

UNIVERSIDADE DO ALGARVE

**Morphodynamic Evolution of
Fetch-limited Beaches**

Ana Rita Carrasco

Doutoramento em Geociências,
especialidade em Dinâmica Litoral

2012

UNIVERSIDADE DO ALGARVE

**Morphodynamic Evolution of
Fetch-limited Beaches**

Ana Rita Carrasco

Doutoramento em Geociências,
especialidade em Dinâmica Litoral

Tese orientada por: Doutor Óscar Manuel Fernandes Cerveira Ferreira
(Universidade do Algarve)

Doutora Paula Maria dos Santos Freire
(Laboratório Nacional de Engenharia Civil)

2012

Nome: Ana Rita Zarcos Carrasco
Faculdade: Faculdade de Ciências e Tecnologia
Universidade: Universidade do Algarve
Orientadores: Prof. Doutor Óscar Ferreira e Doutora Paula Freire
Título da Tese: Evolução Morfodinâmica de Praias de Fetch-limitado

RESUMO

A presente tese analisa a evolução morfodinâmica de uma praia lagunar de fetch-limitado, localizada no sistema de ilhas barreira da Ria Formosa. Para tal, consideraram-se três escalas temporais de análise: curto-termo, médio-termo e longo-termo. Pretendeu-se determinar: (a) quais os mecanismos forçadores que regem o transporte sedimentar na praia; (b) qual a evolução morfológica da praia de médio a longo-termo, e (c) qual a importância das intervenções humana na dinâmica morfológica da praia.

A curto-termo termo (ao longo de um ciclo de mare), o transporte sedimentar foi localmente determinado com recurso à aplicação de traçadores fluorescentes, através da quantificação das variações morfológicas e taxas de transporte. A evolução da praia a médio e longo-termo (entre meses e de anos a décadas) foi obtida através da análise de levantamentos topográficos e análise de fotografia aérea vertical. No final, propõe-se uma breve metodologia destinada a avaliar a suscetibilidade a inundações de ambientes costeiros de fetch-limitado. A metodologia proposta identifica zonas com perigosidade a inundações, quantifica o risco associado e equaciona as medidas de gestão local mais apropriadas.

Palavras-chave: *praia lagunar, fetch limitado, escalas temporais, transporte sedimentar, inundações.*

Name: Ana Rita Zarcos Carrasco
Faculty: Faculdade de Ciências e Tecnologia
University: Universidade do Algarve
Supervisors: Prof. Dr. Óscar Ferreira and Dr. Paula Freire
Title: Morphodynamic Evolution of Fetch-limited Beaches

ABSTRACT

This thesis examines the morphodynamic evolution of a fetch-limited backbarrier beach located in the Ria Formosa barrier island system. Three different scales of analysis were ascribed: a short-term scale, a medium-term scale, and a long-term scale. Main issues addressed were: (a) the factors governing sediment transport under very limited-fetch conditions; (b) the morphological evolution at medium to long-term, and (c) the role of human interventions in beach morphology.

At short-term (over the tidal cycle) sediment transport patterns were locally determined by employing fluorescent tracer techniques, and quantifying morphologic variations and transport rates. The medium- to long-term evolution (between months and from years to decades) was set based in topographic surveys and aerial photograph analysis. Finally, a general framework was developed for flood hazard assessment at fetch-limited coastal environments. This framework embraces the hazard zones identification, risk analysis and the associated most reasonable management options.

Keywords: *fetch-limited, backbarrier, timescales, sediment transport, flood hazard.*

RESUMO ALARGADO

As praias de fetch-limitado distribuem-se ao longo de estuários, baías, zonas lagunares, deltas, lagos, entre outros ambientes, caracterizados por ondas de curto período (2-3 s) e com alturas na ordem dos centímetros ($H_s = 0.10$ m a 1.0 m), em função das condições de 'fetch' local (comprimento de água sobre o qual um determinado vento sopra). Embora estes ambientes costeiros sejam dos mais densamente povoados, os estudos convencionais sobre praias arenosas tendem a concentrar-se em praias oceânicas, o que têm resultado num pior entendimento acerca da sua evolução e morfodinâmica. Recentemente, surgiu a necessidade se desenvolver e prosseguir com estudos dedicados à colheita de dados morfológicos e hidrodinâmicos neste tipo de ambientes. Apesar dos seus recursos naturais poderem não se apresentar imediatamente atrativos, as praias de fetch-limitado têm elevado valor pela sua singularidade ecológica, participando ativamente na dinâmica sedimentar local.

A presente tese analisa a evolução morfodinâmica de uma praia lagunar de fetch-limitado, localizada no sistema de ilhas barreira da Ria Formosa (sul de Portugal), ao longo de diferentes escalas temporais. O sistema de ilhas barreira da Ria Formosa foi designado como Reserva Natural em 1978, Parque Natural em 1987, e nos últimos anos como Rede Natura 2000. É caracterizado por uma elevada diversidade faunística e têm importância nacional e internacional como local de nidificação e migração de aves. A investigação científica costeira neste sistema de ilhas barreira tem sido até então dedicada principalmente à dinâmica litoral da margem oceânica, descurando a dinâmica

sedimentar protagonizada pela margem lagunar. Recebendo contribuição mínima da agitação oceânica, o desenvolvimento de onda na margem lagunar é maioritariamente dependente dos ventos locais e do fetch disponível para geração de onda, normalmente na ordem dos poucos quilómetros de comprimento. Nestas condições, as alturas de ondas de não tempestade são da ordem de poucas dezenas de centímetros ($H_s = 0.1 - 0.2$ m).

Em particular, esta tese foca a sua atenção na margem lagunar da Península do Ancão (extremo Oeste do sistema de ilhas barreira da Ria Formosa), onde as condições de fetch são espacialmente as mais reduzidas ao longo de toda o sistema (fetch < 2 km); à praia é atribuída a condição de 'fetch muito limitado'. A praia é particularmente estreita (~100 m), de baixa elevação vertical (~2 m acima do nível médio do mar) e comporta quatro setores morfológicos principais: a alta praia, a face de praia, o terraço de maré e um banco arenoso (no final do perfil transversal). A parte superior da praia contacta com um extenso campo dunar que se prolonga até à praia oceânica. A parte inferior da praia contacta diretamente com o canal do Ancão. O comportamento morfodinâmico da praia é, na sua globalidade, aqui descrito ao longo de três escalas temporais distintas: a curto-termo (variação da praia à escala diária), a médio-termo (variação da praia de meses a anos), e a longo-termo (variação da praia de anos a décadas). Como objetivos específicos pretendeu-se (a) determinar quais os mecanismos forçadores que regem o transporte sedimentar na praia; (b) caracterizar a evolução da praia entre meses e de anos a décadas, e (c) avaliar a importância de intervenções humanas na dinâmica morfológica da praia.

Os fatores que regem o transporte sedimentar (análise de curto-termo) foram determinados com recurso à aplicação de traçadores fluorescentes. Realizaram-se duas campanhas de campo, em 2006 e 2008, durante dois períodos de não tempestade e em

condições de marés vivas. As duas campanhas contemplaram por si próprias, diferentes escalas temporais de amostragem: a primeira ao longo de apenas um ciclo de maré, e a segunda contemplou um ciclo completo entre marés vivas e marés mortas. Os traçadores fluorescentes foram colocados durante a baixa-mar, na face de praia e no banco arenoso (final do perfil topográfico, junto ao canal do Ancão). O regime de correntes foi caracterizado com recurso a equipamento específico para medição de correntes (dois correntómetros eletromagnéticos e um Aquadopp profiler). Nas duas campanhas recolheram-se amostras sedimentares e procedeu-se à execução de levantamentos topográficos no início e no final do período de monitorização. Definiu-se a variabilidade morfologia típica ao longo de um ciclo de maré ($0.03 \text{ m}^2 \text{ m}^{-1}$), o transporte sedimentar diário (máximo $0.03 \text{ m}^3 \text{ d}^{-1}$), bem como o regime de ventos (máximo 12 m s^{-1}), as velocidades de correntes de maré (máximo 0.5 m s^{-1}) e os respetivos limiares de corrente para despoletar transporte de fundo (u_{cr} ; $u_{cr} = 0.008 \text{ m s}^{-1}$ para a face de praia e $u_{cr} = 0.005 \text{ m s}^{-1}$ para o banco arenoso). As ondas geradas pelo vento foram caracterizadas visualmente (recurso a régua graduada) durante a primeira campanha, enquanto, durante a segunda campanha foram caracterizadas através de modelação numérica ($H_s < 0.1 \text{ m}$ e $T_{\text{mean}} \sim 1.0 \text{ s}$). As técnicas de aplicação de traçadores fluorescentes foram ainda discutidas no contexto das taxas de transporte obtidas. De acordo com os padrões observados, efetuou-se a distinção entre transporte por advecção e dispersão que caracteriza este tipo de ambiente. Os resultados obtidos demonstraram que para praias de fetch muito limitado, as técnicas de aplicação de traçadores fluorescentes devem ser conduzidas com prudência, e requerem a realização de testes prévios para determinar a quantidade ideal de traçador a utilizar e o respetivo tempo de adequação à camada superficial de transporte.

A evolução morfodinâmica da praia a médio-termo incluiu a definição dos intervalos de variabilidade volumétrica da praia ao longo de três anos consecutivos (entre 2005 e 2008). Efetuaram-se levantamentos topográficos com periodicidade mensal e trimestral em 10 perfis transversais à área de estudo. Comparou-se a variabilidade volumétrica total da praia e a variabilidade volumétrica de cada setor morfológico, com as condições de vento dominantes para no mesmo período de análise; o vento foi tido em conta como indicador das condições de agitação local. Avaliou-se ainda a dominância de variações transversais vs. longilitorais ao longo da área de estudo. Os resultados obtidos na análise de médio-termo corroboram os resultados obtidos com as duas campanhas de curto-termo, ou seja, variabilidade volumétrica reduzida. Para o período de análise (2005 a 2008) a variação volumétrica na alta praia e face de praia foi de $0.18 \text{ m}^3 \text{ m}^{-1}$ e $4.88 \text{ m}^3 \text{ m}^{-1}$, respetivamente, enquanto a variação máxima volumétrica no terraço de maré e no banco arenoso foi $4.50 \text{ m}^3 \text{ m}^{-1}$ e $-3.45 \text{ m}^3 \text{ m}^{-1}$, respetivamente. Os quatro sectores morfológicos verificaram a mesma tendência de evolução mensal, alternando entre períodos de acreção e erosão sedimentar, o que sugere relativa homogeneidade na praia; os sectores morfológicos não apresentaram trocas sedimentares significativas entre si. A análise volumétrica interanual revelou que as zonas com maior mobilidade sedimentar se localizam no terraço de maré (no banco de areia e perto do canal do Ancão), nos limites entre a face de praia e o terraço de maré e entre o banco arenoso e o terraço de maré. Não foi observada sazonalidade significativa nos resultados obtidos. Na verdade, a praia não se demonstrou imediatamente reativa à maioria das condições de vento observadas, exibindo uma evolução lenta e contínua numa escala temporal de meses a anos. Durante o período de análise dominaram ventos de W-NW com intensidade média na ordem dos $\sim 4 \text{ m s}^{-1}$ (máximo de 17 m s^{-1} para o período de análise).

Observou-se interligação entre a evolução morfológica da praia a médio e longo-termo. Mesmo operando a escalas de tempo diferentes, as duas análises foram complementares na medida em que tendências observadas na primeira ajudaram na compreensão da segunda. A evolução de longo-termo (de anos a décadas) foi obtida através da análise de fotografia aérea vertical entre 1947 e 2007. A área de estudo revelou uma tendência média de variação de linha de costa de 0.05 m ano^{-1} , com avanço significativo do campo dunar na direção do canal do Ancão (para terra). Morfológicamente, as principais alterações tiveram lugar no canal do Ancão e nas suas imediações. Foram distinguidos quatro períodos distintos de alteração: de 1947 a 1976, de 1976 a 2001, de 2001 a 2005 e de 2005 a 2007.

Os resultados obtidos demonstraram que a praia lagunar esteve sujeita a diferentes mecanismos forçadores nos últimos 60 anos, revelando duas respostas morfológicas distintas: uma resposta natural da praia, condicionada apenas pelos mecanismos forçadores naturais (vento, onda e corrente de maré) e uma outra resposta “modificada”, como resultado de intervenções humanas. As intervenções humanas decorreram essencialmente entre 1996 e 2001 e consistiram em dragagens ao longo do canal do Ancão e a recolocação da barra do Ancão para uma posição poente. As dragagens motivaram a transposição do eixo do canal do Ancão e a criação do banco arenoso, com conseqüente progressão da linha de costa para o canal. A recolocação da barra do Ancão estabeleceu um novo regime de correntes locais.

As intervenções efetuadas incutiram alterações morfológicas na praia, bastante diferentes das observadas, em períodos sem intervenção humana (ex. entre 2005 e 2008 com a análise de médio-termo). A previsão de evolução da praia a longo-termo mostrou-se uma tarefa dificultada devido à complexidade dos processos que nela decorrem e devido à inerente fragilidade do sistema, i.e., fraca capacidade para retornar

a uma fase morfológica anterior. As intervenções humanas deixaram forte herança no sistema, inculcando mudanças morfológicas dificilmente atenuadas ou combatidas pela evolução natural da margem lagunar. Na verdade, os resultados demonstraram que as praias de fetch muito restricto, como é o caso da margem lagunar da Península do Ancão, podem permanecer relativamente inalteradas por um longo período, devido às condições de baixa energia. Neste cenário, a própria praia revela um ‘atraso’ na resposta morfológica aos mecanismos forçadores dominantes. Estas observações são de extrema importância, não só para a compreensão global a longo-termo do comportamento deste tipo de praias, como também podem ser bastante úteis a nível de gestão costeira local.

Ainda no âmbito da análise de longo-termo, a presente tese incluiu uma proposta metodológica para aferir o potencial de inundação em ambientes costeiros de fetch limitado. A metodologia é dedicada apenas a zonas costeiras com risco de inundação forçado pela variabilidade na maré astronómica, sobrelevação meteorológica e contribuição fluvial (ex. zonas estuarinas, lagunas costeiras, deltas, etc). Possui como principal vantagem metodológica o facto de se basear na combinação de duas abordagens distintas: inundações costeiras e inundações fluviais. Abrange a identificação de zonas com perigosidade, o mapeamento de risco de inundação e consideração acerca de medidas de gestão local ambientalmente mais sustentáveis. Na determinação do potencial de inundação esboça dois tipos de variáveis: as que afetam os níveis de água (maré astronómica, sobrelevação meteorológica da maré, subida do nível médio e contribuição fluvial) e as que afetam os impactos de inundação (ocupação humana, geomorfologia e ecologia). A metodologia desenvolve-se ao longo de três etapas principais: (1) a identificação das fontes de perigosidade (determinação de níveis de inundação para os períodos de retorno de 1, 10 e 100 anos), (2) o mapeamento da inundação para diferentes cenários temporais (1, 10 e 100 anos), e (3) a análise de risco

e proposta de medidas de gestão costeira face aos cenários de inundação obtidos. A análise de risco a inundações é discutida no contexto ecológico e humano: o risco ecológico relaciona-se com o potencial de inundação áreas de dunas, paisagens protegidas e habitats, enquanto o risco humano relaciona-se com o potencial inundação de áreas com ocupação humana.

As medidas de gestão costeira propostas assentam maioritariamente sobre uma perspetiva de ‘adaptação’ às condições impostas pela inundação (proposta de um Guia Estratégico de Adaptação). A opção de ‘adaptação’ é considerada a mais adequada do ponto de vista financeiro, diminuindo o impacto económico, social e urbano de intervenções drásticas (por exemplo obras de proteção costeira). Esta estratégia equaciona a manutenção e modificação de usos em zonas de risco de inundação. A maior parte dos usos propostos são usos de ‘valor acrescentado’, contribuindo para uma utilização sustentável das zonas costeiras, incluindo o reforço do valor ecológico e fortalecimento das atividades económicas, ao mesmo tempo que os riscos potenciais de inundação são minimizados. A estratégia proposta ajuda os gestores costeiros: (a) a identificar as zonas de risco elevado e moderado; (b) a implementar um processo orientado e flexível na adaptação de usos em ambientes costeiros de fetch-limitado; e (c) a considerar as medidas de gestão costeira não só para enfrentar a ‘prioridade de conservação de áreas em risco’, mas também para aumentar o seu potencial económico.

Esta metodologia foi aplicada à margem lagunar da Península do Ancão. Os cenários de inundação obtidos tiveram como base o ano de 2010. Os níveis de inundação prevista para 1, 10 e 100 anos de retorno períodos obtidos foram de 2.08 m, 2.45 m e 3.11 m MSL (nível médio do mar), respetivamente. Metodologicamente os níveis de inundação podem revelar alguma incerteza relacionada com erros na aplicação de distribuições probabilística aos níveis de maré e às próprias projeções de subida do

nível médio do mar. No entanto, outros dados e informações recolhidas durante eventos de inundação local (por exemplo, fotografias e visitas de campo) possibilitaram a validação dos níveis obtidos. Os níveis de inundação obtidos foram projetados sobre Modelos Digitais de Elevação (espaçamento de 0.5 m), obtidos com base em levantamento LIDAR (Light Detection And Ranging) de Novembro de 2009 (erro vertical e horizontal de 5-10 cm). Para o caso de estudo em questão, os impactos mais significativos das inundações em ecologia estão relacionados com a interrupção temporária de local e espécies animais que povoam a zona de duna subaérea (principalmente na parte oriental da península). Os impactos das inundações em áreas de ocupação humana fazem-se sentir sobretudo em residências, acessos a residências e passadiços. Especificamente, para este caso de estudo, a adaptação para usos de ‘valor acrescentado’ e a correta gestão dos usos existentes é rentável do ponto de vista económico e social, contribuindo para o aproveitamento global e sustentável de toda a ilha barreira.

É importante realçar que os resultados obtidos nesta tese são uma importante contribuição para o conhecimento científico sobre a evolução morfodinâmica de praias de fetch-limitado. No entanto, ainda subsistem algumas questões relativas aos intervalos de variação morfológica neste tipo de ambientes. Depois da análise às praias de fetch muito limitado (fetch < 2 km, menor energia de onda), a investigação deve futuramente seguir para condições mais energéticas (fetch > 10 km). Deverá tentar estabelecer-se uma escala de variação morfológica, em função de diferentes comprimentos de fetch e consoante os principais mecanismos forçadores. Em futuros tópicos de investigação, e em margens lagunares, deverá ainda ser caracterizada a relação existente entre variabilidade morfológica e fatores ecológicos locais (ex. abundância de algas e diversidade de espécies animais no terraço de maré e face de praia).

ACKNOWLEDGEMENTS

Doing this thesis was a very long journey. I could write it as an amazing fairy tale, full with peculiar characters and its hilarious places, full of magic, dragons and gnomes, and all of those pleasant details that are part of a fantastic history. I could hear myself as an old storyteller talking about dates, places, and memories. Memories of fascinating battles in dark woods, or in dangerous seas that I was able to cross because I was not alone but surrounded with the bravest of the army's. This work could never be done without you all who encouraged and supported me.

I would like to express my sincere gratitude to my supervisors, Dr. Óscar Ferreira and Dr. Paula Freire, for their strong guidance and unwavering support. My unique experience during this journey gave me two people to count on for insight and advice. Their knowledge, comprehension and friendship made this thesis possible. Óscar suggested that I take a step back and look at the bigger picture. Paula usually recommended getting to the essence of the problem and focusing on the specifics. I now realize that such combination provided me with a strong foundation, not only for doing science, but to face world. I acknowledge the frequent science discussions that I kept with Óscar over these years. I am certain that we both proved that describing coastal processes in fetch limited is not an easy task. I am also truly grateful to Dr. Ana Matias for her invaluable insights during results discussion, always teaching me to explore different perspectives.

This research would not have been possible without the support of CIACOMAR/CIMA working group and many of its dedicated and talented researchers (past and present): Tiago Garcia, Ana Vila-Concejo, André Pacheco, Ana Matias, Isabel Mendes, Francisca Rosa, Margarida Ramires, Júlio Cunha, Pedro Almeida, Mara Nunes, Carlos Loureiro, Erwan Garel, Selman Gabriel, and Simon Connor. I would like give special thanks to Ana Matias, Isabel, and Francisca for showing a genuine interest in my work and encouraging me to finish it.

To my friends, I will always be grateful: Ana Luísa, Frutinha, Catarina Sequeira, JSO, Ken, Hugo, Joni, Pipinha, Silvia, Catarina Santos, Tiagilha, Fred, Liliana, Pedro Coelho, Celso, Baco, Pedrilha, Cristina, Bruno, Ana Sofia, Alexandra e Marisa, for reminding me that there is so much in this world to experience, so much more than science. A special thanks to João Janeiro and Joel for their friendship and the challenging ‘good mornings’ that had accompanied me trough every day of this journey.

Finally, I extend heartfelt gratitude to my parents João Carlos and Eugénia for believing in me and in everything I have chosen to do, and to my brother João Pedro for making me feel safe over all these years. Thanks to Hélio for being so genuine, for your support, love and your amazing smile.

It was a pleasure to share this journey with you. We will meet in other battles.

INSTITUTIONAL AND FINANCIAL SUPPORT

The work was funded by:

- Fundação para a Ciência e a Tecnologia, PhD grant reference SFRH/BD/37366/2007; and
- Fundação para a Ciência e a Tecnologia, Research fellowship under the “IDEM – Inlet Dynamics Evolution and Management at the Ria Formosa” (contract n° POCI/MAR/56533/2004).

Data collection was funded by the following scientific projects:

- “IDEM – Inlet Dynamics Evolution and Management at the Ria Formosa” from Fundação para a Ciência e a Tecnologia (contract n° POCI/MAR/56533/2004); and
- “BERNA - Beach Evolution in Areas of Restricted Fetch: Experimental and Numerical Analysis” from Fundação para a Ciência e a Tecnologia (contract n° POCTI/CTA/45431/2002).

Other support:

- Tide data was kindly supplied by **Puertos del Estado**, Ministerio do Fomento, Gobierno de España; and
- **Sociedade POLIS Litoral Ria Formosa SA** provided technical reports and raw data regarding management uses at Ria Formosa barrier system.

CONTENTS

Resumo	i
Abstract.....	iii
Resumo alargado	v
Acknowledgements	xvii
Contents	xxi
List of Figures.....	xxv
List of Tables	xxix
CHAPTER 1. INTRODUCTION	1
1.1. Fetch-limited beaches: Why study them?	2
1.2. Fetch-limited beaches: What to study about them?	4
1.3. Thesis outline and contribution of authors	5
CHAPTER 2. REVIEW OF FETCH-LIMITED BEACHES	9
2.1. Low-energy and Fetch-limited beaches	10
2.2. Human modifications to fetch-limited environments: a brief overview of dredging and nourishment	13
2.3. Research in barrier islands facing low-energy conditions	14
2.4. Ria Formosa backbarrier	16
CHAPTER 3. SHORT-TERM SEDIMENT TRANSPORT AT A BACKBARRIER BEACH.....	19
Abstract	20
3.1. Introduction.....	21
3.2. Field site.....	23
3.3 Methods	24
3.3.1. Fluorescent Tracer data	24
3.3.2. Grain-size data.....	27
3.3.3. Morphological data.....	28
3.3.4. Driving mechanisms data	28
3.4. Results.....	31
3.4.1. Grain-size characteristics and tracer transport	31
3.4.2. Morphological variability	33
3.4.3. Driving mechanisms	34
3.5. Discussion	39
3.6. Conclusions.....	43
CHAPTER 4. SEDIMENT TRANSPORT MEASUREMENTS WITH TRACERS IN VERY LOW- ENERGY BEACHES.....	45
Abstract	46

4.1. Introduction.....	47
4.2. Field site.....	48
4.3. Methods	50
4.4. Results.....	53
4.5. Discussion and Conclusions	60
CHAPTER 5. MORPHOLOGICAL CHANGES IN A BACKBARRIER.....	63
Abstract.....	64
5.1. Introduction.....	65
5.2. Field site.....	66
5.3. Methods	67
5.4. Results.....	69
5.5. Discussion and Conclusions	74
CHAPTER 6. NATURAL AND HUMAN-INDUCED COASTAL DYNAMICS AT A BACKBARRIER BEACH	79
Abstract.....	80
6.1. Introduction.....	81
6.2. Field site.....	83
6.2.1. Regional setting	83
6.2.2. Human activities	85
6.3. Methods	87
6.3.1. Large-scale data collection	88
6.3.2. Small-scale data collection.....	90
6.4. Results.....	93
6.4.1 Large-scale evolution and morphological changes	93
6.4.2. Small-scale evolution, wind, grain-size, and volumetric changes.....	98
6.5. Discussion.....	103
6.5.1. Linking timescales.....	103
6.5.2. Beach inheritance and resource value	108
6.6. Conclusions.....	109
CHAPTER 7. FLOOD HAZARD ASSESSMENT AND MANAGEMENT AT FETCH-LIMITED COASTAL ENVIRONMENTS.....	111
Abstract.....	112
7.1. Introduction.....	113
7.2. Methodology	115
7.2.1. Flood assessment terminology	115
7.2.2. Framework variables	117
7.2.3. Development of the framework.....	118
7.2.3.1. Hazard sources	120
7.2.3.2. Flood hazard mapping	121
7.2.3.3. Risk analysis and management.....	122
7.2.4. Sites for application of the framework	127
7.3. Test case: Ancão backbarrier	128
7.3.1. General characteristics	128
7.3.2. Framework application.....	131

7.3.2.1. Step1: hazard sources	133
7.3.2.2. Step2: flood hazard mapping	134
7.3.2.3. Step3: risk analysis and management	134
7.4. Applicability of the method	140
7.5. Conclusions: benefits of the proposed framework	143
CHAPTER 8. FINAL CONSIDERATIONS	145
8.1. General conclusions	146
8.2. Critical assessment.....	150
8.3. Future work.....	152
REFERENCES	155

LIST OF FIGURES

Figure 1.1.	Definition of spatial and temporal scales involved in coastal evolution. Large-scale coastal landforms evolve over long timescales, whereas small-scale coastal features respond over short timescales [adapted from Cowell and Thom, 1994].	5
Figure 3.1.	Field site location, showing Ancão Peninsula backbarrier, and (inset) a vertical aerial photograph (taken in 2007) with the surveyed profiles and a representative beach profile (M.H.W. = mean high water and M.L.W. = mean low water, based on field data) with instrument position (ECM = electromagnetic current meter, ADP = acoustic Doppler profiler); FT1 and FT2 (fluorescent tracers), deployed during fieldwork are also shown.....	25
Figure 3.2.	Photographs of the field site: (a) fetch distribution on a vertical aerial photograph from 2007; (b) view to NW of the narrow sandy foreshore (July 2007); (c) high shell content in muddy sediments on the tidal flat (October 2006); and (d) from offshore, Ancão tidal channel, offshore sand bank (with shore-normal depression) and tidal flat (January 2006).....	26
Figure 3.3.	Map of tracer concentration at (a) beach face, and (b) sand bank, 24 h after tracer release. Locations of injection points and FT mass centroids are shown (metric coordinates referred to Portuguese Melriça Grid, datum 73)	33
Figure 3.4.	Surface variations between surveys represented as a contour map of isopachs. The numbers (#n) are the topographic profile number. Metric coordinates refer to the Portuguese Melriça Grid, datum 73 (referenced to mean sea level)	34
Figure 3.5.	Driving mechanisms observed during fieldwork: (a) time-average wind intensity and direction; (b) time-average current velocity at the beach face; and (c) time-average velocity at the sand sand bank. The dashed lines in (b) represent ECM data gaps due to equipment malfunction.....	36
Figure 3.6.	Cross-shore velocity component for the first 10 min of data recorded by the electromagnetic current meter (ECM; ~10 cm of water depth above the current meter)	37
Figure 3.7.	Time-averaged shear velocity (\bar{u}_*) and critical shear velocity (u_{cr}) considering d_{10} ($u_{cr}d_{10}$) and d_{50} ($u_{cr}d_{50}$) at (a) beach face, and (b) sand bank	39
Figure 4.1.	Field site location (a) at the Ancão Peninsula backbarrier (Ria Formosa barrier system), overlapped by the scheme of cross-shore and alongshore components at the field site (b); EM corresponds to the position of the current meter placed at the beach face and ADP corresponds to the	

	position of the acoustic doppler profiler placed at the sand bank. Tracer1 and tracer2 represent the locations of fluorescent tracer injection points at the beach face and sand bank, respectively.....	49
Figure 4.2.	Time-averaged currents at the sand bank; data recorded at the lower cell of the equipment (0.7 m above the sensor). Positive alongshore values mean flood, and negative values mean ebb; positive cross-shore values mean offshore (directed towards the Ancão tidal channel) and negative values mean onshore.....	54
Figure 4.3.	Map of tracer concentration at the beach face. Locations of injection points, tracer mass centroids, and number of tagged grains are shown (cross-shore and alongshore).....	56
Figure 4.4.	Map of tracer concentration at the sand bank. Locations of injection points, tracer mass centroids, and number of tagged grains are shown (cross-shore and alongshore)	57
Figure 4.5.	Sediment transport variation during the field experiment: (a) daily Q and Qcumulative at the beach face; and (b) daily Q and Qcumulative at the sand bank.....	60
Figure 5.1.	Field site location and aerial photograph with the location of the analyzed representative profiles (S1, S2 and S3)	68
Figure 5.2.	Wind climate (average magnitude and direction); volume variability at each beach sector, and correlation matrixes (volume and slope) between sectors.....	70
Figure 5.3.	Sediment distribution at the beach-face and sand spit between April 2006 and March 2008.....	72
Figure 5.4.	Profile envelope (maximum, minimum and average volume profile), volume change at each profile during the analyzed period, and volume correlation matrix between profiles.....	73
Figure 6.1.	(a) Field site location, showing Ancão Peninsula backbarrier; and (b) a vertical aerial photograph (taken in 2007) showing the main beach morphologies, profile <i>a</i> , and profile <i>j</i>	84
Figure 6.2.	Photographs of the field site: (a) view of the backshore (June 2006); (b) sandy foreshore (December 2008); (c) high shell content in the tidal flat (October 2006); (d) Ancão tidal channel, sand bank (intercut by the secondary tidal channel), and tidal flat (January 2006); (e) view of aeolian sediment accumulation in the backshore (February 2008); and (f) other view of the sand bank (January 2007).....	86
Figure 6.3.	(a) Surveyed area and beach compartments: backshore, beach face, and nearshore (tidal flat and sand bank). Secondary tidal channel is also shown. Mean elevation is referred to MSL; (b) profile <i>i</i> envelope and standard deviation for the period April 2005 to March 2008; (c) representation of beach face and sand bank reference limits.	92

Figure 6.4.	(a) Ancão backbarrier shoreline evolution between 1947 and 2007; and (b) shoreline displacements between 1947 and 2007 at the study area (aerial photo from 2005).....	96
Figure 6.5.	Field site evolution between 1947 and 2007; beach profile evolution between 1944 - 1945 and 2008	97
Figure 6.6.	(a) daily mean wind direction; and (b) daily and monthly wind maximum velocity	100
Figure 6.7.	Grain size distribution (d_{50}) at profile <i>d</i>	100
Figure 6.8.	Volumetric variations at (a) backshore; (b) beach face; (c) tidal flat; (d) sand bank; and (e) overall area.....	101
Figure 6.9.	Inter-annual elevation changes between 2005 and 2008. Positive elevation changes are expressed with brighter color tones; DEMs were reconstructed as triangular irregular networks in ArcGis 9.3	102
Figure 6.10.	Beach and nearshore displacements towards Ancão channel between 2005 and 2008	104
Figure 7.1.	Schematic methodology for the flood hazard assessment and management of fetch-limited coastal environments	119
Figure 7.2.	Map of Ria Formosa barrier system showing the locations of the Ancão Peninsula and Praia de Faro village (left), and aerial photograph of Praia de Faro village (right).....	129
Figure 7.3.	Land uses of Ancão Peninsula	132
Figure 7.4.	Examples of inundation attained at: (a) Ancão backbarrier during the equinoctial tide of October 2006 (with a maximum storm surge of 14 cm); (b) Praia de Faro bridge during the equinoctial tide of March 2010 (with a maximum storm surge of 58 cm; photograph courtesy of Elsa Caetano); (c) the eastern part of Ancão backbarrier during the equinoctial tide of September 2011 (with a maximum storm surge of 10 cm); and (d) the western part of Ancão backbarrier during the equinoctial tide of March 2010 (photograph courtesy of Elsa Caetano)	133
Figure 7.5.	(a) Lognormal distribution fitting to annual maximum tide levels; and (b) representative topographic profile at Ancão backbarrier showing the main morphological segments (backshore, beach face, and nearshore) and inundation levels.	135
Figure 7.6.	Hazard map for Ancão Peninsula for flood zones < 1 yr return period (constant flooded), 1 - 10 yr (frequently flooded), and 10 - 100 (infrequently flooded) (lain over a 2009 orthophoto)	136
Figure 7.7.	Risk map for occupancy and ecology at Ancão Peninsula.....	137

LIST OF TABLES

Table 3.1.	Grain size parameters. FT = fluorescent tracers, d_{50} = median, d_{10} = limit of 10% of the finer population.....	32
Table 3.2.	FT transport velocities and volumetric transport (Q). U_x is the velocity in the longshore direction and U_y is the velocity in the cross-shore direction	32
Table 3.3.	Time-averaged flow conditions during field experiments and thresholds for bedload transport (u_{cr}) at each morphology. Negative longshore velocity means S-E (ebb) and negative cross-shore velocity means N-E (towards the Ancão tidal channel). $u_{crd_{10}}$ and $u_{crd_{50}}$ are determined for tagged population.....	38
Table 4.1.	Tide, wind, waves, and currents during the fieldwork experiment	58
Table 4.2.	Observed rates of transport based on tracer displacement. u_{bf} and u_{sb} correspond to the daily mass centroids velocity at the beach face and sand bank, respectively (accounting for both cross-shore and the alongshore velocity components); negative values of u correspond to flood and onshore directed tracer displacements; Q represents the daily transport from centroid positions (accounting for Q_x and Q_y), Q_x represents the daily alongshore, and Q_y represents the daily cross-shore transport; negative values of Q_y correspond to onshore tracer displacement, and negative values of Q_x correspond to tracer displacements towards flood. l is the daily immersed cross-shore length of each morphology.....	59
Table 6.1.	Medium- and long-term datasets.....	89
Table 6.2.	Total RMS error associated with georeferenced aerial photographs (in metres).....	90
Table 6.3.	Shoreline displacements between 1947 and 2007 (positive values indicate seaward or northeast displacement, i.e., towards the Ancão channel), backbarrier morphologies and related changes.	98
Table 6.4.	Correlation coefficients between morphology volumes and wind conditions ($p < 0.05$ when $r > 0.39$)	103
Table 7.1.	Permitted uses in flooded areas, developed within the proposed framework	124
Table 7.2.	Example of an Adaptation Strategy Guidance	126
Table 7.3.	Morphological characterization of Ancão Peninsula backbarrier, and social context	131

Table 7.4.	Delimitation of flood hazard zones at Ancão Peninsula and risk estimates for each zone	138
Table 7.5.	Adaptation Strategy Guidance for Ancão Peninsula.....	141

CHAPTER 1

INTRODUCTION

1.1. Fetch-limited beaches: why study them?

Fetch-limited beaches are found in estuaries and bays (e.g., Chesapeake Bay, USA); behind ocean barriers (e.g., Pamlico Sound, USA); adjacent to inlets (e.g., Tapora Bank, New Zealand); deltas (e.g., Menderes River, Turkey); eroding thermokarst (e.g., Yensei Bay, Russia); and glacial outwash fans (e.g., Canal Baker, Chile), amongst other places (Cooper et al., 2007). Although these types of environments are often located near densely populated areas, conventional studies of sandy beaches have focused on high-energy environments (e.g., Wright and Short, 1984; Lippman and Holman, 1990), which resulted in a poor understanding of the evolution and morphodynamics of fetch-limited beaches. The term ‘fetch-limited’ does not appear in the geomorphological literature prior to the early 1990s, and even over the ensuing decade it is difficult to find more than one or two papers per year that refer to fetch-limited or fetch-restricted coasts (Cooper et al., 2007). These days, a simple search on *Web of Knowledge* (all databases, 1899-present) demonstrates the still low scientific profile of these types of shores, with only 143 results for ‘low-energy beaches’, 21 results for ‘fetch-limited beaches’, and 27 for ‘backbarrier beaches’ (checked on 12 December 2011). Data sets in fetch-limited environments are incredibly scarce at a worldwide level. Portuguese research on fetch-limited processes at present is limited to just two places: the Tagus estuary (e.g., Freire and Andrade, 1999; Oliveira et al., 2006; Freire et al., 2009), and the Ria Formosa Barrier system (Ancão Peninsula backbarrier; e.g., Ciavola et al., 1997a; Carrasco et al., 2009). The results presented herein are the most recent contribution to the study of fetch-limited environments in Portugal.

While oceanic beaches respond rapidly to changes in energy conditions, fetch-limited beaches adjust slowly to shifts in energy conditions (Jackson et al., 2002a). The

delay in morphological response may give rise to features that are not representative of dominant wave conditions, but are a remnant of other energetic wave conditions (Costas et al., 2005). The low capacity to return to a prior morphological stage (Eliot et al., 2006) is an environmental ‘weaknesses’, and often hinders local management decisions, since there are few studies about profile response for this type of beach that could help to predict changes (e.g., Nordstrom, 1980; Jackson and Nordstrom, 1992). It is essential to develop and proceed with studies, including collection of morphological and hydrodynamic datasets, and it is essential to generate data that accurately report coastal dynamics on these types of shore; that is the main concern of this thesis.

Fetch-limited shores have a different economic resource potential from ocean beaches because of differences in wave energy, nearshore water depth, water temperature, landform shape and surface characteristics, amongst others (Nordstrom, 1992). Although their resources may not be immediately appealing, they have value because of their uniqueness and because they are located close to population centres (namely backbarrier shorelines). Backbarrier beaches are important counterparts of barrier systems, actively participating in local coastal dynamics. Like other fetch-limited shores, they can create a large variety of habitats, including beach, marsh and tidal flat (e.g., Kraeuter and Fegley, 1994; Botton and Loveland, 2003), often with a higher ecological value and biodiversity than oceanic beaches. Their low perceived value often results in a loss of beach habitat as the shoreline is modified to accommodate human uses or shore-protection methods (Nordstrom, 1992). A better understanding of these shorelines is important from a coastal management perspective, as the pace of development increases along lower energy waters (Lewis et al., 2007).

1.2. Fetch-limited beaches: what to study about them?

Hitherto, research on low-energy beaches has repeatedly adopted the morphodynamic classifications and morphological models used to describe high-energy beaches. However, recent research has demonstrated that viewing low-energy beaches as scaled-down versions of high-energy beaches is unsatisfactory (e.g., Nordstrom, 1992; Carrasco et al., 2011a). Crucial questions about beach dynamics – namely, the type and the related time of beach response – are yet to be asked, let alone answered, in fetch-limited morphodynamics. There remains a lack of knowledge about sediment transport patterns at different timescales and their dependency on the main causative forcing mechanisms (e.g., wind, tide, currents, river influence, amongst others), as well as the magnitude of human impacts.

The main objective of this research was to determine the morphodynamic time-scaling variability of a backbarrier beach located in a multi-inlet barrier system (Ria Formosa barrier system, Portugal). It includes the characterisation of beach morphology and process controls, including wind (and wind-generated waves), and tidal currents on a fetch-limited shoreline located on the Ancão Peninsula backbarrier. Three different scales of analysis were ascribed: a short-term scale (daily variability), a medium-term scale (months to years), and a long-term scale (decadal shoreline variability), covering the timescale spectrum from “instantaneous” to “event” (*sensu* Cowell and Thom, 1994; see Figure 1.1).

Research issues addressed in this thesis include:

(1) Determination of the site-specific controls on **short-term beach morphodynamics**, including an analysis of waves, tide, wind data, and sediment transport through the

definition of the main net surface changes at a daily timescale and from spring to neap tide;

(2) Characterisation of **beach dynamics at medium to long-term scale of analysis**, including the evolution rates of the major beach morphologies and an evaluation of human impacts in the long-term evolution; and

(3) Definition of **flood hazard in fetch limited coastal environments**, definition of an Adaptation Strategy Guidance to face coastal flooding events, and dedicated to support management decisions in fetch-limited environments.

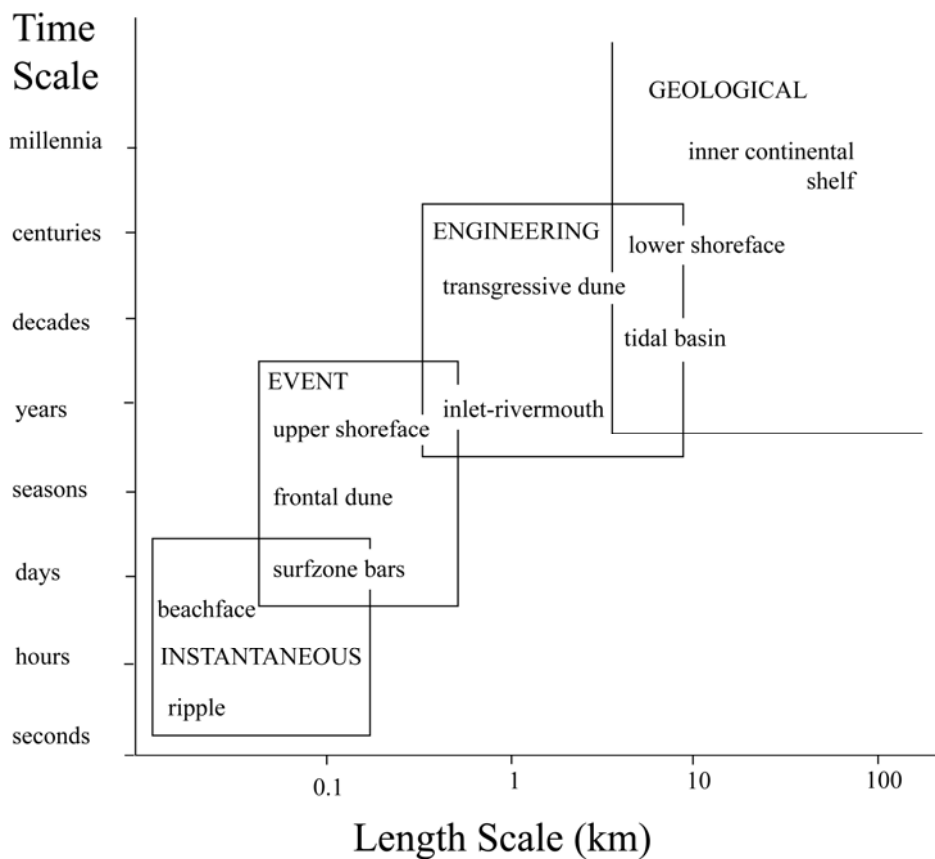


Figure 1.1. Definition of spatial and temporal scales involved in coastal evolution. Large-scale coastal landforms evolve over long timescales, whereas small-scale coastal features respond over short timescales [adapted from Cowell and Thom, 1994].

1.3. Thesis outline and contribution of authors

The main chapters of this thesis refer to submitted, in press or already published peer-reviewed international scientific papers. The advantage of presenting a thesis by articles is that each chapter can be read independently; however, this format has the disadvantage of repeating certain details (e.g., study area description). While it is acknowledged that this repetition may hinder the flow of the text, the format has been maintained to preserve the integrity of the original publications. Three additional chapters were also included to improve consistency (Introduction, Review of Fetch-limited Beaches and Final Considerations). The thesis comprises eight chapters:

A brief introduction is given in **CHAPTER 1**, offering a description of low-energy environments and fetch-limited beaches in the context of morphodynamic research. This chapter introduces the research topic and shows why it is important to study it.

CHAPTER 2 illustrates the recent research undertaken in fetch-limited beaches. Describes the study area, the Ria Formosa barrier system and, in particular, the Ancão Peninsula backbarrier.

CHAPTER 3 is reprinted from the *Journal of Coastal Research* (A.R. Carrasco, Ó. Ferreira, A. Matias, A. Pacheco and P. Freire, 2011. **Sediment transport at a backbarrier beach**, 27(6), 1076-1084). This chapter describes the factors governing sediment transport under fair-weather conditions, during the one tidal cycle. A.R. Carrasco and Ó. Ferreira developed the ideas. A. Matias and P. Freire were crucial to for fieldwork execution. A. Pacheco assisted with current-data collection. A.R. Carrasco analysed data and wrote the paper with the help of all co-authors;

CHAPTER 4 is submitted to *Earth Surface Processes and Landforms* (A.R. Carrasco, Ó. Ferreira, A. Matias, P. Freire, X. Bertin, and J. A. Dias. **Sediment transport measurements by tracer in very low-energy beaches**). This chapter describes the factors governing sediment transport under fair-weather conditions encompassing a spring- to neap-tide cycle. A.R. Carrasco and Ó. Ferreira developed the ideas. X. Bertin provided wave-climate data (using the Morsys 2D application). A.R. Carrasco analysed data and wrote the paper with the help of all co-authors;

CHAPTER 5 is reprinted from the *Journal of Coastal Research* (A.R. Carrasco, Ó. Ferreira, P. Freire, and J.A Dias, 2009. **Morphological changes in a low-energy backbarrier**, SI56, 173-177). This chapter provides a brief overview about the of beach variability between months and from months to years. This was the first paper to be published and represented the first data analysis within the scope of the present thesis. A.R. Carrasco analysed data and wrote the paper with the help of all co-authors;

CHAPTER 6 is under review in *Geomorphology* (A.R. Carrasco, Ó. Ferreira, A. Matias, P. Freire. **Natural and human induced coastal dynamics in at a backbarrier beach**). This chapter describes medium- (within years) to long- term (from years to decades) variability of the Ancão backbarrier. A.R. Carrasco analysed data and wrote the paper with the help of all co-authors. Ó. Ferreira and A. Matias provided many critical reviews of the manuscript;

CHAPTER 7 is submitted to *Ocean & Coastal Management* (A.R. Carrasco, Ó. Ferreira, A. Matias, and P. Freire. **Flood hazard assessment and management of fetch-limited coastal environments**). This chapter embraces a methodological proposal to assess the

potential of inundation in fetch-limited coastal environments. A.R. Carrasco analysed data and wrote the paper with the help of all co-authors.

CHAPTER 8 presents the general conclusions, crossover between timescales of analysis and a proposal for future research in fetch-limited environments

CHAPTER 2

REVIEW OF FETCH-LIMITED BEACHES

2.1. Low-energy and Fetch-limited beaches

Low energy beaches are located in sheltered and fetch-limited environments. Sheltered environments occur in the lee of islands, reefs, or submarine ridges (Hegge et al., 1996), being protected to varying degrees from higher energy (deep-water) ocean waves. Fetch-limited environments occur in lakes (e.g., Roy et al., 2001), bays (e.g., Goodfellow and Stephenson, 2005), estuaries (e.g., Jackson and Nordstrom, 1992; Jackson et al., 2002a), and lagoons (e.g., Jackson et al., 2002b; Carrasco et al., 2008). Low energy conditions are created in different settings through the sheltering effect of the adjacent topography (sheltered environments) or the short fetch (i.e., the length of water over which a given wind has blown). Fetch distances that limit wave size (fetch-limited environments; Cooper et al., 2007).

According to coastal classification, fetch-limited beaches, where beach prisms are smaller than open ocean beaches (Jackson, 1999), tend to be morphodynamically reflective (Wright and Short, 1984; Sherman et al., 1994). Fetch length ranges from narrow, shallow lagoons, where onshore winds can only generate significant wave heights less than 0.10 m on the foreshore (Nordstrom et al., 1996), to beaches in the lee of reefs, where significant wave height at breaking is up to 1.0 m (Hegge et al., 1996). Limited fetch conditions produce small, steep waves, sometimes erosive due to short wave periods (Battjes, 1974; Jackson et al., 2002a). Beach morphologies include narrow and planar foreshores (Nordstrom, 1980; Jackson and Nordstrom, 1992; Hegge et al., 1996) with little evidence of bar forms seaward of low still-water levels (Jackson et al., 2002b). Places with higher tidal range, relative to wave height, are characterized by a steep upper foreshore with a broad, flat low-tide terrace (Jackson et al., 2002a). Extreme dissipative conditions prevail on the low tide terrace (Jackson and Nordstrom, 1992).

Sand availability and wind conditions are important factors in the modulation of fetch-limited beaches (Anthony et al., 2006). In fact, wind may be the main source of energy for mobilizing and transport of beach sediments in those environments (Jackson, 1995). Waves are generally wind-generated, with low heights (usually < 0.2 m) and short periods (2.0 - 4.5 s), and with changes that lead to a relatively low-frequency beach response (Nordstrom, 1977; Nordstrom, 1992; Hegge et al., 1996; Masselink and Pattiartchi, 2001; Costas et al., 2005). Higher energetic conditions are achieved when the dominant wind blowing direction is coincident with larger fetch length. Besides wind-waves, currents are particularly important near channels, projecting headlands, and constrictions in bays, and they may be also the dominant agent of sediment transport (Nordstrom, 1992). In conjunction with the orientation of the shoreline to dominant winds and fetch, currents may determine the local dominance of cross-shore or longshore processes (Jackson et al., 2002a). Currents can both stir up and transport sediments, while waves enhance stirring (Brown and Davies, 2009). The relative importance of tides within fetch-limited systems is fundamentally through the lateral shifts in wave processes and propagation associated with tide-driven water-level changes; boat wakes could also have significant impact on such beaches (Nordstrom, 1992; Curtiss et al., 2009).

The relevance of these forcing processes in beach profile modulation has been discussed by several authors, who demonstrate the foreshore to be the most active part of profile (e.g., Jackson, 1995). Profile changes were mainly defined by sediment removal from the upper foreshore during high-energy events and subsequent deposition in the lower foreshore, whereas the tidal terrace is kept relatively stable (Jackson and Nordstrom, 1992). Only during storms waves are of a sufficient magnitude to promote important sediment transport, otherwise beaches remain static for long periods of time

and are only episodically active (Nordstrom, 1980). According to Nordstrom (1992), the depth of mobilization on the upper foreshore is small, and the active beach may be only a thin veneer of unconsolidated material. Rates of change are thus low, and surveyed profiles at fetch-limited beaches generally reveal little change in morphology, either alongshore or cross-shore (Nordstrom, 1980). In contrast to most oceanic beaches, changes to fetch-limited beaches can remain for long periods, since they usually have very low recovery rates (Nordstrom, 1992).

On the upper foreshore, wrack lines are an important feature of low energy beaches, because fair weather wave conditions are insufficient to modify debris deposited during storm events (Jackson et al., 2002b). Wrack, including human litter, seagrass, leaves, and other organic material, shelters underlying sediment deposits, preventing resuspension and beach erosion from low-energy return flow. Wrack permits the accumulation of sediment, because sand usually filters through debris, but hinders the aeolian resuspension of sediment. Just as low wave energy facilitates wrack accumulation, low wave energy may be partially responsible for a lack of dune development. Algal mats on the seaward tidal flat work in a similar manner, reducing the sediment supply (covering loose sediments) and stabilising the platform (Lewis et al., 2007).

Previous studies (Ekwurzel, 1990 in Goodfellow and Stephenson, 2005; Jackson and Nordstrom, 1992; Hegge et al., 1996; Travers, 2007) noted differences between the typical Wright and Short (1984) model of ocean-barrier beach dynamics and fetch-limited beach dynamics. Modal conditions following a storm event may not be an immediate beach response to high energy event but a reaction of the system's memory to previous events, because of the beach lagging behind causative forcing mechanisms. The variability inherent in the beach response is mostly dependent on the natural

resistance of the beach profile and on the magnitude of seasonal changes. Besides natural forcing factors, fetch-limited beaches are also subject to other factors acting at short-term scales, such as human interventions, which may leave long-term inheritance in profile shape.

The geomorphology and morphodynamics of sheltered, low-energy coastal settings has received less attention than open ocean coastlines. Research dedicated to low-energy environments, particularly concerning fetch-limited areas and backbarrier systems, is scarce (e.g., Jackson et al., 2002a; Carrasco et al., 2008; Pilkey et al., 2009). In contrast, studies on the morphology of open-ocean beaches and on the relevant forcing mechanisms are widely represented in the coastal literature. The findings of this study should contribute to a better understanding of the different timescales of change in a fetch-limited backbarrier subjected to very low-energy conditions.

2.2. Human modifications to fetch-limited environments: a brief overview of dredging and nourishment

Permanent or seasonal human modifications (e.g., occupation or marine exploitation) are conspicuous on nearly every fetch-limited shore in the world (Nordstrom and Roman, 1996). Many human-altered beaches bear little resemblance to their potential state under natural conditions, and many beaches are created where none would occur naturally (Nordstrom, 1992). There are numerous types of impacts, and many have profound effects for many years. For instance, sediment deposits in backbarrier marshes, tidal creeks, bays, estuaries, and lagoon environments behind barrier islands and spits have all been used in the past for beach fill. They are an attractive source because they are protected from ocean waves and are often close enough to the project

beach to allow direct transfer of the material by pipeline. This eliminates the need for separate transport and transfer operations (Nordstrom, 1992). However, backbarrier areas are highly important elements in the coastal ecosystem and are sensitive to disturbance and alteration by dredging. Dredging is mostly done in overwash deposits and relict flood-tidal shoals, which may be ecologically important because they often provide suitable substrate for marsh growth, creating a great variability of habitats (e.g., Kraeuter and Fegley, 1994; Botton and Loveland, 2003). On retreating barriers, backbarriers may comprise a reserve of sand that will be recycled into the active beach deposits as retreat progresses. Flood-tidal shoals at an active inlet may be suitable as borrowing sites because the material removed is likely to be replaced by ongoing inlet processes. However, dredging material from active flood-tidal shoals can adversely alter both the hydraulic conditions in the inlet and wave action on adjacent shores.

As with sediment dredging, beach nourishment can also produce negative effects. Beach nourishment can enhance shore protection, but can also contribute to a decrease in habitat suitability by creating higher berms and wider backshores than would occur under natural conditions (Jackson et al., 2010). Studies of human projects need to predict the above effects over a short time horizon, helping to minimize negative events. Knowledge about short- and long-term patterns of sediment transport in these environments will provide important insights into predicting profile response-type.

2.3. Research on barrier islands facing low-energy conditions

Lewis et al. (2007) identified nearly 7500 actively evolving fetch-limited barrier islands worldwide. More of these islands occur around Australia than any other country. These barrier islands exist in every state and along every coast. Though barrier islands along

open ocean shorelines are the focus of hundreds of studies because they are simultaneously highly dynamic features and subject to intense development pressures (e.g., Hayes, 1979; Stutz and Pilkey, 2002), few studies look exclusively at fetch-limited barrier islands (Lewis et al., 2007). To some extent, the focus on fetch-limited systems has been developed by Nordstrom and Jackson, who were mostly devoted to estuarine beach research (e.g., Nordstrom, 1977; Jackson et al., 2002a). Indeed, it is tempting to attribute the merit of research done on this topic to both workers, in particular the outstanding case studies presented in Nordstrom (1980), Jackson (1995) and, Jackson et al. (2002a). The latter, especially, provides an extensive description of low-energy shorelines in marine and estuarine environments. We should also not forget Nordstrom's (1992) book, containing an overall picture of sediment dynamics in estuarine beaches, with an important spotlight on estuarine beach natural values.

Other references to barrier islands within low energy environments include Pizzuto (1986; Delaware Bay, USA); Tanner and Demirpolat (1988; describing 'low energy beach ridges' in Laguna Madre, USA); Lewis et al. (2005; Chesapeake Bay and Delaware Bay, USA); Andrade et al. (2004; describing 'marsh areas' in the Ria Formosa, Portugal); Cooper et al. (2007; with a collation of geomorphological settings on low energy beaches of North America, the Pacific and Mozambique coast); Pilkey et al. (2009; presenting the global distribution and morphology of active fetch-limited barrier islands); and Carrasco et al. (2008; defining types of backbarrier evolution in the Ria Formosa, Portugal). More recently, there has been an effort to study not only fetch-limited barrier islands, but also other types of fetch-limited beaches. Indeed, there was a significant peak in the output of publications on fetch-limited environments in 2009. The most relevant in terms of beach morphodynamics were Silveira and Psuty (2009; focused on sediment transport on the bayside coast of Sandy Hook, New Jersey);

Dolphin and Green (2009; with a detailed account of short-term wave modification in Manakau Harbour, New Zealand); Freire et al. (2009; with simple wave-tide classification of fetch-limited beaches in the Tagus estuary and Ria Formosa); and Ashton et al. (2009; particularly interesting in its exploration of self-organization in the evolution of fetch-limited shorelines).

2.4. Ria Formosa backbarrier

The Ria Formosa is a highly dynamic multi-inlet barrier island system located in the Algarve region, Southern Portugal. These islands are true barrier islands in that they contain the six required elements needed to impose the distinction of ‘barrier island’ to a littoral sand body: (1) an unconsolidated, elongated body of sediment (typically sand), (2) backed and fronted by a body of water, (3) fronted by a shoreface, (4) bounded by inlets with tidal deltas, (5) sitting on a barrier platform, and (6) “protecting” a mainland shoreline (Oertel, 1985).

The origin of the Ria Formosa is not clear, and several geological hypotheses for the system’s genesis have been proposed (Dias, 1988; Pilkey et al., 1989; Bettencourt, 1994). Dias (1988) and Pilkey et al. (1989) followed the Hoyt (1967, in Pilkey et al., 1989) model, suggesting that the origin of the sand islands is related to changes in sea-level during and after the glacial period, i.e., the Ria’s Holocene evolution fits within the classical shoreface transgression model. As on other fetch-limited barrier islands, the Ria Formosa backbarrier forms a continuum, ranging from linear sand bodies morphologically indistinguishable from transgressive open-ocean barriers (Pilkey et al., 2009). The entire backbarrier covers an area of $8.4 \times 10^7 \text{ m}^2$ (Andrade, 1990), being characterised by: i) extensive saltmarsh areas with a dense distribution of shallow

meanders composed of silt and fine sand (Bettencourt, 1994); ii) large sand flats partially flooded and reworked during spring tides (Pilkey et al., 1989); and iii) a complex network of natural and partially-dredged channels, which narrow and shoal in the upper regions of the system (Andrade et al., 1998; Salles, 2001).

The backbarrier receives minimal ocean swell and is dependent on local winds for wave development, being a typical fetch-limited environment. The main hydrodynamic controls and shoreline morphology differs over short distances due to differences in fetch length and wind exposure. Common characteristics include wave heights in the order of centimetres, and waves driven primarily by local winds and occasional high-energy events (i.e., storms and/or high tides). Unlike open-ocean islands, fair-weather waves exert almost no control on the islands, because the limited fetch prevents fair-weather wave heights from exceeding 0.1 m (see typical H_s values in Carrasco et al., 2011a). Even then, the wide mudflats prevent most waves from reaching the barriers and reduce the energy of the few waves that reach the shore (Lewis et al., 2007). Since most of the backbarriers are near tidal channels and some of them under the direct influence of inlets, the other main hydrodynamic control is the tidal current. At other locations in the system, dune overwashes are the main cause of morphological changes, leading to washover fans in the backbarrier (e.g., Barreta Island, Matias, 2006)

The Ria Formosa barrier system has been the focus of several PhD theses (e.g., Andrade, 1990; Bettencourt; 1994; Salles, 2001) and scientific papers (e.g., Ciavola et al., 1997a; Balouin et al., 2005; Garcia et al., 2010). Research interest in this barrier system has until now been devoted to inlet dynamics, overwash sedimentary dynamics (e.g., Vila-Concejo et al., 2004a; Matias et al., 2008, Pacheco et al., 2010), and beach profile dynamics (e.g., Almeida et al., 2010; Ferreira, 2011); a few publications were concerned with local management issues (Dias and Neal, 1992; Matias et al., 2004).

Most studies were focused on the open ocean coast and only a few works describe sediment dynamics on the lagoon side (Andrade, 1990; Andrade et al., 2004; Carrasco et al., 2008). The dynamics of the lagoon (and backbarrier areas) is presently an important research topic. Besides being an important element of the overall coastal system, the lagoon serves as the main ‘feeder’ of the local economy. Indeed, several economic activities take place in the system (e.g., aquaculture, fishing, shipping, mining and tourism), carrying a fragile combination of different and often-competing economic activities (Dias, 1988). The lagoon is a very low-lying area with maximum depth of 2 m (below mean sea level), supporting great sedimentary and morphological variability (Andrade, 1990). It was designated as a Natural Reserve in 1978, a Natural Park in 1987, and is now part of the Natura 2000 network, with the aim of achieving a rational and sustainable exploitation of its resources. This system is characterized by high faunal diversity, has national importance as a nest-building zone and international relevance for bird migration. Moreover, it is considered a noteworthy wetland area worldwide, and is protected by the RAMSAR and BERNA conventions.

The overall backbarrier has an intrinsic natural/ecological susceptibility to natural hazard events. The process of managing resources involves a complex net of cultural norms, economic constraints, and legal and political perceptions, amongst other issues, making management a difficult task. The findings of this thesis provide a step forward in generating knowledge for local coastal management.

CHAPTER 3

**SHORT-TERM SEDIMENT TRANSPORT
AT A BACKBARRIER BEACH**

Abstract

This paper defines short-term (tidal cycle) sediment transport patterns at a backbarrier beach based on detailed field studies. Fieldwork was planned to record non-storm, spring tide conditions, that enable the definition of background sediment dynamics at the study area. The experiment was set at two beach morphologies: beach face and sand bank. Current meters were deployed at both sites. Fluorescent tracer techniques were applied to determine rates and direction of transport. Topographic surveys and sediment sampling were undertaken.

During the experiment, limited tracer displacement and small morphological changes occurred. The low magnitude changes are representative of predominant low-energy hydrodynamic conditions. Sediment transport was primarily longshore orientated and dependent on the velocity of tidal currents. Tidal currents had the potential for sediment transport only during a short period of the tidal cycle, and had higher velocities during ebb, which results in a net sediment transport orientated towards the nearby inlet. It is suggested that there is a dependence of sediment transport rate at the study site and the variability of tidal currents, which are greatly influenced by the distance to and conditions of the nearby Ancão Inlet.

Keywords: *sediment dynamics, fluorescent tracer, hydrodynamic conditions.*

3.1. Introduction

According to coast classifications, fetch-limited beaches tend to be morphodynamically reflective (Sherman et al., 1994; Wright and Short, 1984), and beach prisms are smaller than on open ocean beaches (Jackson, 1999). Wave regime is characterized by short-period waves and by small wave heights (Nordstrom et al., 1996). Significant wave heights can range from 0.10 m (Nordstrom et al., 1996) to 1.0 m (Hegge et al., 1996). Profile characteristics of sandy beaches include narrow (Jackson and Nordstrom, 1992) and planar foreshores (Nordstrom, 1980; Hegge et al., 1996), frequently without backshore (Nordstrom et al., 1996). When a higher tidal range is present, relative to the wave height, fetch-limited beaches are characterised by a steep, upper foreshore with a broad, flat low-tide terrace (Jackson et al., 2002b). In some areas, intertidal bars are attached to the beach foreshore, implying that sediment may be exchanged between the low-tide terrace and the foreshore; however, these transfers are still not fully understood (Nordstrom et al., 1996).

Fetch-limited environments occur in lakes (e.g., Roy et al., 2001), bays (e.g., Goodfellow and Stephenson, 2005), estuaries (e.g., Jackson and Nordstrom, 1992; Jackson et al., 2002a), and lagoons (e.g., Jackson et al., 2002b). The principal factors affecting the morphodynamics of these beaches are waves, wave- and/or wind-induced currents, and tidal currents (Nordstrom, 1992). Morphological changes might also be the result of storms (Nordstrom et al., 1996). Thus, the profile shape may be inherited and unrelated to contemporary hydrodynamics (Eliot et al., 2006) because modal hydrodynamic conditions following storm events may not be sufficient to return the beach to its original state (Travers, 2007). In the particular case of backbarrier stretches, beach morphology results from the reworking by waves of sediment delivered by tidal

currents from inlets (Nordstrom, 1992). Consequently, the morphodynamic response of the profile is controlled by inherent variability of these forcing factors. Research efforts over these beaches should first attest typical background conditions (fair-weather conditions) and the relative importance of the main forcing factors leading to morphological change. The present study aims to provide this overview and to determine the direction and rate of sediment transport along a backbarrier beach using fluorescent sand tracer. The fluorescent tracer (FT) technique has been used in many studies during the past four decades to determine transport rates (e.g., Inman et al., 1980; Kraus et al., 1982; Vila-Concejo et al., 2004a); however, only a few of these investigations have been made with respect to fetch limited beaches (e.g., Nordstrom et al., 1996; Sherman et al., 1994). The small dimensions and low wave energies of estuarine beaches facilitate the use of tracers (Nordstrom et al., 2003). Despite the significant development of sediment transport measuring techniques in recent years, the use of sand tracers still is one of the best available methods to evaluate longshore transport (Silva et al., 2007). The use of fluorescent sand is simple, and marking can be done easily and rapidly (Ciavola et al., 1998). However, tracer techniques also have some drawbacks, which are essentially related to the high cost of sand tracer experiments and to their moderate accuracy (30 – 60% range; White, 1998). The method must fulfil some basic assumptions: The marked sands should have hydraulic behaviour comparable to the unmarked ones, advection of the tracers should be prevalent over diffusion and dispersion, and the transport system must be in equilibrium (Madsen, 1987). In this study, tracer trends are analysed in conjunction with tidal currents and wind conditions that drive local waves to determine to which forcing mechanism the beach morphology is more reactive under fair-weather conditions.

3.2. Field site

The field measurements took place at the Ancão Peninsula backbarrier, in the south of Portugal (Figure 3.1). The field site is located in the Ria Formosa, a multi-inlet barrier island system. The system extends more than 56 km in length and includes two peninsulas, five islands, and six tidal inlets. Tides in the area are semidiurnal; average ranges are 2.8 m for spring tides and 1.3 m for neap tides, but maximum ranges of 3.5 m can be reached during equinoctial spring tides. Average offshore significant wave height is 0.92 m (Costa et al., 2001); however, the field site behind Ancão Peninsula (Figure 3.1) is sheltered from oceanic waves and is, therefore, exposed to a different wave and current regime. The main forcing mechanisms acting on the field site are tidal currents and waves generated by local wind. The backbarrier beach is limited by the Ancão channel that connects to the Ancão Inlet about 2250 m to the SE (Figure 3.1). Ancão Inlet is a small inlet with a cyclic, eastward migration pattern (Dias, 1988; Pilkey et al., 1989; Vila et al., 1999; Vila-Concejo et al., 2002) and exhibiting an ebb-dominated behavior (Andrade, 1990; Salles, 2001). With the exception of wave regimes generated by exceptionally strong winds, predominant waves are small, in the order of a few centimetres in height (Carrasco et al., 2009) because of extremely limited fetch conditions (maximum, 1500 m; Figure 3.2a). The field site extends over ~150 m (Figure 3.1) and includes a sandy beach with low, narrow, and reflective morphology (Figure 3.2b). Under low wave energy, the steep beach foreshore (~35 m wide) presents a very narrow surf and swash zone. In contact with the foreshore, a tidal flat with a gentle slope is present ($\tan\beta = 0.01$; Figure 3.2c), ending in a small parallel sand bank (30 m of length, with $\tan\beta = 0.06$; Figure 3.2d). Both tidal flat and sand bank, with bedforms absence, are cut off by a small transverse secondary tidal channel. The tidal flat is

mainly sandy ($d_{\text{mean}} = 0.3$ mm) with 9 % of mud ($< 63\mu\text{m}$; Figures 3.2c and 3.2d). The beach face ($\tan\beta = 0.07$) and sand bank are coarser, with d_{mean} values of 0.9 mm and 0.4 mm, respectively.

Human development includes a small number of dwellings (for local fishermen) in the backshore area and an alongshore elevated footpath. Buildings do not interfere with the foreshore sediment dynamics, although might disturb the aeolian transport of dune sand. The footpath is only reached by swash runup in exceptional conditions, and its elevation provides limited effect on aeolian sand transport.

3.3. Methods

The fieldwork campaign took place on the 30th and 31st January 2006 (spring tidal ranges of 3.2 m and 3.4 m, respectively). Data collected and analyzed included, FT data, grain-size data, morphological data and driving mechanisms data (wind and currents).

3.3.1. Fluorescent Tracer data

The preparation of the fluorescent tracer (FT) followed the methodology described by Ciavola et al. (1997a). The tracer material consisted of native sand from the two morphologies collected before fieldwork. The sand was washed, dried and marked in a mixer using orange fluorescent paint. Subsequently, the sand was dried and sieved to remove coarser aggregates. Preparatory tests of sediment mobility involving natural tracers, namely heavy minerals, were undertaken before the field experiment, to attest the adequate portion of tracer to be injected. In agreement with the low rates of transport

reported in literature for fetch-limited beaches (e.g., Nordstrom, 1992), sediment was barely transported.

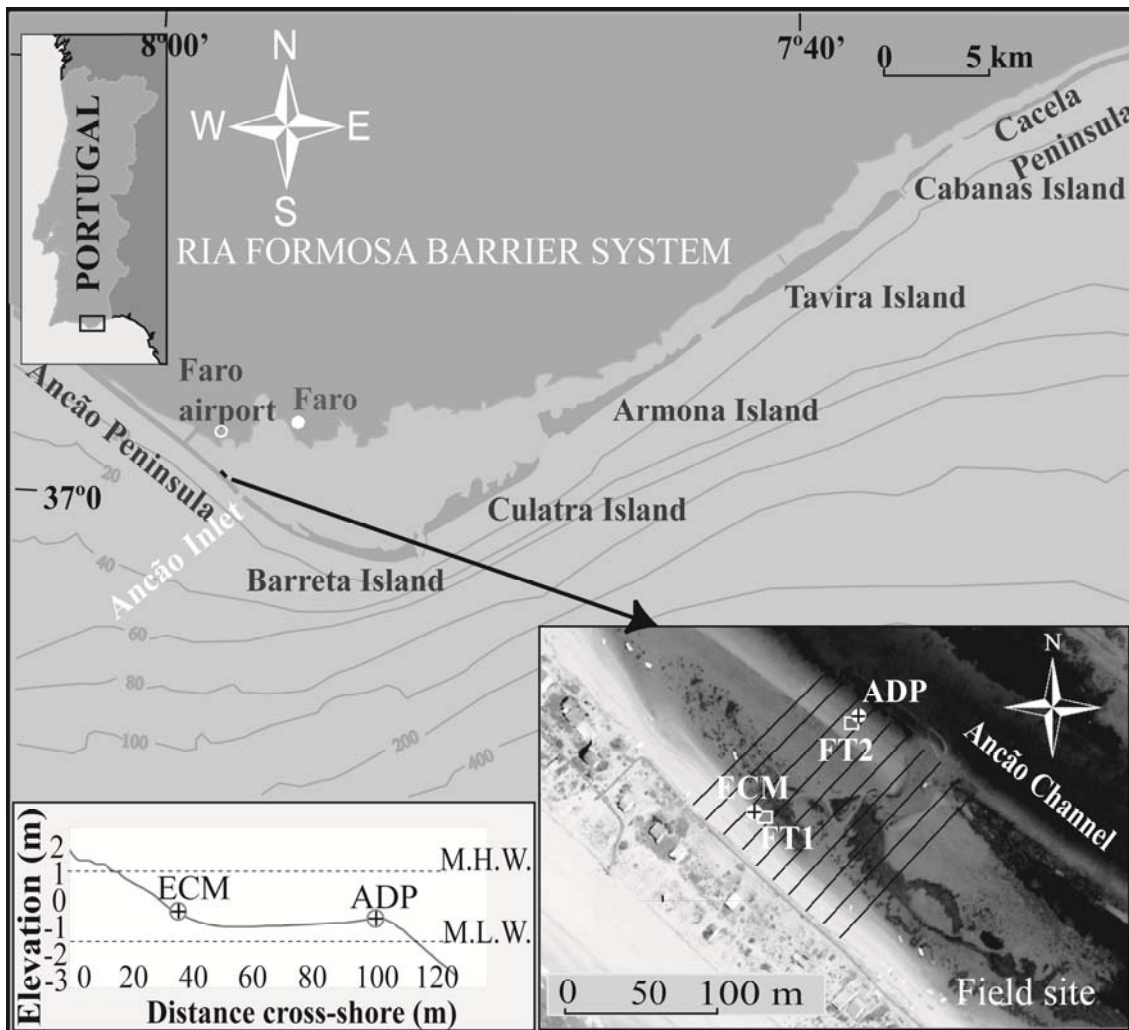


Figure 3.1. Field site location, showing Ancão Peninsula backbarrier, and (inset) a vertical aerial photograph (taken in 2007) with the surveyed profiles and a representative beach profile (M.H.W. = mean high water and M.L.W. = mean low water, based on field data) with instrument position (ECM = electromagnetic current meter, ADP = acoustic Doppler profiler); FT1 and FT2 (fluorescent tracers), deployed during fieldwork are also shown.

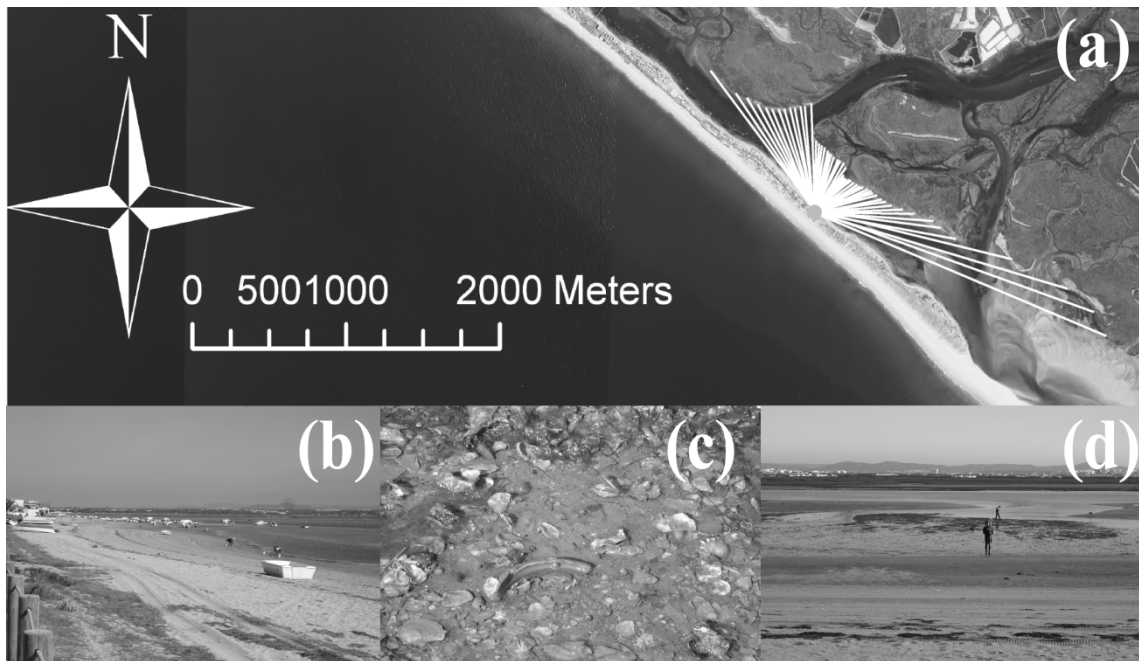


Figure 3.2. Photographs of the field site: (a) fetch distribution on a vertical aerial photograph from 2007; (b) view to NW of the narrow sandy foreshore (July 2007); (c) high shell content in muddy sediments on the tidal flat (October 2006); and (d) from offshore, Ancão tidal channel, offshore sand bank (with shore-normal depression) and tidal flat (January 2006).

Therefore, it was decided to release 200 g of FT, which was found to be adequate to describe local sediment displacement within the time-frame of the expected experiment duration. After washing up with detergent to avoid grain floating, tracer was spread during low tide on the bed along small rectangles, one at the beach face and one at the sand bank (Figure 3.2). FT grains were recovered after two-tidal cycles (~24 h). FT sampling grids (2-dimensional) were established on the basis of grain detection, under a closed device with ultraviolet (UV light). Those sampling grids were marked from the injection point, covering the entire tracer's dispersion cloud. Sampling grid had

20×20 cm spacing over the beach face and on the sand bank. FT grains were counted in laboratory under UV light and the obtained number was extrapolated to the representative area (50×50 cm). The Sampling Integration Method (SIM; Madsen, 1987) was employed to calculate the location (Y) of tracer distribution mass centre,

$$Y = \sum M_i d_i / \sum M_i \quad (3.1)$$

where M_i is the mass of tracers recovered at a sampling point, and d_i is the distance from the injection point. The M_i is obtained by the product of the number of recovered grains at each point of the grid and the average grain mass (obtained using mean grain-size values and assuming only quartz grains). Using the FT, the sediment transport rate, Q ($\text{m}^3 \text{s}^{-1}$), can be computed by

$$Q = N_0 U Z_0 w \quad (3.2)$$

where N_0 is the concentration of sand within the bed (0.60 as suggested by White, 1998, considering a porosity of 40% for medium sands); U is the velocity of the FT mass centroid considering the tide immersion time, Z_0 is the thickness of the moving layer (3.5 mm). Z_0 was measured in the field by digging small trenches on the sampling sites and measuring the tracer depth. Q is provided to the overall beach width (w) of ~150 m.

3.3.2. Grain-size data

Surficial sediment samples were collected in the beginning of fieldwork on the beach face and sand bank. Traditional laboratory dry sieving procedures for unconsolidated clastic sediments were used for the coarse fraction. The pipette method was used for the fine fraction. After sieving the samples at 0.5 phi intervals, grain-size parameters were obtained following Folk and Ward (1957) method, using GRADISTAT (Blott and Pye,

2001). Values of d_{mean} , d_{50} (median) and d_{10} (limit of 10% finer population) were computed.

3.3.3. Morphological data

Beach surveys were performed with a Total Station during low tides. Ten cross-shore profiles with 10 m spacing (Figure 3.1) were undertaken at the beginning and end of fieldwork. A digital terrain model (DTM) was generated, and volume computations were made based on surfaces comparison. Volume computations errors include equipment error (maximum vertical error of ± 0.003 m, quoted by the manufacturer), fieldwork operational errors (mean horizontal error of 0.01 ± 0.07 m, and mean vertical error of ± 0.002 m, based on test surveys) and surface interpolation method errors (maximum deviation of 12% between tested interpolation methods).

3.3.4. Driving mechanisms data

Wind data were obtained from the nearby wind station of Faro airport (Figure 3.1) (Weather Underground, 2006). Prevailing directions and average speeds were determined (data recorded every 30 min). Visual estimates of wave period and wave height (using a marked ruler) were made at the beach face. Currents were obtained with a bidirectional electromagnetic current meter (ECM, model 802) and with an acoustic Doppler profiler (ADP, Nortek AS Aquadopp, 1MHz). The first was located at the beach face (~ 0.13 m above the bed, shoreline oriented), and the second at the sand bank (~ 0.16 m above the bed, data logged in respect to magnetic North). The ECM time

series have some data gaps because of equipment malfunction (about 1 h, 20 min, during high tide for the first tidal cycle, and about 3 h during high tide at the second tidal cycle). The ADP was deployed buried on a frame at the bottom, with a blanking distance of 0.7 m, and was set to run in burst mode (5 min bursts) from cells spaced each 0.5 m (up to five cells of measurement, during high-tide slack). For both current meters, time average values were determined for cross-shore and longshore components. For ECM, the time averaged velocities represent a near-bed velocity (one single point of measurement), whereas for ADP, the time average velocities were taken at different levels of the water column. For both current sampling locations, velocity profiles were reconstructed from the bed to the surface following the power law profile (Soulsby and Humphery, 1990). Depth-average velocity is derived from the measured velocities by

$$U(z) = (z/0.32h)^{1/7} \bar{U} \quad (3.3)$$

where z is the height above sea floor for each cell, $U(z)$ is the current speed at height z , \bar{U} is the depth-averaged current speed and h is the water depth of each cell. Although authors recognise some method limitations, profile reconstruction can be used to approach the near bed velocity in the study area, where the superimposition of waves onto the tidal current is small and no bedforms are present.

Time-average shear velocity (\bar{u}^*) was estimated following a linear regression of $u(z)$ on $\ln(z)$, as proposed by Soulsby (1997)

$$\bar{u}^* = mk \quad (3.4)$$

where m is the gradient of the regression line and k is the von Karman's constant (= 0.4). Based on grain-size parameters, the thresholds of bed load transport were

calculated for the tagged sand population of both analysed morphologies (beach face and sand bank). The threshold of bed load transport was determined for d_{10} ($u_{cr}d_{10}$) and d_{50} ($u_{cr}d_{50}$) populations. These thresholds (u_{cr}) were compared with \bar{u}^* in order to evaluate which component of the sediment population is carried by the flow. This theoretical approach was analysed and compared with the tracer displacement pattern. The value of u_{cr} was obtained by using its relationship with the critical shear stress

(τ_{cr}),

$$\tau_{cr} = \rho u_{cr}^2 \quad (3.5)$$

The parameter τ_{cr} is associated with the sediment size, through the critical Shields parameter (θ_{cr}) by,

$$\tau_{cr} = \theta_{cr}(\rho_s - \rho)d \quad (3.6)$$

where θ_{cr} depends on the dimensionless form of the bed shear-stress (D_*)

$$\theta_{cr} = [0.30/(1 + 1.2D_*)] + 0.055[1 - \exp(-0.02D_*)] \quad (3.7)$$

$$D_* = [g(s - 1)/\nu^2]^{1/3} d \quad (3.8)$$

where g is the acceleration due to gravity (9.81 m s^{-2}), s the ratio of densities of grain ($\rho_s = 2650 \text{ kg m}^{-3}$) and water ($\rho = 1027 \text{ kg m}^{-3}$), ν is the kinematic viscosity of water ($1.36 \times 10^{-6} \text{ m}^2 \text{ s}^{-1}$), and d is the sediment grain size (in meters).

3.4. Results

3.4.1. Grain-size characteristics and tracer transport

The beach face is composed of coarse sand, whereas sediments from the sand bank are slightly finer and poorly sorted (Table 3.1). Tagging was found to have some effect in the native sand population of the beach face, leading to coarser, tagged grains (Table 3.1). This effect is a consequence of paint adhesion over the grains and generation of grain aggregates. The small amount of tracer release was not limitative for both cross-shore and alongshore tracer transport; the tracer displacement was in the order of a few centimetres (Table 3.2). Despite the limited quantity of tracer that was deployed, the small amount that still remained undisturbed at the injection point sampling grid assured the total tracer recovery (Figure 3.3). Therefore, FT distribution pattern and sediment transport are valid and representative of local field conditions. Tracer displacement around the injection points and small transport distances indicate the coexistence of tracer dispersion and transport by advection over a preferential direction (Figure 3.3). Both FT contours and FT mass-centroid displacement indicate that longshore orientated sediment transport is greater than the cross-shore transport at both morphologies (Figures 3.3a and b). Net alongshore sediment transport is directed towards SE (towards Ancão Inlet). Longshore components of the centroid velocity (U_x) are slightly higher than cross-shore components (U_y) (Table 3.2). Both morphologies present FT displacement velocities of similar magnitude. The sand bank FT has a faster longshore centroid velocity (0.07 m d^{-1}) and a higher overall sediment transport rate than the beach face (Table 3.2).

Table 3.1. Grain-size parameters. FT = fluorescent tracers, d_{50} = median, d_{10} = limit of 10% of the finer population.

Sample	Mean (mm)/classification	Sorting (mm)/ classification	d_{10} (mm)	d_{50} (mm)
Beach face	0.94 (coarse sand)	1.80 (moderately sorted)	0.42	0.99
Beach face (FT)	1.15 (very coarse sand)	1.43 (moderately well sorted)	0.73	1.17
Sand bank	0.38 (medium sand)	2.19 (poorly sorted)	0.13	0.41
Sand bank (FT)	0.37 (medium sand)	1.91 (moderately sorted)	0.16	0.38

Table 3.2. Fluorescent tracer transport velocities and volumetric transport (Q). U_x = the velocity in the longshore direction, U_y = the velocity in the cross-shore direction.

Tracer experiment	Centroid velocity ($m d^{-1}$)		Q ($m^3 d^{-1}$)
	U_x	U_y	
Beach face	0.05	0.04	0.02
Sand bank	0.07	0.06	0.03

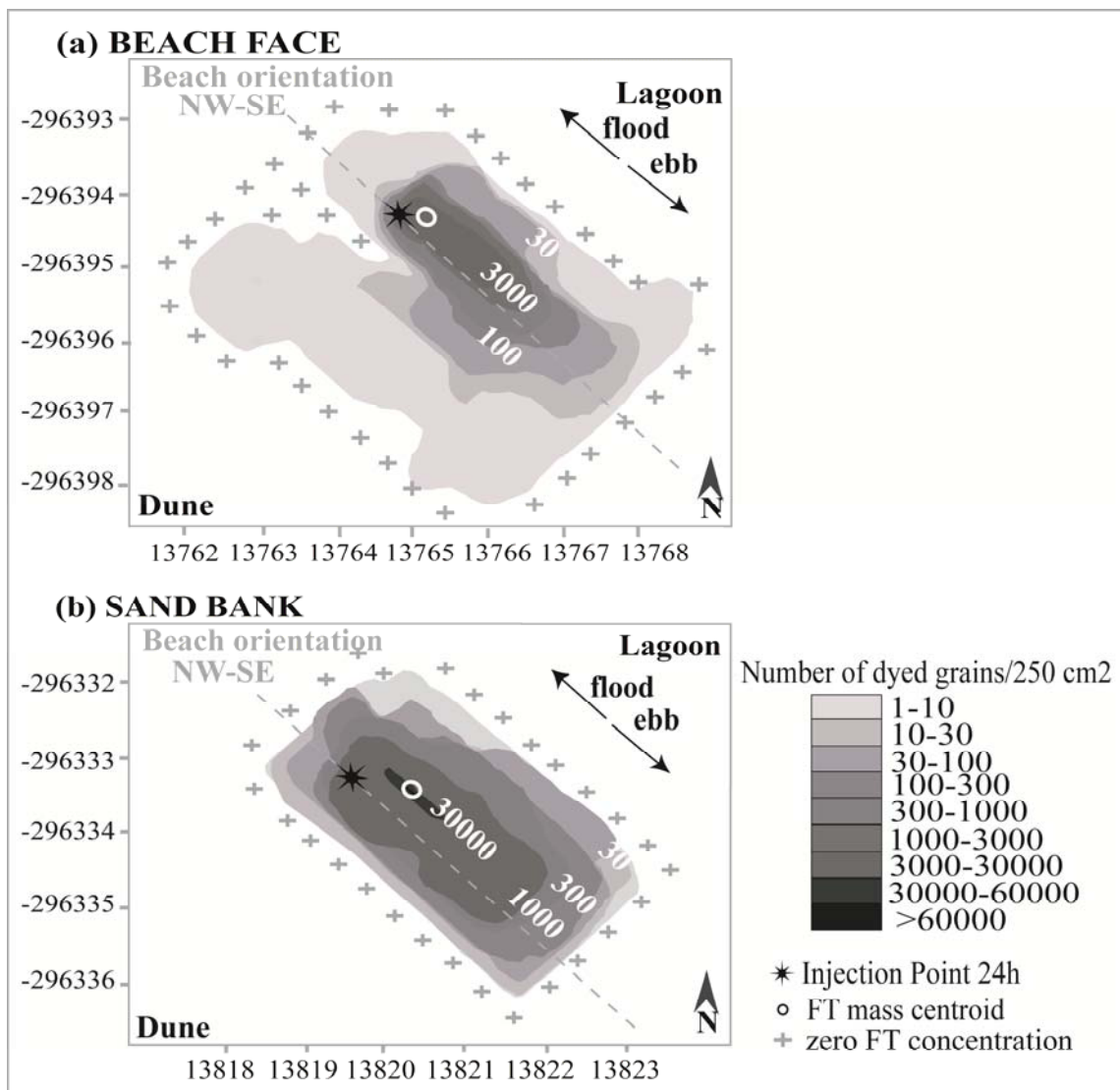


Figure 3.3. Map of tracer concentration at (a) beach face, and (b) sand bank, 24 h after tracer release. Locations of injection points and fluorescent tracers (FT) mass centroids are shown (metric coordinates refer to Portuguese Melriça Grid, datum 73).

3.4.2. Morphological variability

Morphological changes that occurred during the experiment induced a total volumetric change of about $-0.03 \text{ m}^3 \text{ m}^{-2}$ throughout the surveyed area. Changes are globally small, below the 20 cm, with no evident volumetric tendency (Figure 3.4). Erosion is

commonly observed in the lower part of the profile, closest to Ancão tidal channel, while the beach face presents slight tendency toward accretion (Figure 3.4).

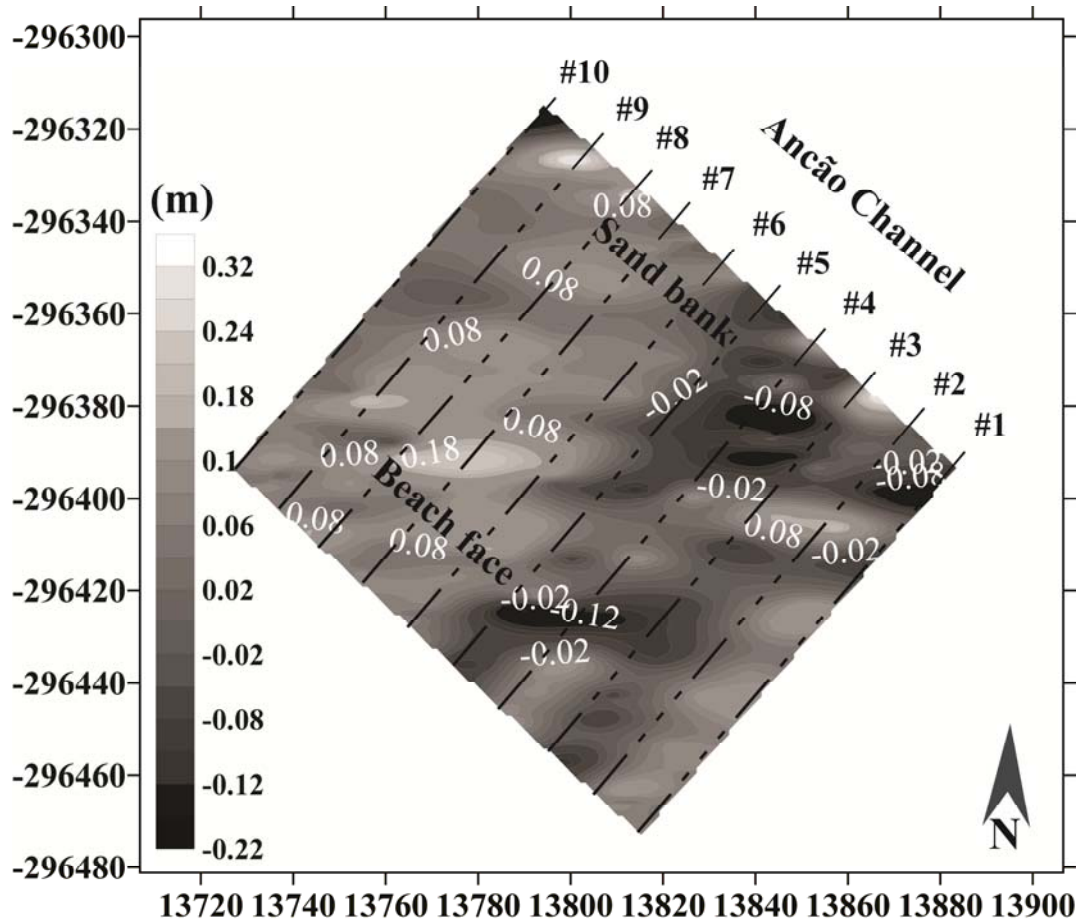


Figure 3.4. Surface variations between surveys represented as a contour map of isopachs. The numbers (#n) are the topographic profile number. Metric coordinates refer to the Portuguese Melriça Grid, datum 73 (referenced to mean sea level).

3.4.3. Driving mechanisms

Prevailing wind conditions during the field experiments were north to northwest with some episodes of north to northeast winds (Figure 3.5a). Mean wind intensity were

about 3 m s^{-1} with a maximum of 6.3 m s^{-1} from the north to northwest. Dominant, low-wind intensities, in association with a reduced lagoon fetch (tens to hundreds of meters; Figure 3.1), drove small height waves ($H_{\text{mean}} = 5 \text{ cm}$, $H_{\text{max}} = 10 \text{ cm}$, and $T_{\text{mean}} < 1 \text{ s}$), with a very limited competence for sediment transport. An example of the cross-shore wave-induced currents can be observed with the plot of the first minutes of the ECM cross-shore instantaneous velocity record, where the velocity peaks might suggest the influence of breaking waves (Figure 3.6). As observed, the instantaneous velocities are generally below 10 cm s^{-1} . Results from the time-average flow velocities show a dominance of the longshore-oriented component over the cross-shore component at both morphologies (Figures 3.5b and c). Maximums of cross-shore time-average velocity at the sand bank are close to 25 cm s^{-1} , occurring during the first tide cycle (Figure 3.5c). At the beach face, maximums of cross-shore time-average velocity are lower, about 6 cm s^{-1} , also during first tide cycle (Figure 3.5b). The ECM denotes equipment malfunction during both tidal cycles, which restricts the degree of discussion based on this equipment.

Currents are stronger at the sand bank, which is closer to the Ancão tidal channel, with maximums of the longshore component close to 50 cm s^{-1} (Figure 3.5c). There is a dominance of the ebb flow (SE/NE), as revealed by higher average velocities during ebb (Table 3.3). On average, \bar{u}^* is higher at the sand bank than at the beach face (Figure 3.7), maximum \bar{u}^* velocities are close to 0.032 m s^{-1} on the beach, while on the sand bank 0.07 m s^{-1} can be reached.

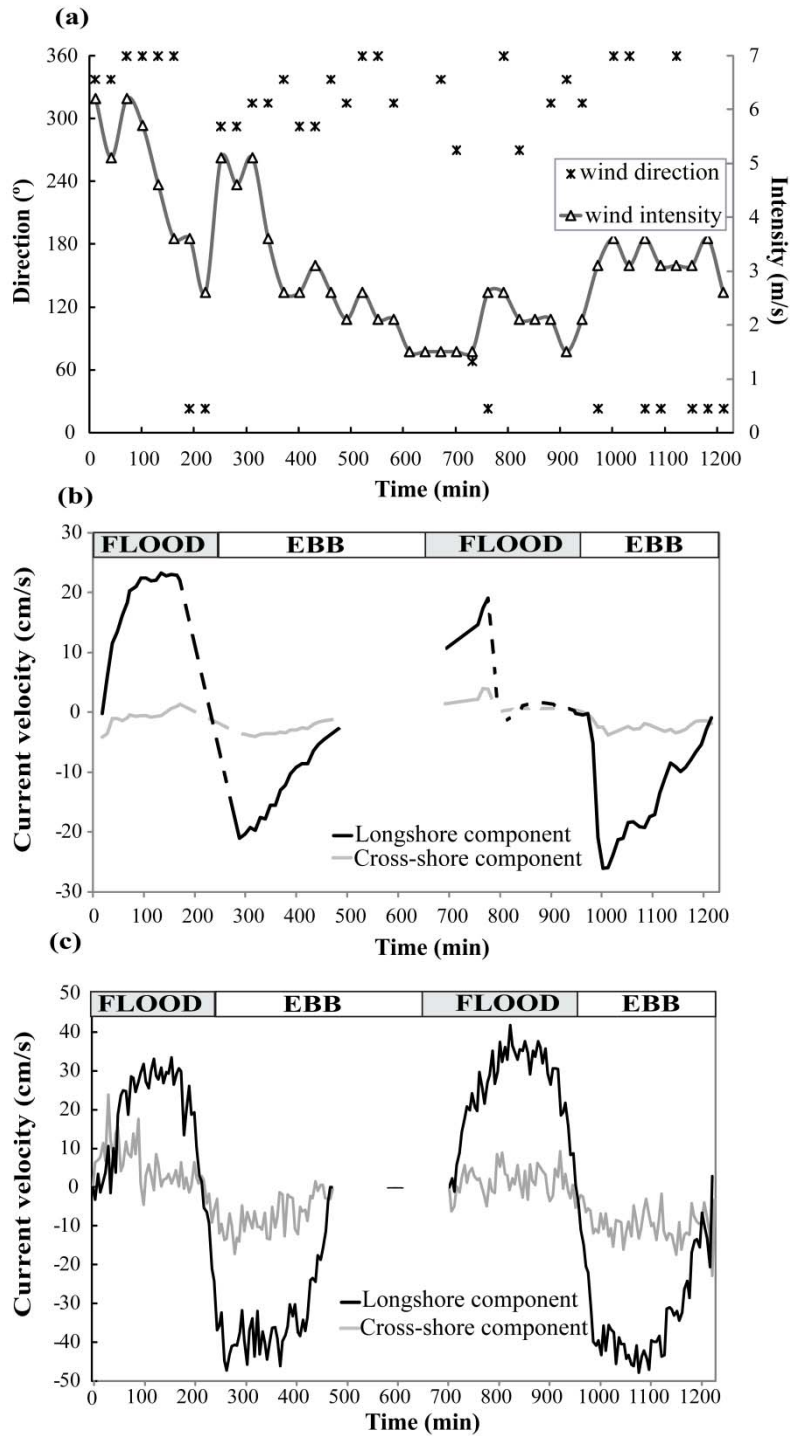


Figure 3.5. Driving mechanisms observed during fieldwork: (a) time-average wind intensity and direction; (b) time-average current velocity at the beach face; and (c) time-average velocity at the sand sand bank. The dashed lines in (b) represent electromagnetic current meter (ECM) data gaps due to equipment malfunction.

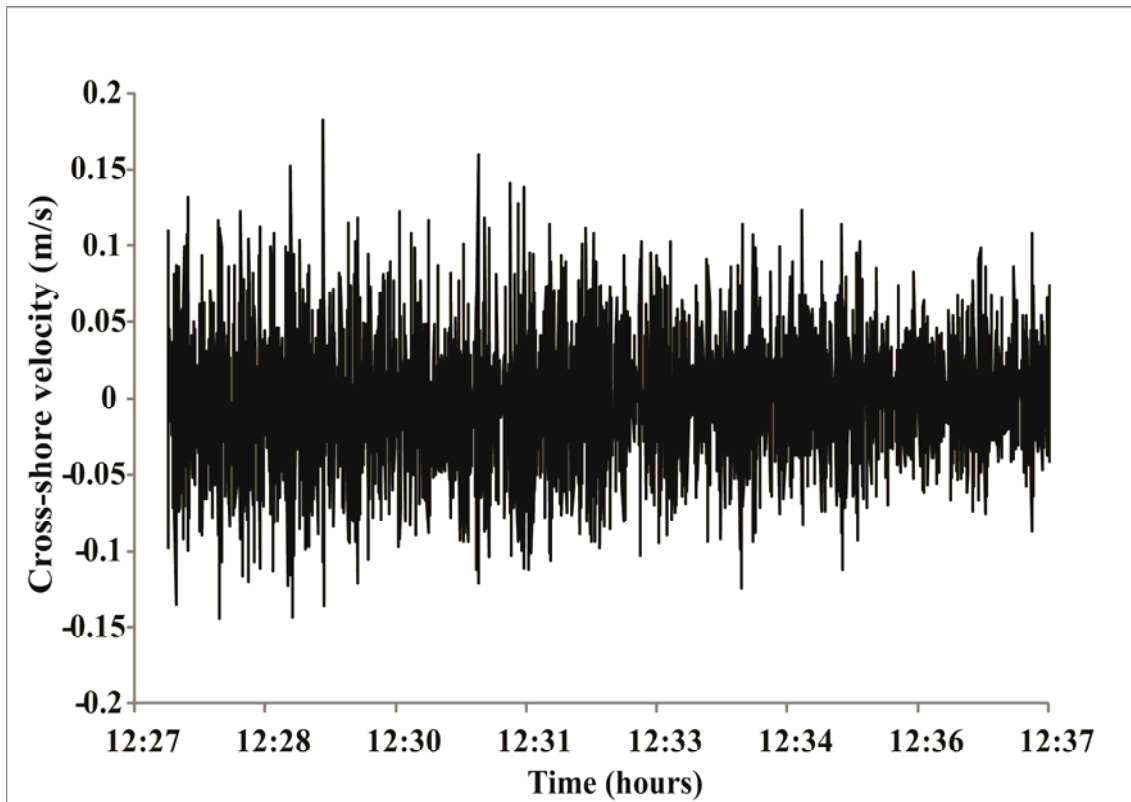


Figure 3.6. Cross-shore velocity component for the first 10 min of data recorded by the electromagnetic current meter (ECM; ~10 cm of water depth above the current meter).

At the beach face, \bar{u}^* represents a near bed velocity (single point of measurement), while at the sand bank, \bar{u}^* represents an approximation through the water column. Calculated u_{cr} at the beach face was higher (both for d_{10} and d_{50} populations) than at the sand bank (Table 3.3 and Figure 3.7). According to estimated thresholds, there is an absence of transport at the beach face for the analysed sediment populations (Figure 3.7a). In contrast, at the sand bank, both sediment populations, d_{10} and d_{50} , can be displaced during about one-half of the tidal cycle. At the sand bank, slender preferential sediment transport occurs during ebb tide (Figure 3.7b).

Table 3.3. Time-averaged flow conditions during field experiments and thresholds for bedload transport (u_{cr}) at each morphology. Negative longshore velocity means S-E (ebb) and negative cross-shore velocity means N-E (towards the Ancão tidal channel). $u_{crd_{10}}$ and $u_{crd_{50}}$ are determined for tagged population.

Morphology	Tide	Time of Exposure (min)	Longshore Velocity ($m s^{-1}$)	Cross-Shore velocity ($m s^{-1}$)	$u_{crd_{10}}$ ($m s^{-1}$)	$u_{crd_{50}}$ ($m s^{-1}$)
Beach face	Flood	243	0.11	0.00	$u_{cr} = 0.006$	$u_r = 0.008$
	Ebb	222	-0.13	-0.03		
Sand bank	Flood	230	0.20	0.02	$u_{cr} = 0.004$	$u_{cr} = 0.005$
	Ebb	240	-0.34	-0.06		

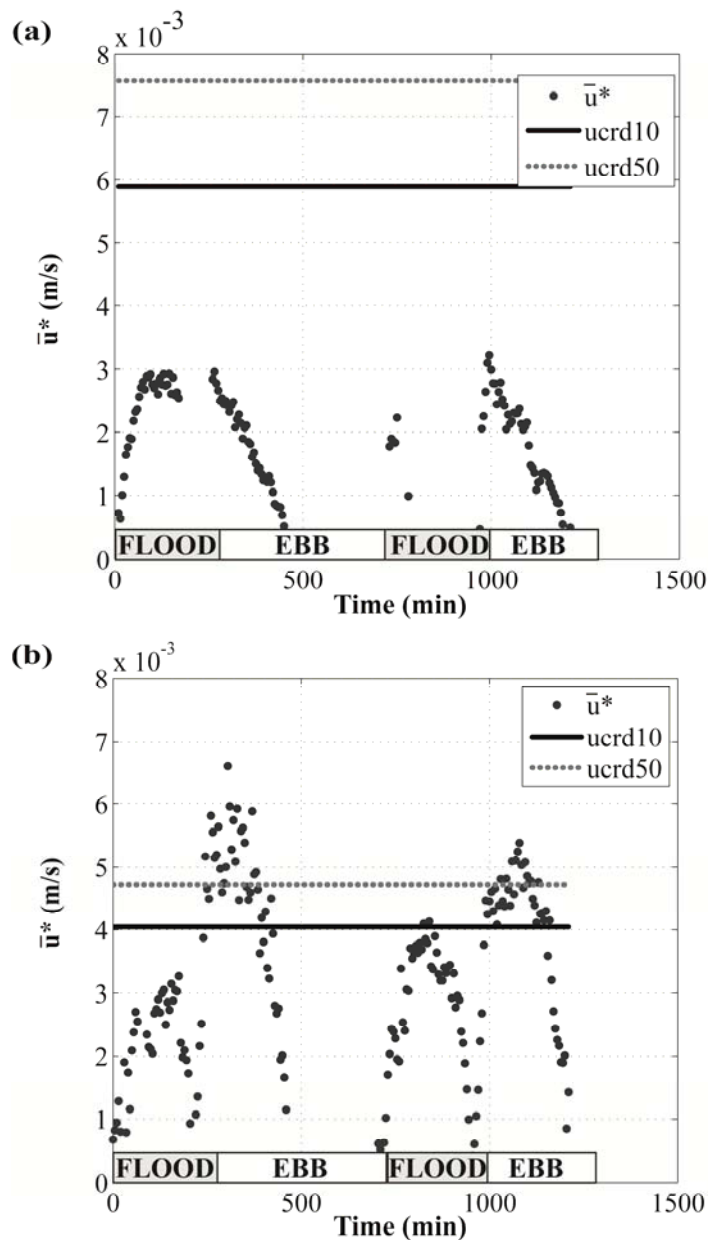


Figure 3.7. Time-averaged shear velocity (\bar{u}^*) and critical shear velocity (u_{cr}) considering d_{10} (u_{crd10}) and d_{50} (u_{crd50}) at (a) the beach face, and (b) the sand bank.

3.5. Discussion

Low rates of sediment transport were recorded during fieldwork, with low FT displacements (Figure 3.3). Relatively higher rates of tracer displacement were observed

at the sand bank ($0.03 \text{ m}^3 \text{ d}^{-1}$; Table 3.2) as a consequence of higher current velocities (Figures 3.5c and 3.7b), and smaller grain size (Table 3.1). The analysis of time-average shear velocity vs. critical shear velocity (Figure 3.7) also indicates a higher potential for sediment transport at the sand bank. At several occasions of the fieldwork duration, currents at the sand bank could displace grains until mean grain-size (Figure 3.7b), whereas \bar{u}^* results for the beach face were lower than required to transport the tagged grain population (u_{cr} , Figure 3.7a). Some dispersion of tagged grains was noticed on the beach face (Figure 3.3a), which implies that at a certain moment in the experiment duration, the thresholds for sediment entrainment were overcome. The velocity profile close to bottom is derived from an approximation of the logarithmic profile, and thus, a small uncertainty might be associated with that approximation. Although computed time-average shear velocities seem not able to induce important sediment transport (Figure 3.7a), instantaneous peak velocities may be responsible for sediment movement. Moreover, the determined threshold (u_{cr}) is affected by the coarsening induced by dyeing of sand (beach face, Table 3.1), and u_{cr} may be overestimated in relation to indigenous material.

Tracer pattern and mass centroid position indicate that transport in the longshore direction is greater than cross-shore transport (Figure 3.3), which implies relatively small sediment exchanges between the morphologies, beach face and sand bank, and confirms the results of Carrasco et al. (2009). Thus, in contrast to the dominant cross-shore transfers proposed in models dedicated to storm response (Nordstrom, 1980; Nordstrom and Jackson, 1992), this study reveals the dominance of transport in the longshore direction for fair-weather conditions. The very limited onshore–offshore transport redistribution observed with the tracer cross-shore dispersion (especially at the

beach face; Figure 3.3a) might just be associated with currents induced by breaking waves (Figure 3.6).

Longshore-orientated transport results from essentially a higher velocity of the tidal-longshore velocity component (maximums of 20 cm s^{-1} and 50 cm s^{-1} on the beach face and sand bank, respectively; Figures 3.5b and c). Moreover, the main wind direction is alongshore (north to northwest; Figure 3.5a), and wind-induced currents might have powered the longshore orientated transport through the field site (NW–SE oriented; Figure 3.1).

The tidal currents become the major agent of transport at the beach in the present hydrodynamic conditions, and even with low rates, transport should be regular because the tidal currents are unremittingly reworking the backbarrier. There is no clear difference between the durations of the ebb and flood (Table 3.3), but measured velocities are not identical in magnitude (Figures 3.5b and c). Recorded ebb currents are stronger than flood currents, e.g., for the sand bank, maximum flood velocities are close to 40 cm s^{-1} , and maximum ebb velocities are almost 50 cm s^{-1} (Figure 3.5c). Ancão Inlet ebb dominance, associated to stronger ebb currents, was previously attested to by Salles et al. (2005) and by Pacheco et al. (2010). Unequal ebb–flood is caused by tidal-wave distortion during the propagation into shoaling water and is a dominant factor in causing residual sediment transport and morphological changes in estuaries (favours seaward displacement, Friedrichs and Aubrey, 1988; Salles, et al., 2005; Moore et al., 2009). The asymmetrical pattern of the time-average velocity variation (Figure 3.7b) suggests preferential sediment transport during ebb conditions, which is in agreement with the ebb-dominant transport computed for Ancão Inlet (Salles, 2001; Salles et al., 2005; Dias et al., 2009).

Higher-velocity currents are generally observed in locations closer to inlets, and rates and directions of sediment displacement are controlled by the local tidal regime. Inlet influence is attenuated with distance, and therefore, the sediment-transport patterns observed at the field site may differ from those operating at other sites along the backbarrier (Carrasco et al., 2008). In the Ria Formosa backbarrier system, changes in inlet position, either natural in origin (migration cycles; Vila-Concejo et al., 2006) or artificial (such as the inlet relocation in June 1997; Vila-Concejo et al., 2004b), have modified hydrodynamic conditions and consequent sediment supply (Carrasco et al., 2008). Therefore, local rates and patterns of sediment displacement will vary according to the changing inlet hydrodynamics (e.g., changes in flood–ebb dominance). The magnitude and direction of the sediment transport may also change, for example, with fluctuations in the tidal cycle (Jackson et al., 1999) or with alterations in the frequency of high-energy events. Transport measurements during equinoctial spring tides (deeper water columns and faster tidal currents) and storm conditions (increased wind speed and wave height), could provide different transport magnitudes. The morphodynamic response is foreseen to be slow, and extremely dependent on the variability of the inherent forcing factors (Nordstrom, 1980; 1992). Therefore, a main issue in fetch-limited environmental studies is still to thoroughly define the ordinary conditions that set the background settings, as was performed in this study. The definition of sediment transport for nonstorm, regular tidal conditions is essential to fully understanding the types of responses under other, more energetic conditions.

Recorded conditions are representative of typical fair-weather conditions, anticipating extremely low rates of transport, when compared with rates at the beach on the oceanside. Vila-Concejo et al. (2004a), measured $950 \text{ m}^3 \text{ tide}^{-1}$ for the Ancão oceanic beach (about 1 km SE of the study area), during calm–moderate, winter, SW

conditions. On the other hand, the Ancão backbarrier beach has low transport rates, on the order of $7 \text{ m}^3 \text{ yr}^{-1}$ extrapolated for the beach face and $11 \text{ m}^3 \text{ yr}^{-1}$ for the sand bank. These rates are even lower than the transport-rate interval compiled by Nordstrom (1992) for estuaries ($30 \text{ m}^3 \text{ yr}^{-1}$ to $14,000 \text{ m}^3 \text{ yr}^{-1}$). This implies that the study area is not only a low-energy beach when compared with the oceanic beach but also is in the lower-energy spectrum of fetch-limited environments, which have almost no wave action and clear tidal-current dominance.

3.6. Conclusions

The morphodynamic behaviour of fetch-limited beaches is generally slow and continuous. Sediment-transport studies are useful tools for determining sediment budgets and, therefore, important in the definition of local management policies. The present work encompasses the definition of patterns of sediment displacement at a backbarrier beach following the application of fluorescent tracer methods. The outcomes of this case study defined the beach's typical morphological changes, its grain size, and its sediment transport, as well as its tidal currents and wind regime under fair-weather conditions. Results obtained from the application of fluorescent tracer and from the current analysis reveal that sediment transport is mainly driven by ebb tidal currents. Moreover, a direct relationship between the patterns of transport and inlet influence is suggested. In other, more energetic conditions, wave action may also play an important role in sediment transport. The obtained results are useful for the discussion about morphodynamic behaviour of low-energy bay beaches, particularly those adjacent to tidal channels. Given the lack of data concerning sediment transport in low-energy

beaches, the quantification of the sediment transport within the present study may provide new insights into such environments.

CHAPTER 4

**SEDIMENT TRANSPORT
MEASUREMENTS WITH TRACERS IN
VERY LOW-ENERGY BEACHES**

Abstract

This study investigates sediment transport at a very low-energy backbarrier beach in southern Portugal, by using fluorescent tracer techniques. Results herein reported points towards the distinction between tracer advection and tracer dispersion in this type of environment. Transport by advection was low (few decimetres per day) as consequence of the prevailing hydrodynamic conditions ($H_s < 0.1$ m, and maximum current velocity of 0.5 m s^{-1}), whereas dispersion was relatively high (few metres per day). Tracer techniques allow distinguishing the broad picture of transport, but revealed the need for improvement to correctly determine the transport rate at a daily scale.

Keywords: *sediment transport, backbarrier, fluorescent tracer.*

4.1. Introduction

The primary agents of sediment dynamics at fetch-limited beaches are waves, tidal currents, and wind-induced drift (Nordstrom, 1992; Jackson et al., 2002a). So far just a few datasets peruses sediment transport patterns in fetch-limited beaches (e.g., Sherman et al., 1994; Nordstrom et al., 2003), turning difficult to establish an immediate association between rates of change and the magnitude of the causative forcing factors. Furthermore, the ‘tradicional’ sediment transport techniques commonly applied on exposed coasts, have been barely tested in very low-energy conditions (low-wave conditions). Only few studies evaluated sediment transport or beach morphodynamics on estuarine beaches (e.g., Sherman et al., 1994; Nordstrom et al., 1996), and even less in backbarrier beaches. Most studies of longshore transport have been conducted on beaches with well developed and gently sloping surf zones, making results difficult to be apply to low-energy environments (Nordstrom et al., 2003).

There are several techniques to directly measure transport, as using sediment tracers, short-term impoundments, and streamer traps, all of which having advantages and drawbacks (Wang et al., 1998; Nordstrom et al., 2003). Sand tracers are frequently used to measure and detail longshore sediment transport (e.g., Ciavola et al., 1997a; Tonk and Masselink, 2005; Silva et al., 2007) being capable of producing integrated results by time (e.g., tide, fortnightly) and space (e.g., surf zone, intertidal area). The small dimensions and low wave energy characteristic of fetch-limited beaches facilitate a priori the use of tracers and enhance the accuracy of measurements in the upper part of the profile, even during strong onshore winds (Nordstrom et al., 2003). But farther tests in very low-energy conditions still needs to be conducted.

Previous results from Carrasco et al. (2011a) were inconclusive in what concerns to the long-term (over days) transport patterns at backbarriers facing low-wave conditions and in the neighbourhood of a tidal inlet. The obtained transport rates were small, and authors were not able to fully discriminate the circumstances of transport for more than one tidal cycle. The present study provides new insights on sediment transport at backbarriers, defining a continuum (daily) pace of change over a spring-to-neap tide cycle. The main research question to be addressed is how much sediment is actually expected to be transported at a very fetch-limited beach during fair-weather conditions, and if that can be easily determined with tracer techniques application.

4.2. Field site

The field measurements took place at Ancão Peninsula backbarrier, in the south of Portugal (Figure 4.1a). Tides in the area are semi-diurnal, average ranges are 2.8 m for spring tides and 1.3 m for neap tides, but maximum ranges of 3.5 m can be reached during equinoctial spring tides. Because is sheltered from oceanic waves (offshore H_s of 0.92 m; Costa et al., 2001), and not frequently exposed to high wind intensities, there is a dominance of fair-weather conditions at this location. With the exception of waves generated by exceptionally strong winds, predominant waves at the field site are small, in the order of a few centimetres in height (Carrasco et al., 2009) due to the limited fetch conditions (maximum 1500 m). Storm-conditions, derivate from storm winds prevail for just a few hours. The backbarrier beach is limited by Ancão tidal channel, which connects to Ancão Inlet about 2250 m to the southeast (Figure 4.1). Ancão Inlet is a small inlet with a cyclic eastward migration pattern (e.g., Vila et al., 1999; Vila-

Concejo et al., 2002), and exhibits an ebb-dominated behaviour (e.g., Andrade, 1990; Pacheco et al., 2010).

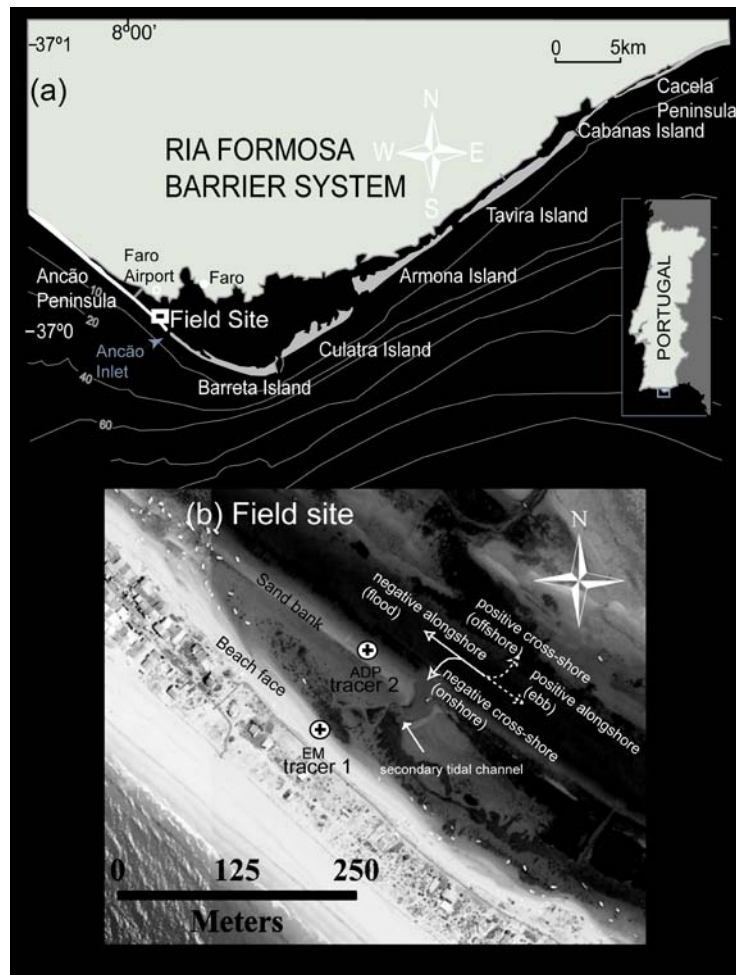


Figure 4.1. Field site location (a) at the Ancão Peninsula backbarrier (Ria Formosa barrier system), overlapped by the scheme of cross-shore and alongshore components at the field site (b); EM corresponds to the position of the current meter placed at the beach face and ADP corresponds to the position of the acoustic doppler profiler placed at the sand bank. Tracer1 and tracer2 represent the locations of fluorescent tracer injection points at the beach face and sand bank, respectively.

The field site extends alongshore over ~100 m and includes a low sandy beach composed of four different morphologies: backshore; beach face; tidal flat; and a detached sand bank (Figure 4.1b). The intermediate-steep beach face (~39 m wide) presents a very narrow swash zone during high tide. In contact with the foreshore, a tidal flat with a gentle slope is present (~44 m wide), ending in a small sand bank (30 m wide) parallel to Ancão channel. Both the tidal flat and sand bank show no bedforms and are cut off by a small oblique secondary tidal channel (Figure 4.1b), which promotes the rise and fall of the tide at the study area. The tidal flat dissipates wave energy during low tide and is mainly sandy with a high percentage of mud (< 63 μ m), and contains seagrass and accumulations of shells.

4.3. Methods

Sediment transport measurements took place from 20 to 27 March 2008, from a spring-to-neap tide period, during fair-weather conditions. Fluorescent tracer was deployed at the beach face and sand bank. The duration of tide immersion (in minutes) per day was determined for each beach segment, based on their topographic elevation and the predicted tidal levels. Currents were obtained with a portable single-axis electromagnetic current meter (EM) and a Doppler profiler (ADP, Aquadopp; Figure 4.1b). The EM was deployed at the beach face (~15 cm above the bed, current directed) and, in non-continuous mode, collecting data frames of 10-15 min each between 21 and 26 March, during the top half tidal cycles at the beach face. The ADP was deployed at the sand bank (0.21 m above the bed, oriented to magnetic North) and collected data from 20 to 27 March. The ADP ran in burst mode (5 min) with an initial blanking

distance of 0.7 m above the sensor (cell spacing of 0.5 m). Mean currents were determined for the lower ADP cell (lower point in the water column, for bedload conditions), for both cross-shore and longshore components.

Wind data were obtained from a nearby wind station, at the fronting Faro Airport (2 km from the field site, without obstacles in between, Figure 4.1; Weather Underground, 2008). Prevailing wind directions and average speeds (30 min observations) were determined. Wind waves were characterized using the morphodynamic modelling system MORSYS2D (see details in Fortunato and Oliveira, 2004; Bertin et al., 2009a). The circulation model ELCIRC used an unstructured grid covering the whole Ria Formosa (Bertin et al., 2009b, Dias et al., 2009) with a resolution ranging from 1000 m along its open boundary to 5 m at Ancão Inlet and at the studied beach. ELCIRC was forced offshore by the regional tidal model of Fortunato et al. (2002), and in the coastal zone by the gradient of wave radiation stresses computed from SWAN outputs using a Galerkin finite element method. Two regular grids were employed for the SWAN model: the first grid with a resolution of 500 m covered the whole Ria Formosa, and the second, nested in the first, had a 20 m resolution and covered the western part of the Ria Formosa. SWAN was forced offshore along its open boundary by time-series of wave spectra originated from the regional wave model of Dodet et al. (2010), and inside the domain by time series of wind measured at Faro Airport. SWAN was also driven by water elevations and current velocities originated from ELCIRC; hourly significant wave height (H_s) and mean wave period (T_{mean}) were determined for the beach face. Wind-waves modelled were validated against wind-wave observations at the study area using a simple marked rod.

Surface sediment samples were collected at the beginning of the fieldwork at both the beach face and the sand bank (along one profile). The usual grain-size parameters, including d_{50} (median) grain size, were obtained following the method of moments. The preparation of the fluorescent tracer followed the methodology described by Ciavola et al. (1997a). The tracer material consisted of native sand collected from the two beach segments (beach face and sand bank) one week before fieldwork. Results from previous experiments (Carrasco et al., 2011a) shown that local rates of transport are extremely low. Consequently, it was decided that placing small amounts of FT (less than 1 kg) would yield acceptable results. Three hundred and fifty grams of tracer were released at each location on 20 March 2008, and sampling was conducted at low tides during the following seven days, near the two tracer release points (tracer1 and tracer2, Figure 4.1b). Tracer sand detection was locally performed with ultraviolet (UV) light over two sampling grids (50×50 cm spacing). Samples were collected at the grid nodes, and tracer grains were counted in the laboratory under UV light. The Sampling Integration Method (SIM, Madsen, 1987) was employed to calculate the location (Y) of the mass centre of the tracer distribution:

$$Y = \sum M_i d_i / \sum M_i \quad (4.1)$$

Where M_i is the product of the number of recovered grains at each point of the grid and the average grain mass (obtained using mean grain size values and assuming only quartz grains), and d_i is the distance from the injection point. Fluorescent tracer is assumed to have a transport rate Q ($\text{m}^3 \text{s}^{-1}$), given by

$$Q = N_0 U Z_0 l \quad (4.2)$$

where N_0 is the concentration of sand within the bed (0.60 as suggested by White, 1998); U is the velocity of the tracer mass centroid considering the tide immersion duration; Z_0 is the thickness of the moving layer; and l is the daily immersed cross-shore length of each beach segment. Z_0 could not be quantified during fieldwork. Previous experiment from Carrasco et al. (2011a) demonstrated that for this type of beach the thickness of the moving layer is very shallow (in the order of millimetres), which difficult its measurement in situ. Thus, Z_0 was characterised based in two empirical approximations related with the two main local forcing factors: the recorded current data, by using the relationship developed by Bertin et al. (2007), and the predicted wave data, by using Sherman et al. (1994) approximation. The estimated Z_0 was of 0.010 m and 0.013 m for the Bertin et al. (2007) and Sherman et al. (1994; with $H_s = 0.06$ m) relationships, respectively. There is no significant difference between them and it was assumed for both segments $Z_0 = 0.01$ m. The net daily sediment transport was termed Q_{bf} for the beach face and Q_{sb} for the sand bank (estimated based on the daily position of the mass centroid). Besides Q , the cross (y) and alongshore (x) components were also determined (Q_{xbf} , Q_{ybf} , Q_{xsb} , and Q_{ysb} ; see orientation in Figure 4.1b).

4.4. Results

During the first few days of the tracer experiment maximum tidal range was 2.98 m, decreasing after 24 March (day 4 after release, Table 4.1). The beach face experienced a shorter duration of immersion than the sand bank, on account of its higher elevation (Table 4.1). Prevailing wind conditions were from the northwest (300-360°) with a few episodes of easterly winds between 20 and 21 March (Table 4.1). Wind intensities were on average close to 5 m s^{-1} with maximum velocities of about 12 m s^{-1} . The predicted

daily maximum H_s was 0.1 m, while the predicted daily T_{mean} ranged from 0.5 s to 1.0 s. Current velocities were higher at the sand bank than at the beach face (maximum of 0.55 m s^{-1} , Figure 4.2), and there was a dominance of the alongshore velocity component. Daily ebb current velocities at the sand bank were higher than flood current velocities, and the residual current was ebb directed (Table 4.1). At the beach face, current velocities were very similar for both ebb and flood, with a maximum of 0.26 m s^{-1} during the flood of 21 March (Table 4.1).

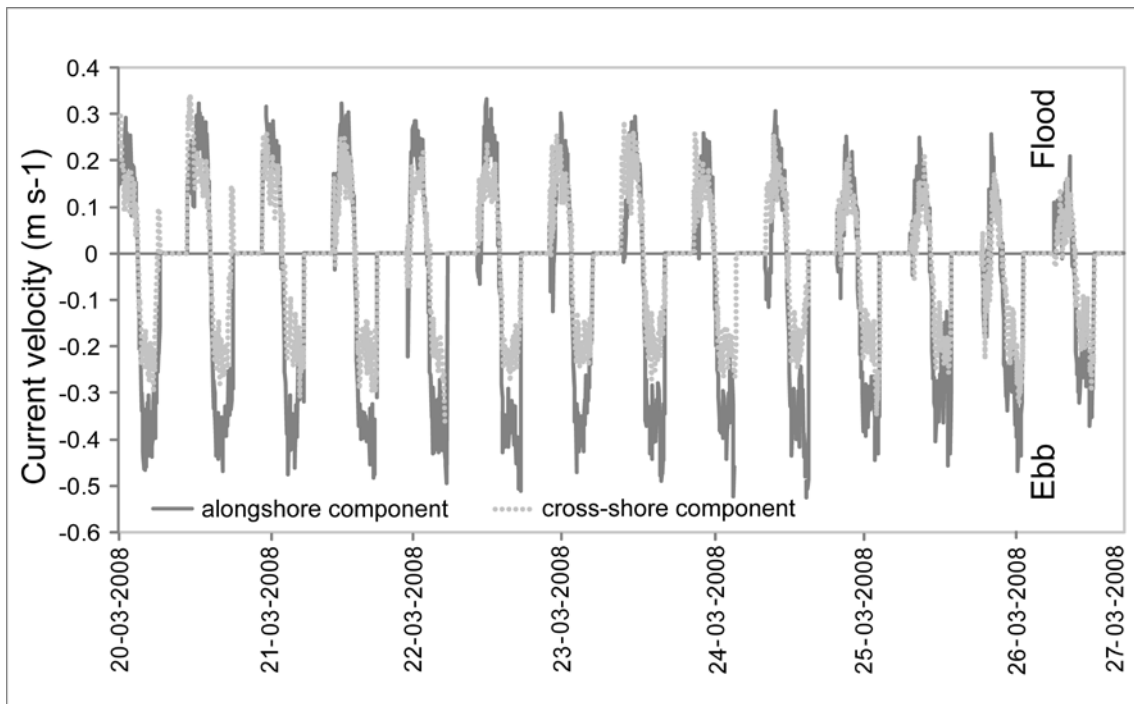


Figure 4.2. Time-averaged currents at the sand bank; data recorded at the lower cell of the equipment (0.7 m above the sensor). Positive alongshore values mean flood, and negative values mean ebb; positive cross-shore values mean offshore (directed towards the Ancão tidal channel) and negative values mean onshore.

The native beach face sediment (before tagging) was formed with coarse sand, whereas the sand bank was formed with medium sand. A small increase in grain size occurred after tagging: mean grain size at the beach face was 0.80 mm before tagging and 0.81 mm afterwards, and at the sand bank mean grain size varied from 0.44 mm to 0.62 mm. This effect is a consequence of paint adhesion over the grains and the generation of grain aggregates. Tracer application provided two distinct results: the overall tracer daily dispersion (isopleths, Figures 4.3 and 4.4) and the daily transport by advection (Table 4.2). Tracer isopleths reveal intense dispersion, mainly alongshore directed: at the beach face, the tracer showed a total alongshore dispersion of ~35 m and cross-shore dispersion of ~9 m (Figure 4.3), and at the sand bank, the tracer showed a total alongshore dispersion of ~28 m and cross-shore dispersion of ~9 m (Figure 4.4). Contrary to dispersion, transport by advection (Q) was small in magnitude (alongshore orientated; Table 4.2). Notwithstanding of being located in the same sandy stretch, the two beach segments operated in a different manner. Q_{bf} between day 1 and day 7 (20 and 26 of March) was about $-0.007 \text{ m}^3 \text{ week}^{-1}$ (flood-directed), whereas Q_{sb} was about $0.011 \text{ m}^3 \text{ week}^{-1}$ (ebb directed, Table 4.2).

Figure 4.5 displays the absolute cumulative transport (Q_{cum}) and daily Q at both locations from spring to neap tide. Q_{cum} increased from spring to neap tide, with higher transport rates during the first few days of fieldwork (spring tides, Table 4.1), while afterwards, transport rate increments reduced, tending towards zero (neap tides, Table 4.1 and Figure 4.5).

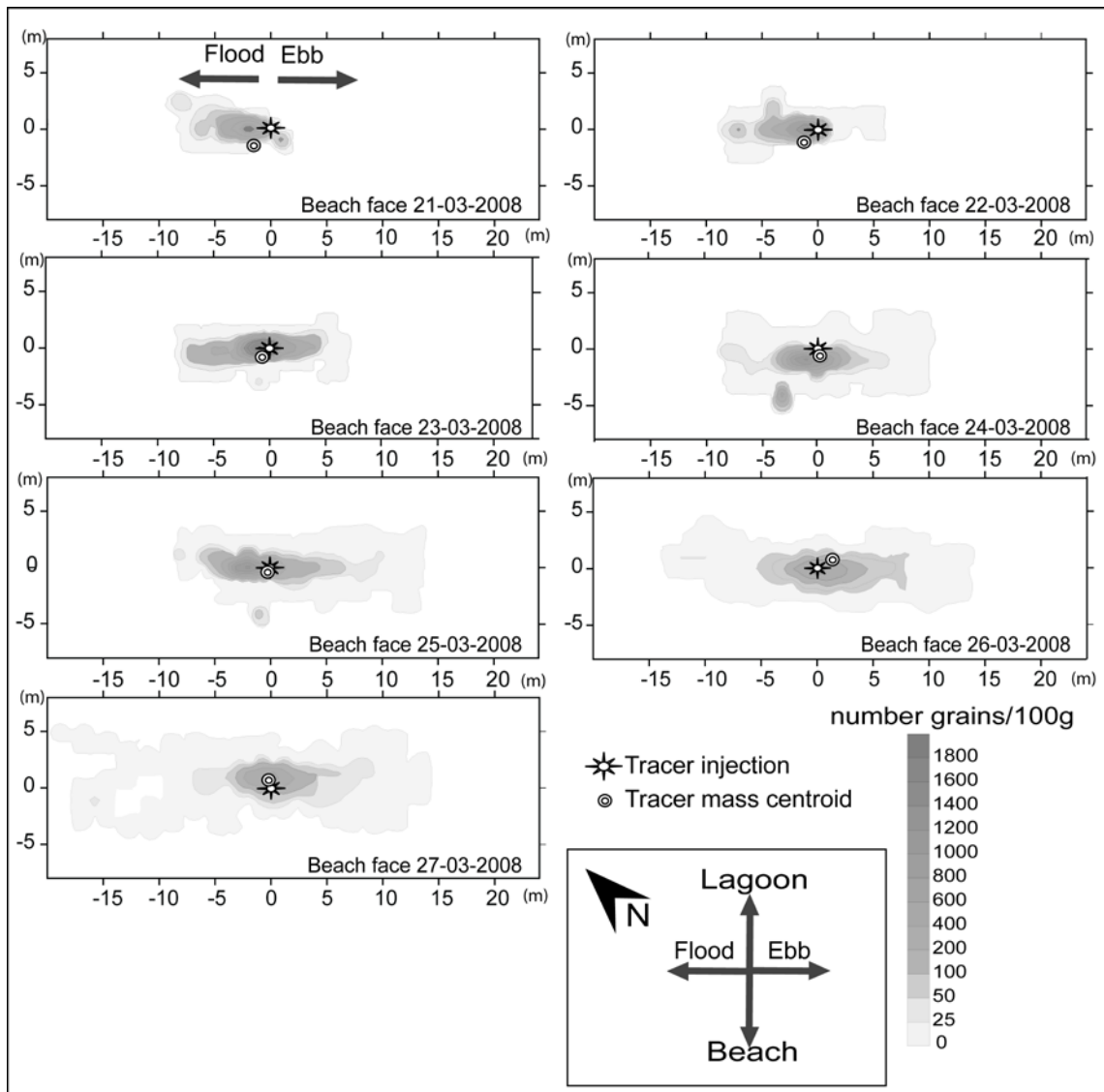


Figure 4.3. Map of tracer concentration at the beach face. Locations of injection points, tracer mass centroids, and number of tagged grains are shown (cross-shore and alongshore).

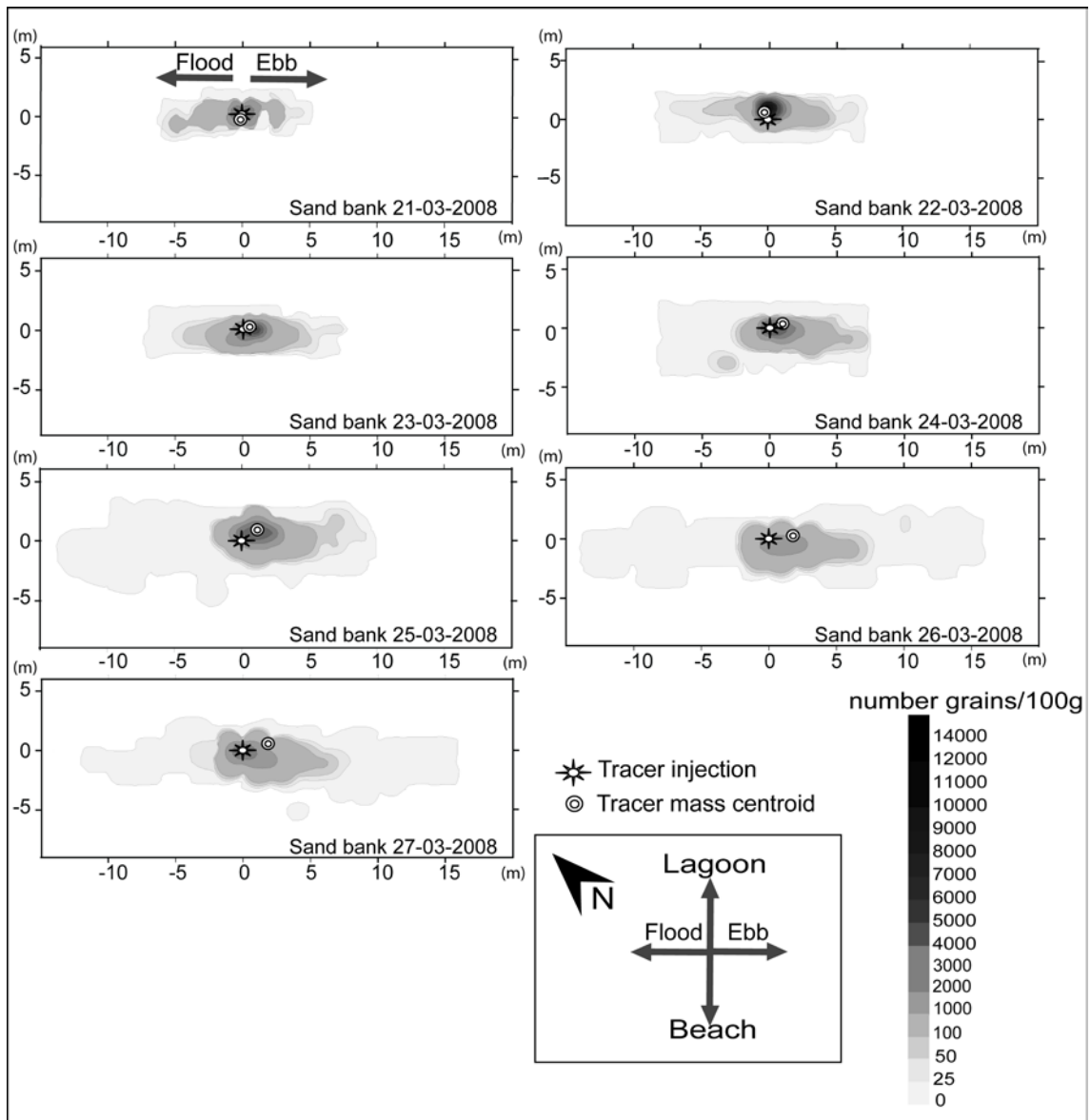


Figure 4.4. Map of tracer concentration at the sand bank. Locations of injection points, tracer mass centroids, and number of tagged grains are shown (cross-shore and alongshore).

Table 4.1. Tide, wind, waves, and currents during the fieldwork experiment.

Parameters	days after release of tracer						
	day 1 (20-03-2008)	day 2 (21-03-2008)	day 3 (22-03-2008)	day 4 (23-03-2008)	day 5 (24-03-2008)	day 6 (25-03-2008)	day 7 (26-03-2008)
Tidal range (m)	2.64	2.98	2.95	2.90	2.75	2.61	2.32
Wind direction(°)	75	250	305	325	323	308	298
Maximum intensity (m s ⁻¹)	8.2	9	12	6.7	7.7	8.2	8.7
Maximum H _s (m)	0.10	0.06	0.10	0.08	0.07	0.08	0.09
T _{mean} (s)	0.86	0.65	0.92	0.82	0.76	0.78	0.78
Mean wave approaching angle (°)	90	233	334	347	347	339	338
Mean current velocity at the sand bank (m s ⁻¹ , flood conditions)	-0.21	-0.23	-0.19	-0.21	-0.18	-0.13	-0.02
Mean current velocity at the sand bank (m s ⁻¹ , ebb conditions)	0.39	0.39	0.40	0.38	0.38	0.36	0.35
Mean current at the beach face (m s ⁻¹ , flood conditions)	-0.14	-0.26	-0.17	-0.17	-0.18	-0.17	-0.12
Mean current velocity at the beach face (m s ⁻¹ , ebb conditions)	NM*	0.17	0.21	0.19	0.15	0.16	0.15
Beach face - time of immersion (min)	416	754	794	772	786	800	833

Sand bank - time of immersion (min)	541	1082	1070	1082	1111	1149	1248
-------------------------------------	-----	------	------	------	------	------	------

Table 4.2. Observed rates of transport based on tracer displacement. u_{bf} and u_{sb} correspond to the daily mass centroids velocity at the beach face and sand bank, respectively (accounting for both cross-shore and the alongshore velocity components); negative values of u correspond to flood and onshore directed tracer displacements; Q represents the daily transport from centroid positions (accounting for Q_x and Q_y), Q_x represents the daily alongshore, and Q_y represents the daily cross-shore transport; negative values of Q_y correspond to onshore tracer displacement, and negative values of Q_x correspond to tracer displacements towards flood. l is the daily immersed cross-shore length of each morphology.

Rates	days after release of tracer							Total
	day 1	day 2	day 3	day 4	day 5	day 6	day 7	
u_{bf} ($m d^{-1}$)	-0.207	0.024	0.100	0.084	-0.134	0.175	-0.261	-0.219
Q_{bf} ($m^3 d^{-1}$)	-0.021	0.002	0.010	0.006	-0.004	0.006	-0.006	-0.007
Q_{xbf} ($m^3 d^{-1}$)	-0.015	0.002	0.007	0.005	-0.002	0.004	-0.005	-0.004
Q_{ybf} ($m^3 d^{-1}$)	-0.015	0.002	0.008	-0.003	-0.004	0.004	-0.002	-0.010
u_{sb} ($m d^{-1}$)	-0.018	0.057	0.071	0.038	0.002	0.021	-0.028	0.143
Q_{sb} ($m^3 d^{-1}$)	-0.001	0.004	0.005	0.003	0	0.002	-0.002	0.011
Q_{xsb} ($m^3 d^{-1}$)	-0.001	-0.002	0.008	0.003	0	0.002	0.002	0.012
Q_{ysb} ($m^3 d^{-1}$)	-0.002	0.007	-0.004	0.004	0	0.001	-0.003	0.003
l_{bf} (m)	16.7	16.6	16.9	11.3	5.2	5.7	3.6	-
l_{sb} (m)	20.9	20.9	20.9	20.9	20.9	20.9	20.9	-

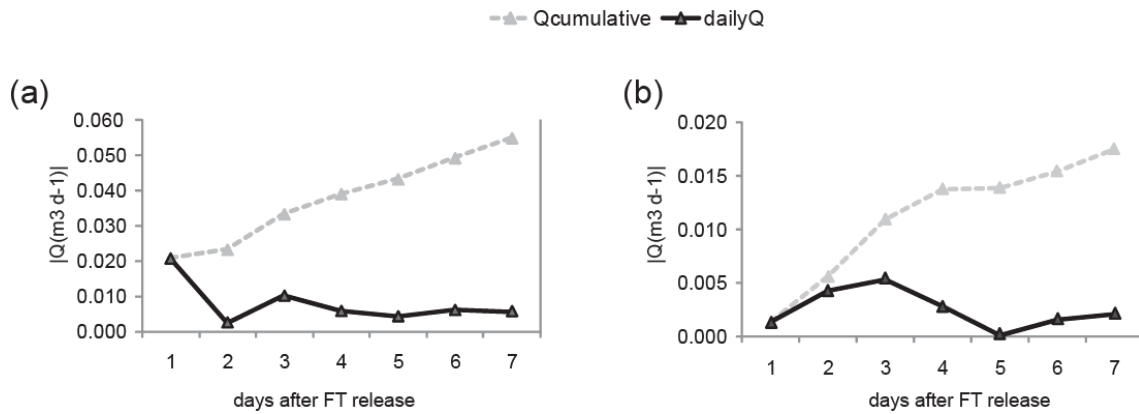


Figure 4.5. Sediment transport variation during the field experiment: (a) daily Q and Qcumulative at the beach face; and (b) daily Q and Qcumulative at the sand bank.

4.5. Discussion and Conclusions

This study demonstrate that in backbarrier beaches facing low-wave conditions (maximum fetch < 2 km) and lapped by tidal channels, sediment transport occurs mostly during spring tide conditions, tending towards very small values (or zero) at neap tides (approaching a tidal range pattern; Figure 4.5). With wind velocities below 12 m s^{-1} and $H_s < 0.1 \text{ m}$ (and $T_{\text{mean}} \sim 1.0 \text{ s}$), sediment transport is mainly governed by tidal currents (magnitude and direction; in agreement with Carrasco et al., 2011a), approaching rates of transport in the order of few cubic decimetres per week (below $0.01 \text{ m}^3 \text{ week}^{-1}$). This dependency is more evident in locations closer to the tidal channel (at sand bank): sediment transport and mean tidal current changed simultaneously (e.g., decrease of current velocities after day 3 caused decrease of transport, Tables 4.1 and 4.2). Higher transport took place during ebb, because ebb velocities were greater than flood velocities (about 0.2 m s^{-1} of difference), as locally testified by Salles et al. (2005) and Pacheco et al. (2010). Transport rates were distinct between spring and neap tide since there is a local distinction between maximum ebb

(and flood) velocities over the spring to neap tidal cycle (Figure 4.2; Dias et al., 2009). Dispersion and transport rates outlined by Carrasco et al. (2011a) were even smaller than the rates found in this study, reporting smaller wind intensities and wind-induced wave heights.

Given the absolute current speeds involved (maximum 0.5 m s^{-1}) and current asymmetry (Figure 4.2) herein reported, a greater net alongshore transport was expected to be obtained when compared to other studies reporting similar constrains (e.g., Ciavola et al., 1997b). The analyses of transport over several tidal cycles gave new insights about this technique. Tracer techniques were found helpful for determining sediment transport rates, but revealed complexity in defining the daily tracer movement under very low-energy conditions. Transport by advection was difficult to be estimate, with values in the order of cubic decimetres per day (Table 4.2), while dispersion was relatively high (few metres alongshore), reflecting the redistribution of a large number of tracer grains located around the mass centroid (bi-directional forcing by ebb and flood cycles, Figures 4.3 and 4.4). Tracer advection was not prevalent over diffusion and dispersion, and the transport system was not in equilibrium, as postulated by Madsen (1987). Furthermore, the higher transport rate values found after the first tide (e.g., $0.021 \text{ m}^3 \text{ d}^{-1}$ at the beach face, Table 4.2) were derived from the tracer initial dispersion process, suggesting that tracers need to be firstly incorporated/adjusted to the transport surficial active layer (more uniform rates after day 2, Table 4.2) to correctly represent the local sediment transport conditions (advection). Contrary to the present analysis, in higher energetic environments, causative forcing factors interact with beach at higher scale level and tracers have a relative quick adjustment to the active transport layer (e.g., Ciavola et al., 1997a; Balouin et al., 2005). The relationship between forcing

and response processes is stronger and more tendentious, with dominance of tracer's advection.

The obtained findings are likely of being observed in backbarrier beaches facing analogous hydrodynamic conditions. At those areas and for the use of tracer's techniques it is recommended to:

- perform small scale experiments (with different colours or at nearby sites) to determine the optimal tracer quantity;
- use small tracer amounts (e.g., hundreds of grams or less) to permit full tracer removal from the injection point;
- allow time for tracer adjustment and incorporation at the active transport layer; and
- perform a detailed sampling (high density grid) along several days/weeks to get representative advection values (disregarding tracer dispersion caused by cyclic ebb/flood conditions).

The tracer results analysis must also be very careful in both the interpretation of daily changes as well as relating it with the causative forcing. A wider application of tracer studies in other fetch-limited conditions will contribute to improve the knowledge on sediment transport techniques in this type of environments.

CHAPTER 5

**MORPHOLOGICAL CHANGES IN A
LOW-ENERGY BACKBARRIER**

Abstract

Profile characteristics of low energy sandy beaches include narrow foreshores that are often steep, with reflective swash zones. Seaward of the foreshore a low gradient terrace is generally present, acting as a wave energy filter. Low magnitude changes are usually associated to this type of environments, either cross- or longshore. To examine the short- (between months) and medium-term (from months to years) morphological changes at Ancão backbarrier (Ria Formosa), data from monthly cross-shore surveys was used. The degree of morphological mobility was given by the volumetric variability within specific morphologic units (foreshore, tidal flat and sand spit) and through the analysis of three cross-shore sections. Results show low medium-term variability, not seasonally distributed, and without a direct connection to changes on average wind intensity. The three morphologies are not interdependent and do not show a clear relation on sediment exchanges between them. Low intensity short-term changes are however present, which seem to be related with net sediment adjustments. Although the morphology and beach slope changes do not indicate a linear pattern of sediment exchange across the profile, cross-shore transport seems to dominate the small scale short-term process, mainly at the foreshore, being related with changes in wind direction (erosion associated to S-SE directions). At the medium- to long-term scale of evolution (years to decades) beach morphodynamics is probably more related with other forcing factors (e.g., inlet position, currents intensity and direction) rather than wind conditions.

Keywords: *backbarrier, variability, wind climate.*

5.1. Introduction

The term low energy has been applied to beaches in environments ranging from narrow, shallow lagoons, with non-storm significant wave heights smaller than 0.25 m (Nordstrom et al., 1996), to beaches in the lee of reefs, where the significant breaker height is up to 1.0 m (Hegge et al., 1996). Locally generated waves are found in fetch-limited conditions (e.g., enclosed lagoons) while non-locally generated waves are characteristic of sheltered environments (e.g., lee of islands; Jackson et al., 2002a). In fetch-limited environments the wave climate reflects the wind conditions affecting the surrounding coastal area. Due to the short-period waves, fetch-limited sandy beaches tend to be morphodynamically reflective with low wave amplitudes and steep foreshores (Wright and Short, 1984; Sherman et al., 1994; Jackson et al., 1999). Locally waves are less affected by wave refraction and may approach the shoreline at relatively larger angles, increasing the potential for strong longshore currents for a given wave height (Jackson et al., 2002a). At these environments, beach morphology includes narrow foreshores (Jackson and Nordstrom, 1992), planar (Nordstrom, 1980; Hegge et al., 1996) and without backshore (Nordstrom et al., 1996), with little evidence of bar forms seaward of low still-water levels (Jackson et al., 2002b). Extreme dissipative conditions prevail on the low tide terrace, and beach profile change is usually restricted to the foreshore (Jackson and Nordstrom, 1992). Survey profiles generally reveal little change in morphology, either alongshore or cross-shore (Nordstrom, 1980). The magnitude of beach mobility is a function of the controls that increase or decrease susceptibility to erosion (Jackson and Nordstrom, 1992). Sand availability and wind conditions are important factors in beach morphotype modulation (Anthony et al., 2006). Moreover, tidal range, coupled with changes in wind wave energy will affect the

location of the beach forms. Tidal range affects the vertical distribution of the wave-energy over the profile, and consequently determines the width of the beach and the duration that waves break at any elevation. Tidal currents may also be an important process on estuarine sites, controlling patterns of beaches evolution (Nordstrom, 1992; Carrasco et al., 2008).

Several models of beach change identify the variability of beach stage through time as a result of seasonal and short-term changes in wave height, associated with storm cycles (Nordstrom, 1980). Magnitude of morphological changes will be dependent on the energy/duration of these events. Modal conditions following a storm event may not be sufficient to return the beach to its original state (Travers, 2007). Therefore, the variability inherent to the beach response will be mostly dependent on the natural resistance of the beach profile and the magnitude of the seasonal changes. The aim of this paper is to discuss the short- (between months) and medium-term evolution (months to years) of a sandy beach located in a backbarrier system. Beach volumetric mobility, in terms of cross- and longshore transport dominance, is discussed within the prevailing wind conditions.

5.2. Field site

The field site is located at the backbarrier of the Ancão Peninsula, which belongs to the Ria Formosa, a multi-inlet barrier island system located in Southern Portugal. Ria Formosa includes two peninsulas and five islands, and extends over 56 km (Figure 5.1). Tides in the area are semi-diurnal, average ranges are 2.8 m for spring tides and 1.3 m during neap tides. Maximum ranges of 3.5 m can be reached on spring tides. Offshore wave climate in the area is moderate to high (Ciavola et al., 1997a), with average

offshore significant wave height of 0.92 m (Costa et al., 2001). Incident oceanic waves do not reach the study area and have no influence on its evolution.

The field site extends over ~100 m (Figure 5.1) and presents a sandy beach characterized by a low, narrow and intermediate morphology. The steep beach foreshore ($d_{\text{mean}} = 0.7 \text{ phi}$) and the low wave energy result in a narrow surf/swash zone. A gently sloping low tide terrace ($d_{\text{mean}} = 1.9 \text{ phi}$) is present, ending at a parallel sand spit ($d_{\text{mean}} = 1.2 \text{ phi}$) cut-off by a small transverse secondary tidal channel (Figure 5.1). The overall beach profile exhibit a convex-curvilinear shape between the segmented and convex-curvilinear morphotypes, presented by Travers (2007). Main forcing mechanisms acting at the backbarrier include tidal currents and waves generated by local wind over a low fetch distance. Waves are considerably small being on the order of few centimetres ($H_{\text{mean}} \sim 5 \text{ cm}$, $T_{\text{mean}} < 1 \text{ s}$), with the exception of waves generated by exceptional strong winds. Human occupation includes small number of fisherman houses in the backshore, which do not affect the backbarrier sediment dynamics; these edifications might only disturb the lower aeolian sediment transport from and to the dune.

5.3. Methods

Monthly topographic data were gathered for the field site from March 2006 to March 2008 (during low spring-tide conditions). The degree of the morphological mobility is given by volumetric variability (m^3), over successive surveys (18 surveys). Three main morphological sectors, within the survey area, were split for volumetric and processes analysis: foreshore*, tidal flat and sand spit**.

* in this chapter the foreshore includes the backshore and the beach face

**in this chapter the sand bank is designed as sand spit

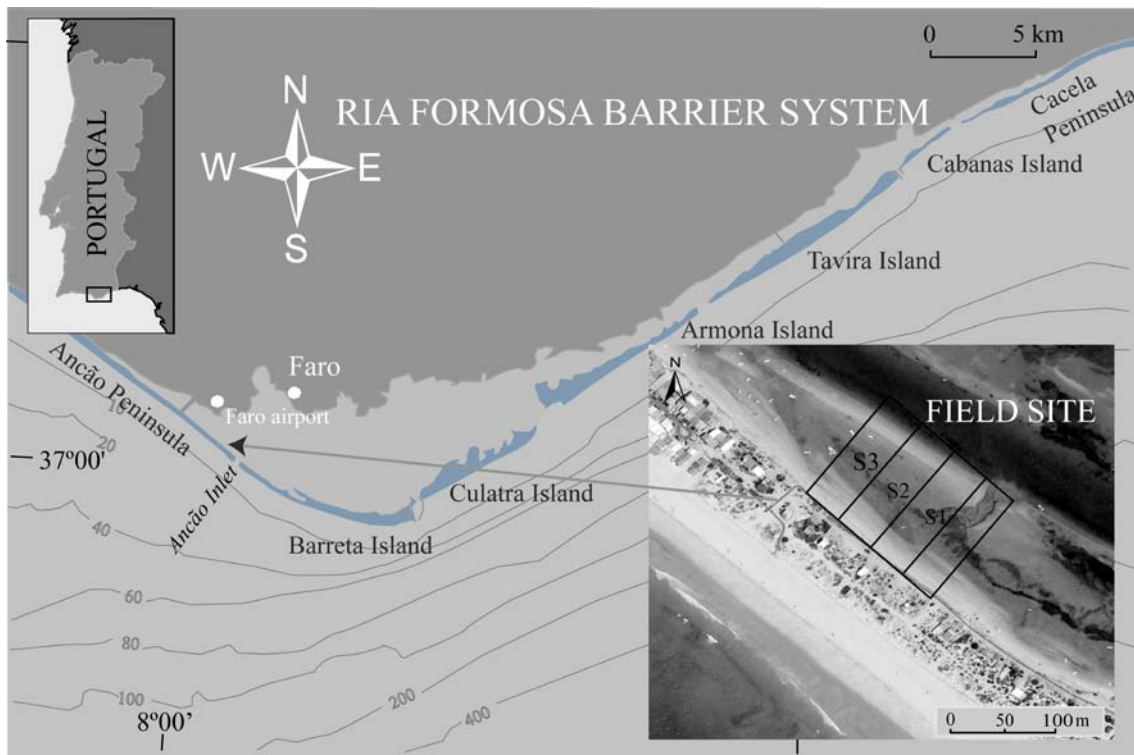


Figure 5.1. Field site location and aerial photograph with the location of the analysed representative profiles (S1, S2 and S3).

To each sector, surfaces were created using the kriging method interpolation (SURFER[®] 8 software package) and volume computations were made above a defined level. Results contain the errors associated to the equipment accuracy (use of Total Station maximum vertical error of ± 0.003 m) and to the volume interpolation method (maximum deviation of 12% in relation to other tested methods). Besides volume, slope was also determined. Sediment samples were collected in some parts of the beach profile (beach-face and sand spit) at each 3-month surveys, and analyzed by traditional sieving and grain size procedures.

Three representative cross-shore profiles (of 123 m length), were defined and taken for each survey by employing the *slice* command tool (SURFER[®] 8 software package):

S1 is the eastern profile, S2 the middle profile, and S3 the western profile (Figure 5.1). Volumetric changes and profile envelope were determined to each location. Sector analysis and sediment distribution allows quantifying cross-shore transferences between morphologies, whiling profile analysis is used to determine the response heterogeneity along the surveyed area, and smaller scale morphological changes.

Wind data were obtained from a close wind station (Faro airport, Weather Underground, 2008). The prevailing directions and average wind speeds were monthly determined and discussed with the topographic data results (sectors and profile volumetric variability). An indication of the morphological dependence between the three sectors and between each profile, is given by the application of the *Pearson correlation* (level of significance of 0.05), found to be statistically significant for $r > 0.45$. This approach was used to analyse the degree of correlation between variables (volumes, slope, and wind conditions).

5.4. Results

Most of the wind occurrences for the study period are related with S-SW wind conditions (average 4 m s^{-1}), with greater speeds associated to SW winds (Figure 5.2). Variations in the mean wind speed are small, ranging from 3 to 4.5 m s^{-1} (Figure 5.2). Three different periods of wind direction can be underline: until September 2006 (predominance SW conditions), until February 2007 (predominance S-SE conditions), and until July 2007 (predominance SW conditions). The volumetric variability of all morphologies is of very low magnitude, without showing any particular seasonal variation. With exception of January 2008, where accretion in the foreshore occurs

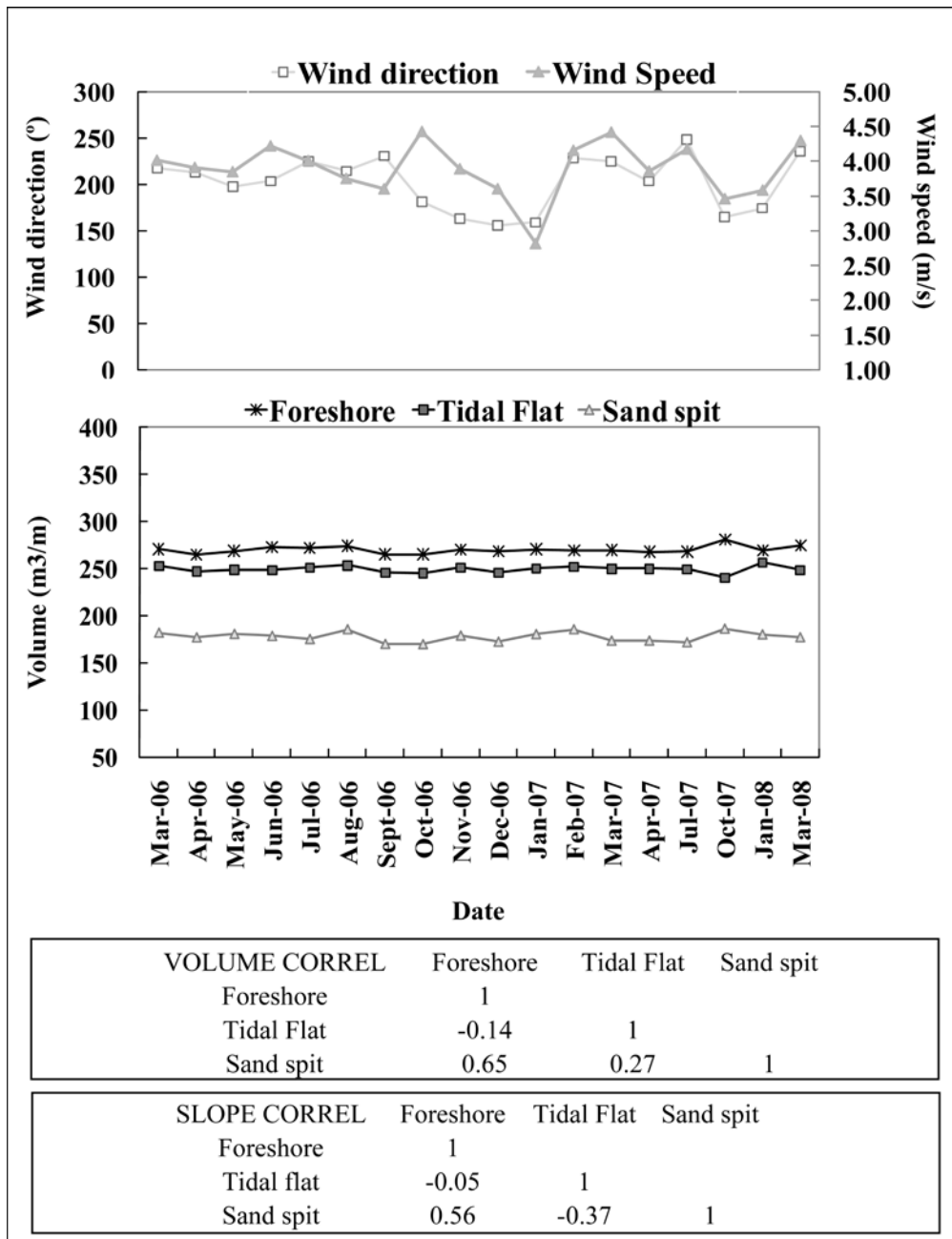


Figure 5.2. Wind climate (average magnitude and direction); volume variability at each beach sector, and correlation matrixes (volume and slope) between sectors.

simultaneously to erosion at the tidal flat, the three sectors present homogeneity in the volumetric tendency (Figure 5.2), with all showing similar evolutionary trends. Volumetric differences can only be account when considering the cumulative volume

variation between March 2006 and March 2008. A positive overall elevation at the uppermost part indicates a cumulative spatially-averaged accretion at the foreshore of $+3.58 \text{ m}^3 \text{ m}^{-1}$. On the contrary, at the lower part of the profile, the tidal flat and sand spit, exhibit cumulative erosion of $-4.74 \text{ m}^3 \text{ m}^{-1}$ and $-4.80 \text{ m}^3 \text{ m}^{-1}$, respectively. The overall slope changed little throughout the two years of analysis: at the foreshore

within the sector limits (e.g., January 2007 and October 2007, Figure 5.3). There is, however, no linear pattern between periods of sediment coarsening dominance and summer/winter conditions.

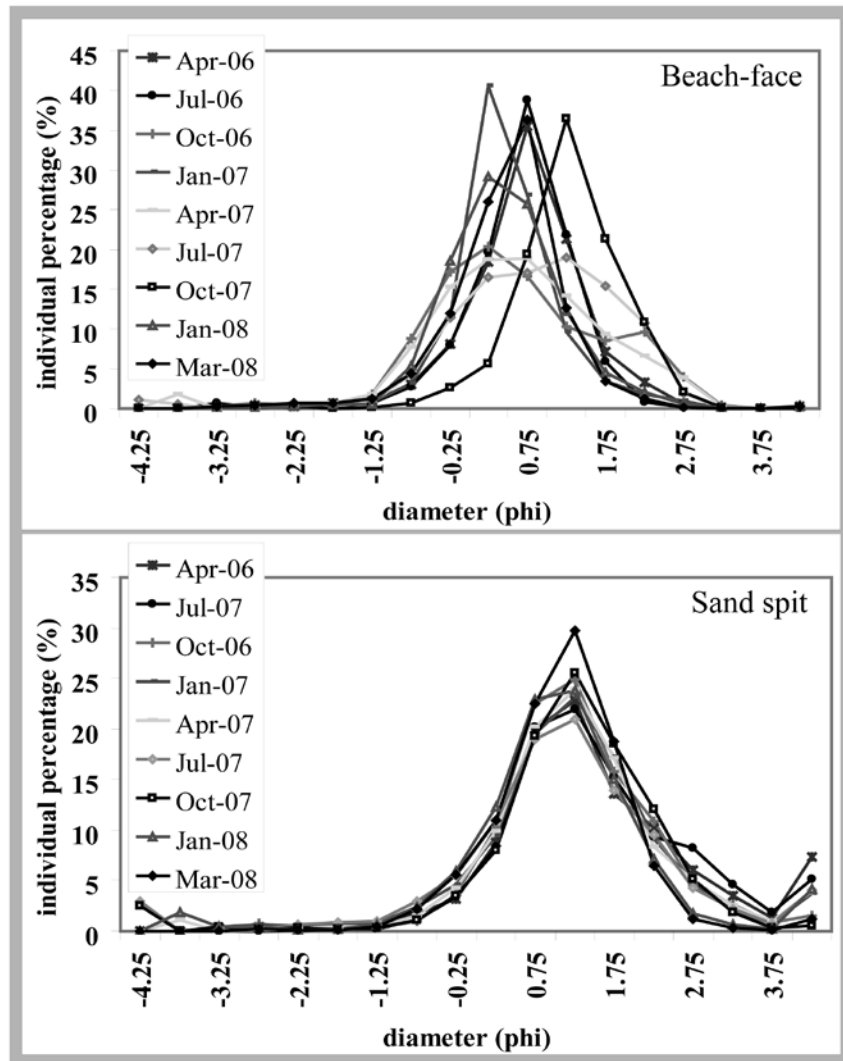


Figure 5.3. Sediment distribution at the beach-face and sand spit between April 2006 and March 2008.

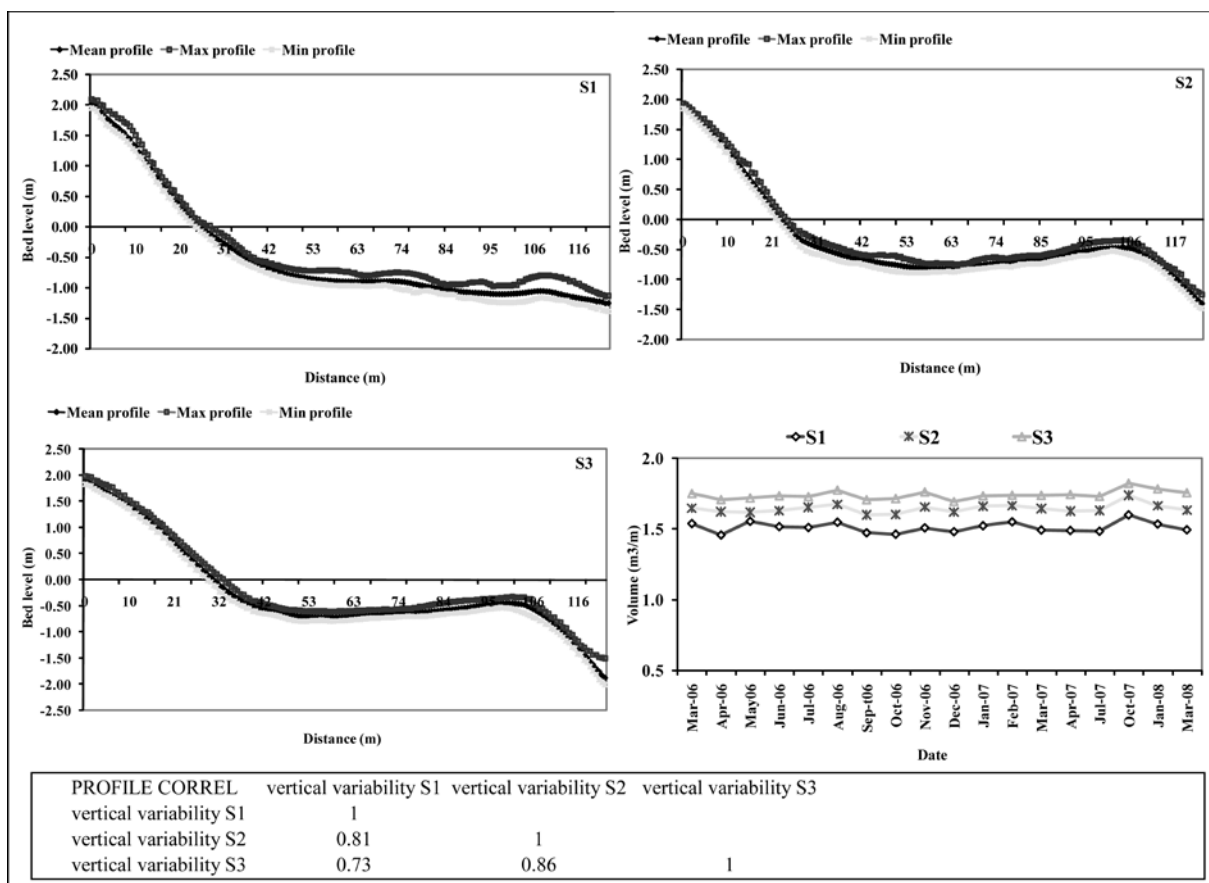


Figure 5.4. Profile envelope (maximum, minimum and average volume profile), volume change at each profile during the analysed period, and volume correlation matrix between profiles.

The *Pearson correlation* coefficients obtained between profiles (Figure 5.4) show a positive significant relationship ($r > 0.45$), indicating that they all follow the same tendency (Figure 5.4). Profile results show cumulative vertical erosion between March 2006 and March 2008: $0.04 \text{ m}^3 \text{ m}^{-1}$ at S1, $0.03 \text{ m}^3 \text{ m}^{-1}$ at S2, and $0.04 \text{ m}^3 \text{ m}^{-1}$ at S3. Volume changes at profiles located in the western part (S2 and S3, Figure 5.1) are better correlated ($r = 0.86$). These profiles also present a higher volume. S1, at the eastern part, shows greater beach mobility (Figure 5.4). Maximum vertical displacements are of 0.38 m, 0.32 m and 0.51 m, for S1, S2, and S3, respectively (profile envelope, Figure 5.4). The mean vertical variability was similar between the three profiles (0.2 m).

5.5 Discussion and Conclusions

The morphological variability of the field site do not follow the sedimentary pattern observed at oceanic exposed beaches or even the typical sedimentary exchange observed at other low-energy beaches, as those studied by Nordstrom (1977), Nordstrom (1980), and Jackson and Nordstrom (1992). Volumetric changes are generally very small (volume and slope, Figure 5.2) and do not allow to confirm a tendency of transport, at a medium-term scale (months to years). The absence of significant changes characterizes the beach typical condition (Figure 5.2). Mean vertical variability, through the morphologies is about 0.03 m between March 2006 and March 2008. Seasonality at the volumetric changes was not observed for the analyzed period (Figure 5.2). Moreover, there is no cyclical beach pattern following high energetic periods, as the one observed in similar low-energy environment (storm/non-storm cycles, Nordstrom, 1980). The overall tendency illustrates a homogeneous tendency of

accretion/erosion for the three considered sectors, with low/moderate correlation between them. The fact that two populations present positive correlations means that one of them might have a direct/indirect effect on the other, or that they evolve together in the same direction (Jackson and Nordstrom, 1992). Only the foreshore and sand spit presented positive moderate correlation. However, none of these sectors presented a significant correlation with the tidal flat (Figure 5.2). This means that do not exists relevant cross-shore relation between them. The significant positive correlation of foreshore and sand spit indicates that they are exposed and react equally to the same forcing factors. The tidal flat is probably more resilient to the forcing mechanisms, due to the existence of some cohesion induced by fine sediments (silt and clay).

The moderate correlation between the vertical variability of the three profiles ($r > 0.45$; $p > 0.95$), indicates that most of the surveyed area is affected by the same processes, having the same evolutionary trend (Figure 5.4). Positive correlations also show that there are no direct alongshore net sediment transferences from one profile to the others, able to indicate erosion at one site and accretion at the other. Since the evolution seems to follow the same trend at all profiles, it can be suggested that cross-shore exchanges dominate over longshore, in which regards the induced morphological changes. The observed cross-shore dominance, do not excludes the longshore transport occurrence, but solely that it is not responsible for the major changes at a monthly scale. These changes do not imply a net loss or gain of sediment but simply re-arrangements of sediment, as stated by Voulgaris and Collins (2000), within each morphological limit.

Even admitting the relative beach stability at medium-term scale (months to years), a few low magnitude changes (accretion/erosion) can be observed through the profile, at a shorter-term scale of analysis (between months, Figure 5.2). The cumulative variability at the foreshore, points to an accretion tendency between 2006 an 2008,

while at the tidal flat and sand spit it is observed erosion (low magnitude changes). In general, the foreshore is the sector reporting greater short-term volumetric variability (Figure 5.2), which can be in part related with site specific differences like width and slope (Jackson and Nordstrom, 1992). The foreshore includes the beach-face that is associated to the maximum energy concentration, leading to the incorporation of higher rates of sediment displacement (Nordstrom and Jackson, 1992; Hegge et al., 1996; Makaske and Agustinus, 1998; Travers, 2007). Higher variability is, therefore, observed in the grain size distribution curves, indicating a higher short-term cross-shore gradient within the beach-face, when compared with the lower part of the profile (sand spit, Figure 5.3). Sediment mobility is explained by the displacement of small sand ripples, for specific periods, controlled by locally generated waves (field observations).

The observed short-term changes can be reported to changes in wind direction by morphological realignment to the prevailing wave induced characteristics. S-SE conditions are frequently associated to erosion, while transition to the SW domain is associated with accretion (Figure 5.2). This type of situation has been previously attested for other low energy beaches. Jackson et al. (2002a) observed that changes in wind direction and wave angle might be able of inducing changes on longshore transport and consequent parallel retreat/advance of the beach profile. Since the response of the profile is proportional to the increase in the wave energy level (Jackson et al., 2002a), the obtained lower variability indicate that wind intensity, and consequent generated wave climate (extremely reduced fetch, Figure 5.1), were not energetic enough to cause significant profile changes (Figure 5.2 and 5.4). Hence, the beach was not reactive to most of the observed wind conditions. A low correlation between wind speed and beach volume was observed (Figure 5.2), and therefore it can be assumed that waves were just responsible for second order readjustments in the beach profile.

The overall time of beach response is slow and continuous, and the medium- to long-term morphological evolution (years to decades) is probably more related with changes on the tidal currents regime (Carrasco et al., 2008) rather than to the wind regime. Changes in tidal currents are intrinsically related with changes in Ancão Inlet position (Figure 5.1), which depends on inlet migration (circa. 40-100 m yr⁻¹, Vila-Concejo et al., 2002), and inlet relocation (as in June 1997, Vila-Concejo et al., 2004b). Changes in inlet hydrodynamics will reaffirm or dissipate the potential of currents, leading to other trends, when evaluating longer scales. Further efforts should be focused in a longer period of analysis, in order to define a typical short- to medium/long-term beach profile response.

CHAPTER 6

**NATURAL AND HUMAN-INDUCED
COASTAL DYNAMICS AT A
BACKBARRIER BEACH**

Abstract

This study contributes to the understanding of very low-energy, fetch-limited environments by reporting the evolution of a backbarrier beach (Ancão Peninsula, southern Portugal). It includes two temporal timescales, one a large-scale evolution for the past 60 years based on aerial photograph analysis, and the other a small-scale beach evolution based on monthly topographic surveys performed during three years of monitoring. The investigation attempts to unravel similarities and dissimilarities in the patterns of change between them, and to define the causative forcing mechanisms.

Each timescale denounced a different rate of evolution, the first reporting a modified beach response-type, and a second, reporting a natural beach response-type. At large-scale, short-term events led to the development of a new compartment in the beach (a sand bank) and proved to be of paramount importance to the evolution of the beach system. Human activities (“soft management” approaches) caused significant changes in the backbarrier shore, which remained in the system’s memory. Changes under natural forcing were much smaller, were less influential on the area’s evolution, and were not sufficient to counteract or mask the consequences of human activities. Backbarrier shores have a valuable geological and ecological potential that needs to be sustained on a permanent basis. The findings of the study should contribute to a better understanding about the large- and small- scale changes in other backbarriers characterised by similar very low-energy conditions.

Keywords: *backbarrier, morphological changes, human activities.*

6.1. Introduction

Low-energy estuarine beaches are geographically more extensive than oceanic beaches (Vila-Concejo et al., 2010); however, they have received less scientific attention which has resulted in a poorer understanding of their evolution and morphodynamics. Hitherto, research on high-energy beaches has produced a range of morphodynamic classifications and morphological postulations that describe or predict nearshore morphotypes. Although high-energy beach parameterizations have been applied to low-energy environments, recent research has questioned the usefulness of these traditional indices for labelling beaches along relatively low-energy coastlines (Nordstrom, 1992; Hegge et al., 1996; Masselink and Pattiaratchi, 2001; Gómez-Pujol et al., 2007). Viewing low-energy beaches as scaled-down versions of high-energy beaches has been found to be an insufficient approach (Carrasco et al., 2011b). Beaches exposed to high wave energy generally undergo rapid erosion and accretion as a response to storm onset and passage (Nordstrom, 1980; Dail et al., 2000; Jackson et al., 2002a), whilst low-energy beaches tend to exhibit a relatively low-frequency response (Masselink and Pattiaratchi, 2001). Moreover, fetch-limited beaches are subject to a high variety of forcing factors acting at short time scales, including human changes, which may leave enduring inheritance in profile shape. Contrary to most oceanic beaches, changes in fetch-limited beaches can remain for a long period of time, since they usually have very low recovery rates (Nordstrom, 1992).

Research efforts on fetch-limited beaches have been focused not only on identifying the main forcing factors and their relative importance in sediment transport, but also on predicting the beach morphological response over time (Jackson, 1995; Nordstrom et al., 1996; Eliot et al., 2006; Travers, 2007; Carrasco et al., 2011a).

Predicting morphological changes in fetch-limited environments, or in other coastal systems, is a difficult task due to the complexity of the underlying physical processes involved and because of the sensitivity of system behaviour to natural variability (Karunaratna et al., 2009). Furthermore, there are limits to the predictability of morphological variables, which are related to the issue of scale (Larson and Krauss, 1995; Larson et al., 2002). This requires a better description of the changes occurring over each temporal scale and a better specification for the crossover between the various scales. The main objective of this work is to quantify the large-scale behaviour (from years to decades) of a low-energy beach and to determine how such behaviour relates to small-scale evolution (months to a few years). Also, local and regional spatial frames are integrated to understand how they interact to explain the evolution of the backbarrier environment.

At the beginning of this study, three research questions were raised: (a) does a fetch-limited shore segment approach a quasi-equilibrium state over a few years? (b) does the beach respond to a seasonal hydrodynamic cycle? and (c) what are the main physical processes responsible for change at different timescales? By answering these questions, we intend to provide a basis for the discussion of controls involved in inter-site variability in net budget trends and to contribute to the overall understanding of backbarrier stretches.

6.2. Field site

6.2.1. Regional setting

The field site is located at Ancão Peninsula backbarrier (Figure 6.1), within the Ria Formosa lagoon (southern Portugal). This lagoon is protected by a multi-inlet barrier island system that extends over 56 km in length and includes two peninsulas, five islands and six tidal inlets (Figure 6.1a). Tides in the area are semi-diurnal; average ranges are 2.8 m for spring tides and 1.3 m for neap tides, but maximum ranges of 3.5 m can be reached during equinoctial spring tides. The average offshore significant wave height is 0.92 m (Costa et al., 2001). The field site located at Ancão Peninsula backbarrier (Figure 6.1) is sheltered from oceanic waves, and is therefore exposed to a different wave and current regime from other coastal stretches in the region. With the exception of wave regimes generated by exceptionally strong winds, predominant waves are small, in the order of few centimetres in height (Carrasco et al., 2009). The backbarrier beach is bounded by Ancão channel (Figure 6.1b), which connects to Ancão Inlet, located about 2250 m to the SE. Ancão Inlet is a small inlet with a cyclic eastward migration pattern (Dias, 1988; Pilkey et al., 1989; Vila-Concejo et al., 2002), exhibiting an ebb-dominated behaviour (Andrade, 1990; Salles, 2001, Pacheco et al., 2010). According to Vila-Concejo et al. (2002), Ancão Inlet undergoes an eastward migration cycle that lasts 30–40 years. During these cycles, the inlet migrates to the east with variable migration rates while the width of the channel at the inlet throat remains almost constant.

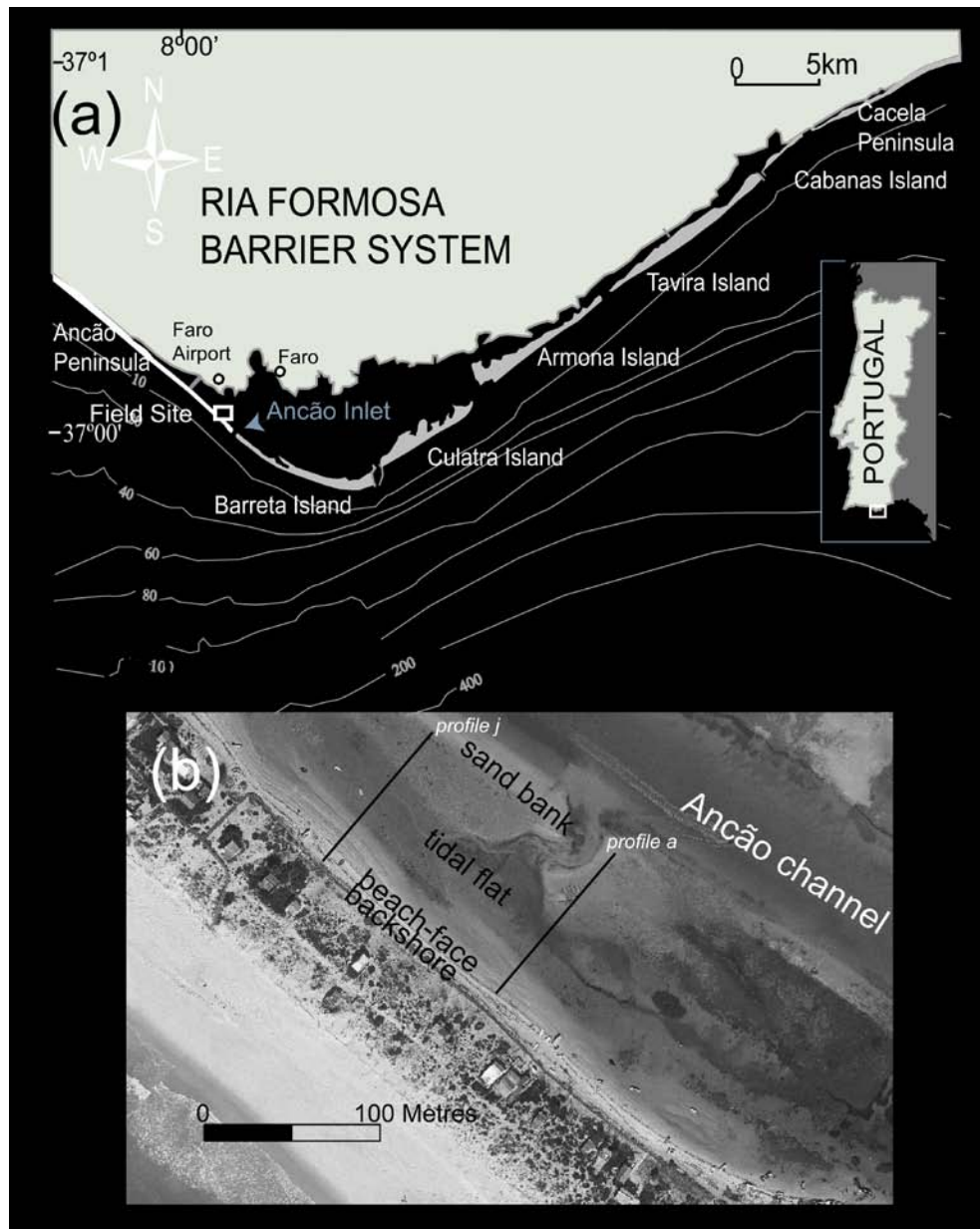


Figure 6.1. (a) Field site location, showing Ancão Peninsula backbarrier; and (b) a vertical aerial photograph (taken in 2007) showing the main beach morphologies, profile *a*, and profile *j*.

The field site extends along the shore over ~100 m and includes a sandy beach with low, narrow, and intermediate morphodynamic behaviour (Figure 6.1b). The beach profile is presently composed of four different morphologies: backshore (Figure 6.2a);

beach face (Figure 6.2b); tidal flat (Figure 6.2c); and a detached sand bank (Figure 6.2d). Under low wave energy, the intermediate-steep beach face (~39 m wide) presents a very narrow swash zone during high tide. In contact with the foreshore, a tidal flat with a gentle slope is present (~44 m wide), ending in a small sand bank (~30 m wide) parallel to Ancão channel. The tidal flat dissipates wave energy during low tide. Both the tidal flat and sand bank show no bedforms and are cut off by a small oblique secondary tidal channel (Figure 6.2d). This secondary tidal channel promotes the rise and fall of the tide at the study area. The tidal flat is mainly sandy with a high percentage of mud, and contains seagrass and accumulations of shells (Figure 6.2c). The backshore and beach face have coarser morphologies (Carrasco et al., 2009).

6.2.2. Human activities

Human occupation at the field site dates from the 1940s. Currently, the site hosts a small number of dwellings (for local fishermen) in the backshore area and an alongshore elevated footpath (Figure 6.1b). An elevated footpath was constructed in the late 90s, instilling shoreline changes. At the moment buildings and footpath do not interfere with the foreshore sediment dynamics, although their presence might disturb the aeolian transport of sand from the dune towards the beach and vice-versa; the footpath is only reached by swash runup in exceptional conditions.

Besides human occupation, other human activities have included dredging operations and the relocation of the inlet during the 1990s. The Ria Formosa system has also undergone an extensive environmental rehabilitation programme to recover the natural dynamic equilibrium while decreasing natural hazards (Ramos and Dias, 2000; Dias et al., 2003).

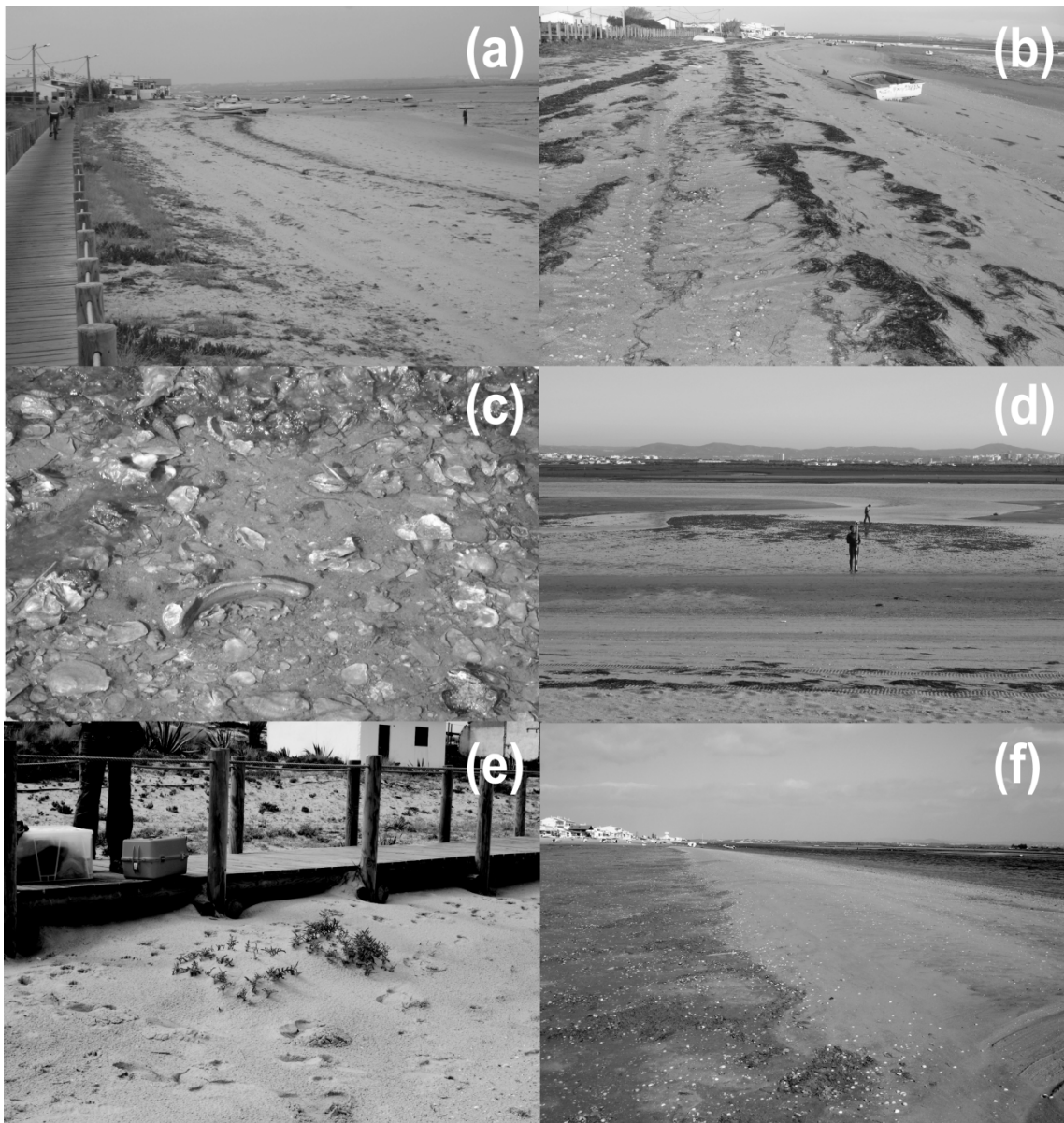


Figure 6.2. Photographs of the field site: (a) view of the backshore (June 2006); (b) sandy foreshore (December 2008); (c) high shell content in the tidal flat (October 2006); (d) Ancão tidal channel, sand bank (intercut by the secondary tidal channel), and tidal flat (January 2006); (e) view of aeolian sediment accumulation in the backshore (February 2008); and (f) other view of the sand bank (January 2007).

This programme has included soft protection techniques such as tidal channel dredging, beach and dune nourishment, and the relocation of two inlets, including Ancão Inlet. Sand renourishment operations close to Ancão Peninsula occurred in 1990, and between 1999 and 2000. In 1990, about 300,000 m³ were dredged from Ancão tidal channel and deposited along Ancão Peninsula. Between 1999 and 2000, about 570,000 m³ were dredged from the entire Ancão tidal channel and placed in the vicinity of the oceanic beach of Ancão Peninsula (Ramos and Dias, 2000). Both dredging operations were responsible for the Ancão tidal channel deepening and channel axis shift, and were performed mainly for navigation purposes, especially to enable fishing boats from western Ancão Peninsula to get out easily through Ancão Inlet.

Ancão Inlet was relocated in 1997 to a more westerly position, improving its hydrodynamic efficiency and reducing navigational difficulties (see inlets positions through time in Vila-Concejo et al., 2006). This relocation effectively brought the inlet closer to the study area, from the former position of 5,600 m (1996) to 1,740 m (2001). Some of the sediment dredged during the relocation of Ancão Inlet was placed in the innermost western end of the inner channel, to protect existing houses (Vila-Concejo et al., 2003) to the west of the study area.

6.3. Methods

This investigation includes two temporal frameworks, (a) large-scale shoreline change over the last 60 years based on aerial photograph analysis, and (b) small-scale beach evolution based on monthly topographic surveys performed during three years of monitoring. Large-scale analysis reports shoreline tendencies and beach width evolution

between 1947 and 2007. This framework provides information on long-term (decadal scale) backbarrier evolution.

The small-scale analysis reports the main beach volumetric tendencies with respect to wind (wave driver) conditions. This framework provides information about the evolution of the backbarrier beach on a monthly/seasonal to yearly timescale.

6.3.1. Large-scale data collection

Shoreline evolution over the last 60 years was calculated by analysing a time-series of georeferenced aerial photographs (1947, 1976, 1989, 1996, 2001, 2005, and 2007). Dates for the set of photographs were chosen according to photo quality and to better discriminate evolution in the more recent decades (Table 6.1). In a first step, the evolution of the overall Ancão backbarrier shoreline was determined to assess the morphological variations in the surrounding area, and in a second step a thorough analysis was conducted just for the study site. For the overall backbarrier shoreline analysis, Ancão backbarrier was sub-divided into two sectors, with the field site being located in sector 1.

The shoreline was defined as the contact between the dune and the beach, since the contact between the water and the beach is highly dependent on the tidal level at the time the photographs were taken. Shoreline limit detection was based on sediment texture and dune vegetation. Digital Shoreline Analysis System from the USGS (DSAS; Thieler et al., 2005) was applied to infer shoreline displacements. DSAS was used for transect-based reference limit-change analysis. With this approach, transects are created perpendicular to a baseline that is positioned landward or seaward of the shorelines under analysis (Thieler and Danforth, 1994). Shoreline change was determined based on

the endpoint rate (EPR), according to Dolan et al. (1991). EPR was calculated by measuring the distance between shorelines along the fixed transects and dividing by the interval of time between pairs of photographs in the series (yielding a shoreline movement between the two measurements, positive values indicating seaward displacement (accumulation; Cowart et al., 2010). In shoreline position data, an estimate of the long-term change based on a shorter-term data set can result in an erroneous value (Dolan et al., 1991). Thus, a minimum of ten years was used to delineate the long-term trend. In the present study the uncertainty in data and methods used for long-term data collection is related to the accuracy of photographic interpretation of the shoreline.

Table 6.1. Medium- and long-term datasets.

Date	Medium-term data (Topographic datasets and number of surveys)	Long-term data (aerial photo datasets)
1947		✓
1976		✓
1989		✓
1996		✓
2001		✓
2005	✓ (7 surveys)	✓
2006	✓ (10 surveys)	
2007	✓ (4 surveys)	✓
2008	✓ (4 surveys)	

The measurement error associated with shoreline delineation methods is well-documented (e.g., Crowell et al., 1991; Dolan et al., 1991). Errors associated with long-term rate-of-change statistics include the inherent aerial photo georeferencing error, which is more significant in areas where changes in shoreline positions are small, as occurs in the case of this study. The RMS error associated with aerial photo georeferencing is reported in Table 6.2. The statistical uncertainty for the long-term

evolution rate at each transect was reported at the 99% confidence interval. The determined mean least square estimate (LSE), which includes the above errors using the EPR method, was 5 m for Ancão Peninsula and 2 m for the field site. The obtained results represent best estimates and can be used to assess general tendencies.

The long-term evolution of the beach profile was assessed by the comparison of recent profiles (2008) with topographic data measured around 1944-1945 (source, Instituto Portuário Transportes Marítimos).

Table 6.2. Total RMS error associated with georeferenced aerial photographs (in metres).

Date	RMS
1947	3.11
1976	1.73
1989	1.46
1996	1.13
2001	0.49
2005*	-
2007	1.39

*orthophoto

6.3.2. Small-scale data collection

Wind data, surficial sediment samples, and topographic data were collected during the monitoring period, from April 2005 to March 2008. Prevailing wind directions and maximum and average wind speeds were accessed every 30 minutes from Faro airport, 2 km north of the study area (Figure 6.1; Weather Underground, 2008). Surficial sediment samples were collected from the main beach morphological compartments. Traditional laboratory dry sieving procedures for unconsolidated clastic sediments were

used for the coarse fraction. The pipette method was used for the fine fraction. Grain-size parameters (e.g., mean, calibration, median- d_{50}) were obtained using the GRADISTAT macro of Excel (Blott and Pye, 2001), which uses the methods of Folk and Ward (1957).

Ten cross-shore profiles (*a*, to the east, through to *j*, to the west, see Figure 6.3a) with 10 m spacing were measured during each survey (Survey 1 to 25, Table 6.1). First and foremost, profiles were analysed to capture cross-shore morphometric variations, and alongshore heterogeneity over the survey area. An average profile was determined for each survey and the standard deviation of elevation for each cross-shore position was computed (Figure 6.3b). Volumes were determined for the main morphologies, in relation to Mean Sea Level (MSL). Kriging was used as the grid-fitting method with 0.5 m spacing. Digital beach elevation models (DEMs) were built with Surfer 9.0. Comparison of DEMs allowed monthly and inter-annual elevation changes, and inherent cross- and long-shore variability, to be assessed. Errors associated with topographic maps and with volume computations resulted from equipment error (maximum vertical error of ± 0.003 m, quoted by the manufacturer), fieldwork operational errors (mean horizontal error of 0.01 ± 0.07 m, and mean vertical error of 0.00 ± 0.002 m, based on test surveys) and surface interpolation method errors (maximum difference between interpolations with different methods of 0.39 %).

The prevailing wind conditions, temporal distribution of sediment grain-size, and volumes of morphologies were jointly analysed. Seasonal backbarrier cross-shore displacements, both seaward (accumulation or advance) and landward (erosion or retreat), were also calculated.

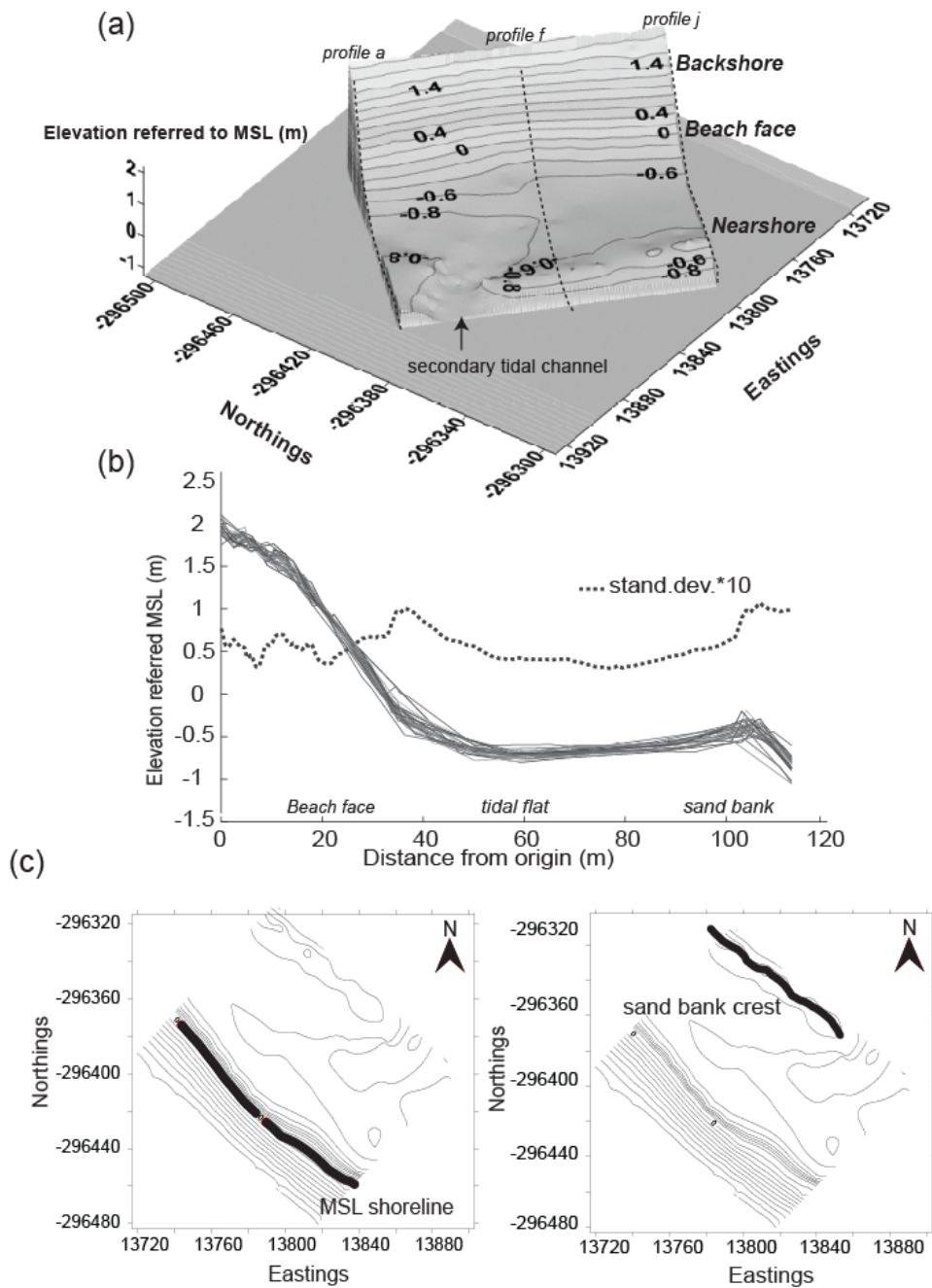


Figure 6.3. (a) Surveyed area and beach compartments: backshore, beach face, and nearshore (tidal flat and sand bank). Secondary tidal channel is also shown. Mean elevation is referred to MSL; (b) profile *i* envelope and standard deviation for the period April 2005 to March 2008; (c) representation of beach face and sand bank reference limits.

In this case, “seaward” refers to displacement towards the northeast (i.e., towards Ancão channel), and “landward” to the opposite direction (i.e., towards the backshore) (Figure 6.1). Reference lines were marked for beach evolution analysis: for the beach face the MSL contour was used, while for the sand bank the crest position was used (Figure 6.3c). Net advance/retreat of the two reference lines was quantified using DSAS.

6.4. Results

6.4.1. Large-scale evolution and morphological changes

The mean shoreline-change rate at Ancão Peninsula backbarrier between 1947 and 2007 was 0.1 m yr^{-1} (EPR, below RMS error). Changes were not uniform along the backbarrier shoreline, comprising two sectors with different mean shoreline-change rate (Figure 6.4a). Sector 1 (containing the field site) presented a maximum shoreline-change rate of 0.7 m yr^{-1} , whereas sector 2 in the eastern part of Ancão Peninsula presented the most dynamic evolution with a maximum backbarrier shoreline-change rate of 4.4 m yr^{-1} , during the 1990s (Figure 6.4a).

Shoreline-change rates at the field site show a significant backbarrier seaward trend (dune field advance towards Ancão tidal channel; Figure 6.4b), with a net average displacement of about 0.05 m yr^{-1} , between 1947 and 2007 (Table 6.3); accretion was greater between 2001 and 2005 (1.22 m yr^{-1} , Table 6.3). Aerial photograph interpretation shows that major shoreline changes over the last 60 years were human-induced. Until 2001 the shoreline remained relatively stable, whilst greater displacements took place between 2001 and 2005 (Table 6.3). The beach, nearshore,

and tidal channel evolved in separate ways, on which basis four main periods of evolution were distinguished (aerial photos, Figure 6.5):

- (a) Between 1947 and 1976, with no major shoreline changes (Figure 6.5). The beach profile was short and the foreshore contacted directly with Ancão tidal channel (see backbarrier morphologies, Table 6.3). Human occupation was limited to small and traditional settlements associated with the fishing industry.
- (b) Between 1976 and 2001, characterised by important changes occurring in the nearshore and Ancão tidal channel; beach remained almost stable. Between 1976 and 1989 there was an increase in human occupation of the dune field, involving the construction of small dwellings as well as other fishermen's settlements; the beach was narrow, and the beach face was the major compartment, with no evidence of a prominent nearshore. A few sand spits were observed at Ancão tidal channel. These spits had limited width and were split by several tidal channels (see photo 1989, Figure 6.5; Table 6.3). The channels in between the sand spits merged to form the tidal flat, and sand dredged from the tidal channel was used to replenish the ocean shore. After 1989, there was a reduction in human occupation of the dune field.

The remaining sand spits were further modified by other dredge operations that took place in Ancão tidal channel during the late 1990s (see dredge channel in photo 1996, Figure 6.5). Simultaneously, the backbarrier beach became wider and another detached compartment (the sand bank) started to form close to Ancão tidal channel (after 1996, Figure 6.5; Table 6.3). The sand bank was an impact of dredging. Besides changes in the density of human occupation,

between 1996 and 2001 an elevated footpath was also constructed across the dune field.

- (c) Between 2001 and 2005, characterised by changes focused on the beach and nearshore (Figure 6.5). By 2001, the backbarrier profile was exhibiting the four well-developed compartments/morphologies: backshore, beach face, tidal flat, and sand bank. High shoreline displacements occurred (seaward) as a consequence of the incorporation of the sand bank into the beach (Table 6.3). The sand bank evolved significantly (became tidal channel margin), and Ancão tidal channel started to communicate with the tidal flat subsequent to sand bank formation, by a small oblique secondary tidal channel that cut the sand bank.
- (d) Between 2005 and 2007, characterised by beach and nearshore stability (Table 6.3). In 2005, both the sand bank and secondary tidal channel were established as important features for the evolution of the upper beach profile.

These morphological changes since 1947, as described, are also visible in profile view (Figure 6.5, bottom right diagram). Both aerial photographs and topographic datasets show the importance of anthropogenic changes. Around 1944 - 1945, in the absence of nearshore morphologies (tidal flat and sand bank), the beach face dipped directly into the Ancão tidal channel. The sandy beach was very narrow when compared with the 2008 topography. Over the ensuing decades since 1944 - 1945, substantial sediment accumulation occurred in the nearshore, which led to the development of both the tidal flat and sand bank, and subsequent seaward shoreline displacement. The Ancão tidal channel migrated towards the mainland (i.e., to the northeast).

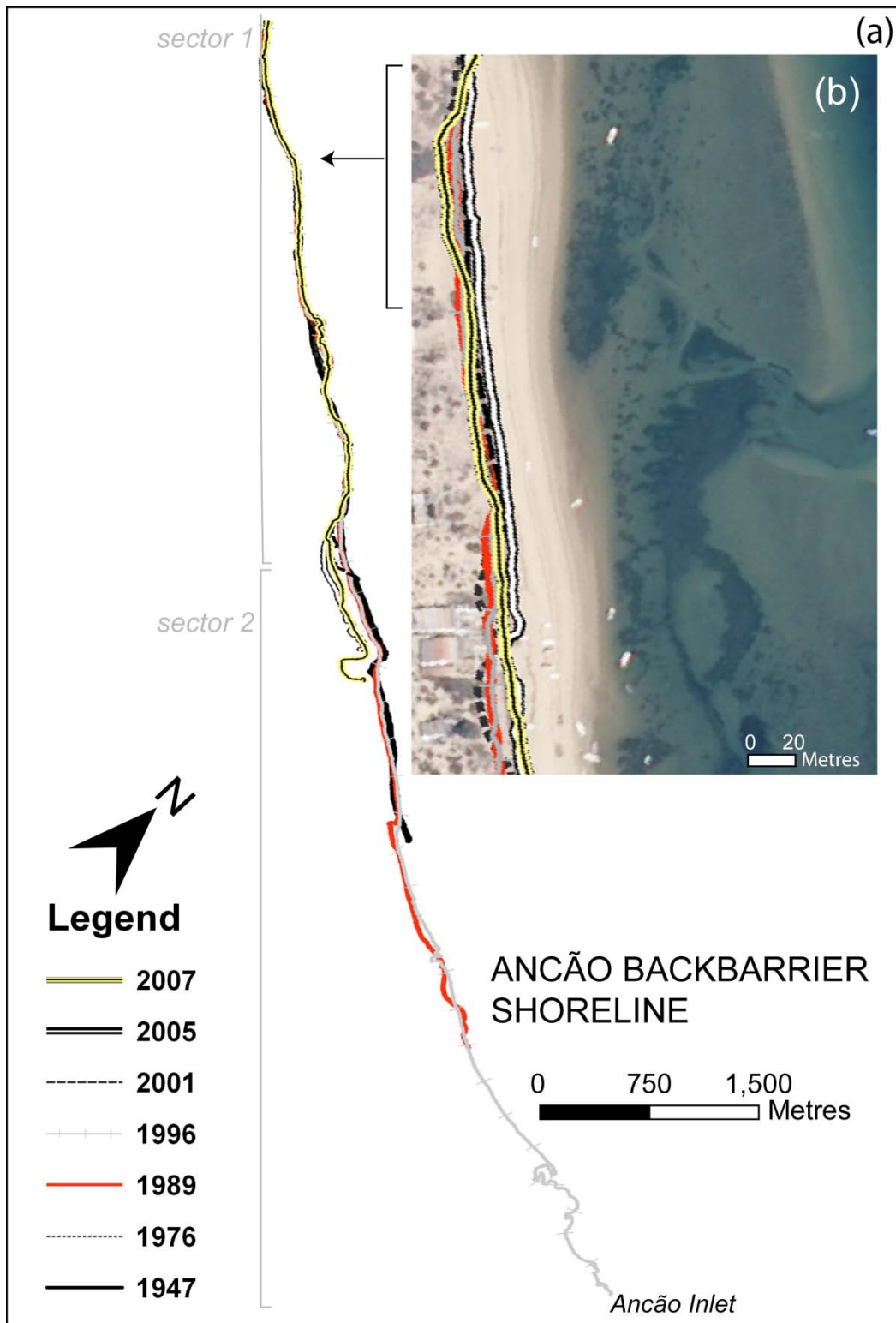


Figure 6.4. (a) Ancão backbarrier shoreline evolution between 1947 and 2007; and (b) shoreline displacements between 1947 and 2007 at the study area (aerial photo from 2005).

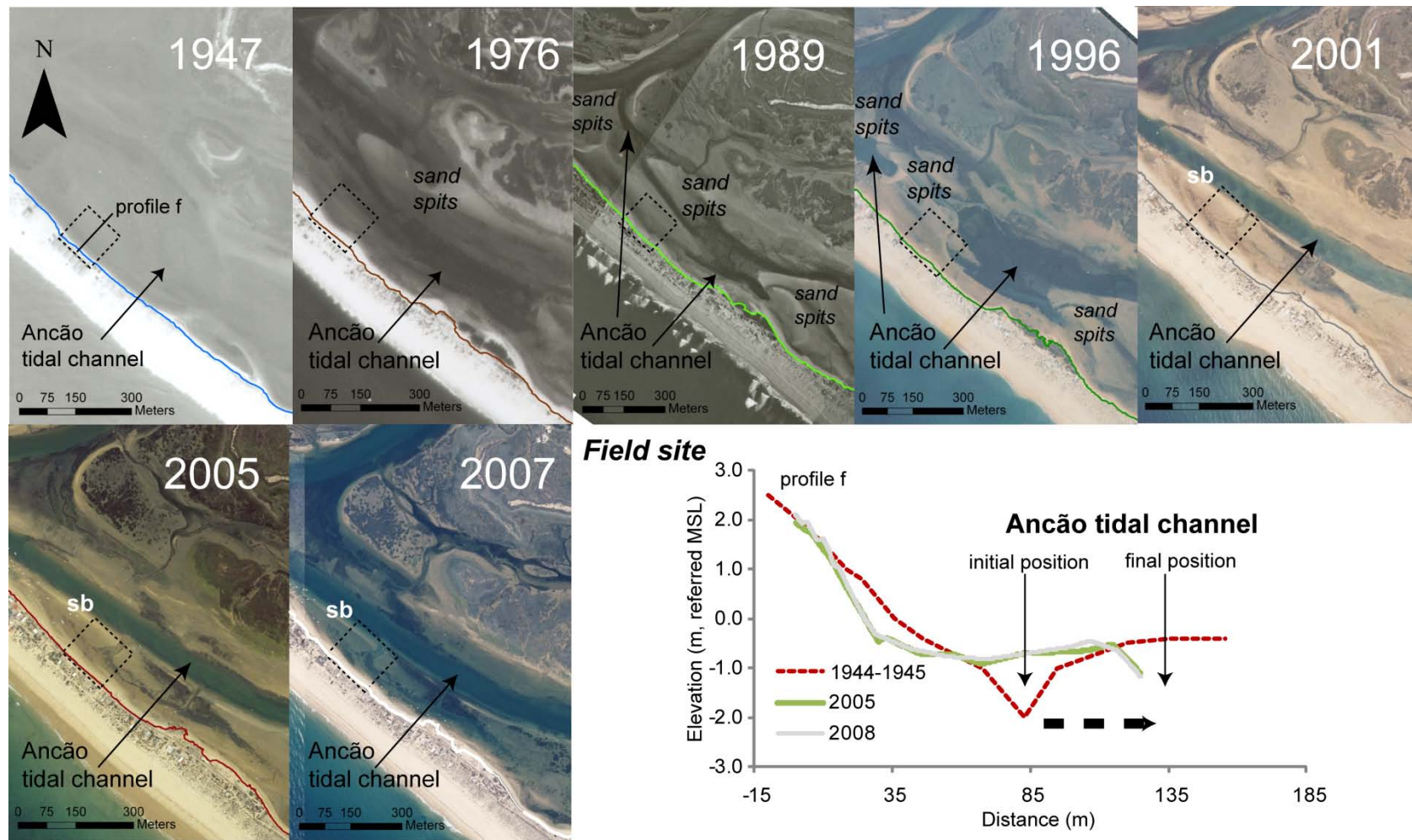


Figure 6.5. Field site evolution between 1947 and 2007; beach profile evolution between 1944 - 1945 and 2008.

Table 6.3. Shoreline displacements between 1947 and 2007 (positive values indicate seaward or northeast displacement, i.e., towards the Ancão channel), backbarrier morphologies and related changes.

Period	Mean displacement (m/yr)	Backbarrier morphologies	Major morphological changes
1947-1976	0.05	<i>backshore beach face</i>	<ul style="list-style-type: none"> • Beach face and nearshore stability
1976-1989	-0.05	<i>backshore beach face tidal flat</i>	<ul style="list-style-type: none"> • sand spit development
1989-1996	0.08	<i>backshore beach face tidal flat</i>	<ul style="list-style-type: none"> • sand spit development • Ancão tidal channel infilling
1996-2001	-0.22	<i>backshore beach face tidal flat sand bank</i>	<ul style="list-style-type: none"> • dredging • sand bank development • tidal channel axis migration with changes in the channel margins
2001-2005	1.22	<i>backshore beach face tidal flat sand bank</i>	<ul style="list-style-type: none"> • sand bank evolving • changes in tidal channel margins
2005-2007	0.15	<i>backshore beach face tidal flat sand bank</i>	<ul style="list-style-type: none"> • nearshore stability

6.4.2. Small-scale evolution, wind, grain-size, and volumetric changes

Between 2005 and 2008, W-NW winds prevailed (Figure 6.6a) with an average direction of 210° during summer and 181° (a higher percentage of NE winds) during winter, with a few episodes of easterly winds (mostly at the end of 2007 and beginning of 2008). Maximum monthly intensities occurred associated with S-SE winds. Wind velocity was generally low to moderate with an average wind velocity of $\sim 4 \text{ m s}^{-1}$ (Figure 6b). Maximum wind velocity occurred in February 2008 (about 17 m s^{-1} , westerly winds; Figure 6.6), with no major high-energy episodes between 2005 and 2008. Maximum wind velocity in 2005 was 15 m s^{-1} (from the SW), in 2006 was 14 m

s^{-1} (from the SW - W), in 2007 was $17 m s^{-1}$ (from the SW), and finally in 2008 was $15 m s^{-1}$ (from the SE).

Beach volume variations were small, with a maximum variation between surveys of $47 m^3$. Slope gradients did not change over the study period. Between 2005 and 2008 the backshore and beach face slopes were in average 0.06 and 0.09, respectively, while at the nearshore, the tidal flat and sand bank slopes were in average 0.01 and 0.02, respectively. Finer sediment was dominant at the tidal flat and sand bank ($d_{50} = 1.3 \phi$), with the tidal flat presenting a relatively high mud content (up to 9%, Figure 6.2c). The beach face was the coarser compartment ($d_{50} = 0.7 \phi$, Figure 6.5). Monthly median grain-size (d_{50}) variations were greater at the backshore and beach face, whereas at the nearshore the sand bank changed less (Figure 6.7).

The total net change in volume across beach morphologies was low and there was an irregular shifting between erosion and accretion around the mean volume (Figure 6.8). Maximum volumetric variation at the backshore and beach-face between 2005 and 2008 was $+0.18 m^3 m^{-1}$ and $+4.88 m^3 m^{-1}$, respectively, whereas maximum volumetric variation at the tidal flat and at the sand bank between 2005 and 2008 was $+4.50 m^3 m^{-1}$ and $-3.45 m^3 m^{-1}$, respectively (Figure 6.8). The nearshore evolved as an independent sub-system, with analogous volumetric variations within it, indicating the absence of cross-shore transport between the tidal flat and the sand bank (Figures 6.8c and 6.8d). The backshore has a minimal variation while beach face shows considerable variation, indicating no similar trend between them (Figures 6.8a and 6.8b). Cross-shore transport between the nearshore and beach face was also limited, at least at the monthly timescale.

Inter-annual analysis revealed that higher mobility occurred in the nearshore (in the sand bank, and close to Ancão tidal channel, Figure 6.9), and at the boundaries between

beach face and tidal flat, and between tidal flat and sand bank. There was no marked seasonality in beach evolution (Figure 6.8e), nor any significant correlation between volume and prevailing wind conditions (Table 6.4).

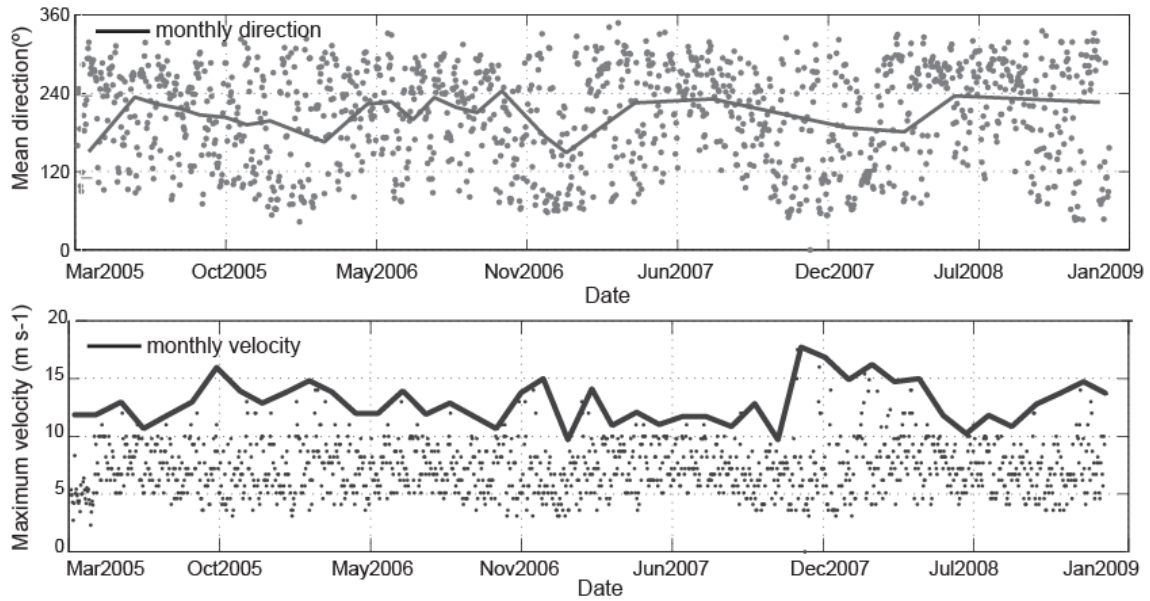


Figure 6.6. (a) daily mean wind direction; and (b) daily and monthly wind maximum velocity.

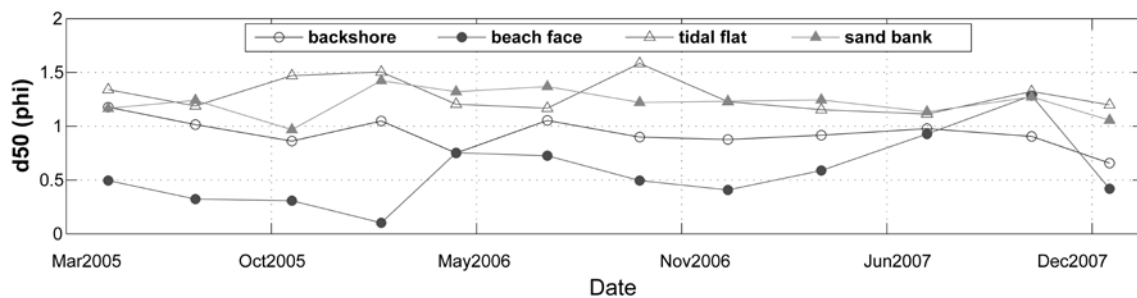


Figure 6.7. Grain size distribution (d_{50}) at profile d .

The results reveal that the influence of wind (and driven wind-waves) on the beach was almost non-existent. The only relationship evident is that the maximum volumetric

variability between 2007 and 2008 (e.g., between the beach face and tidal flat, and scouring of the secondary channel in the sand bank, Figure 6.9) occurred during the prevailing higher-energy wind conditions (higher intensities, Figure 6.6).

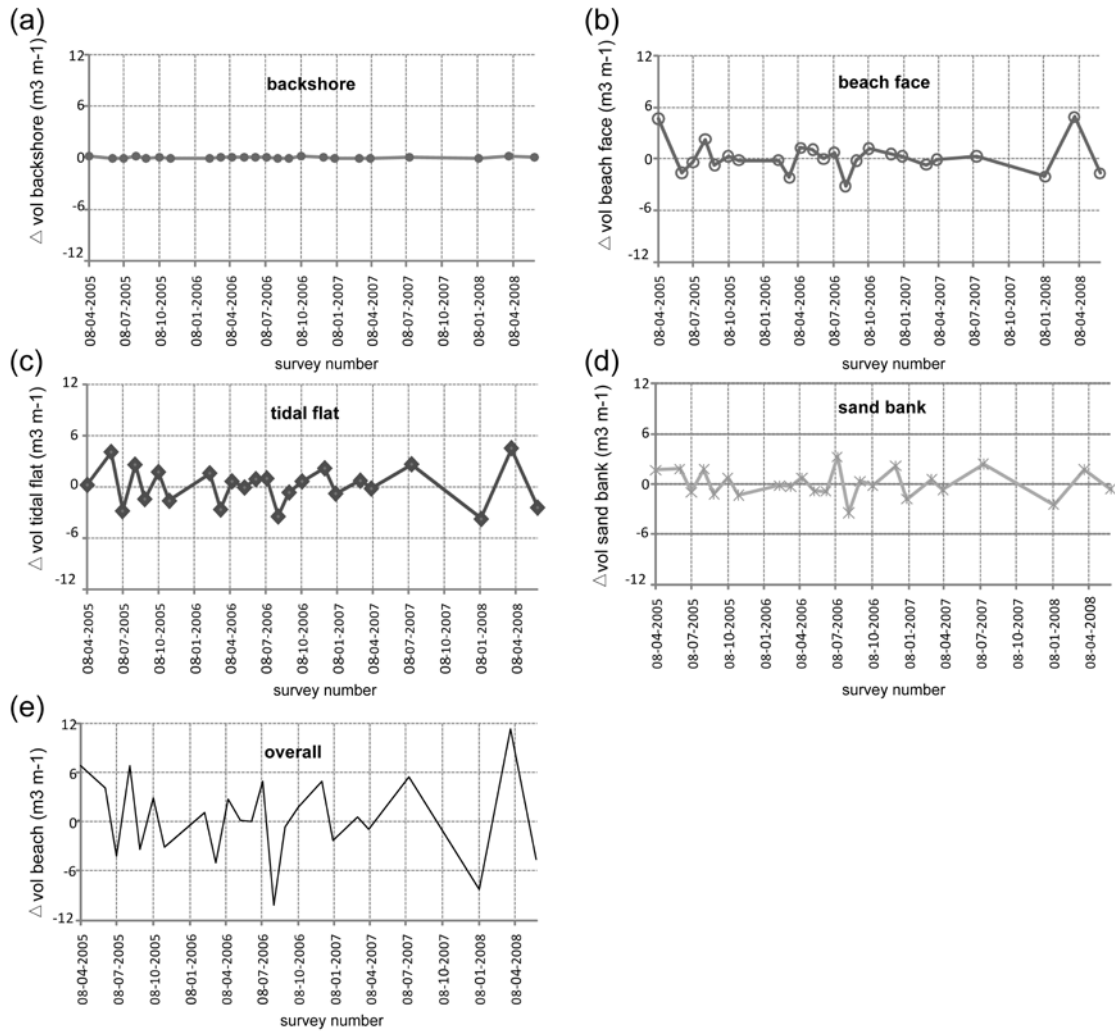


Figure 6.8. Volumetric variations at (a) backshore; (b) beach face; (c) tidal flat; (d) sand bank; and (e) overall area.

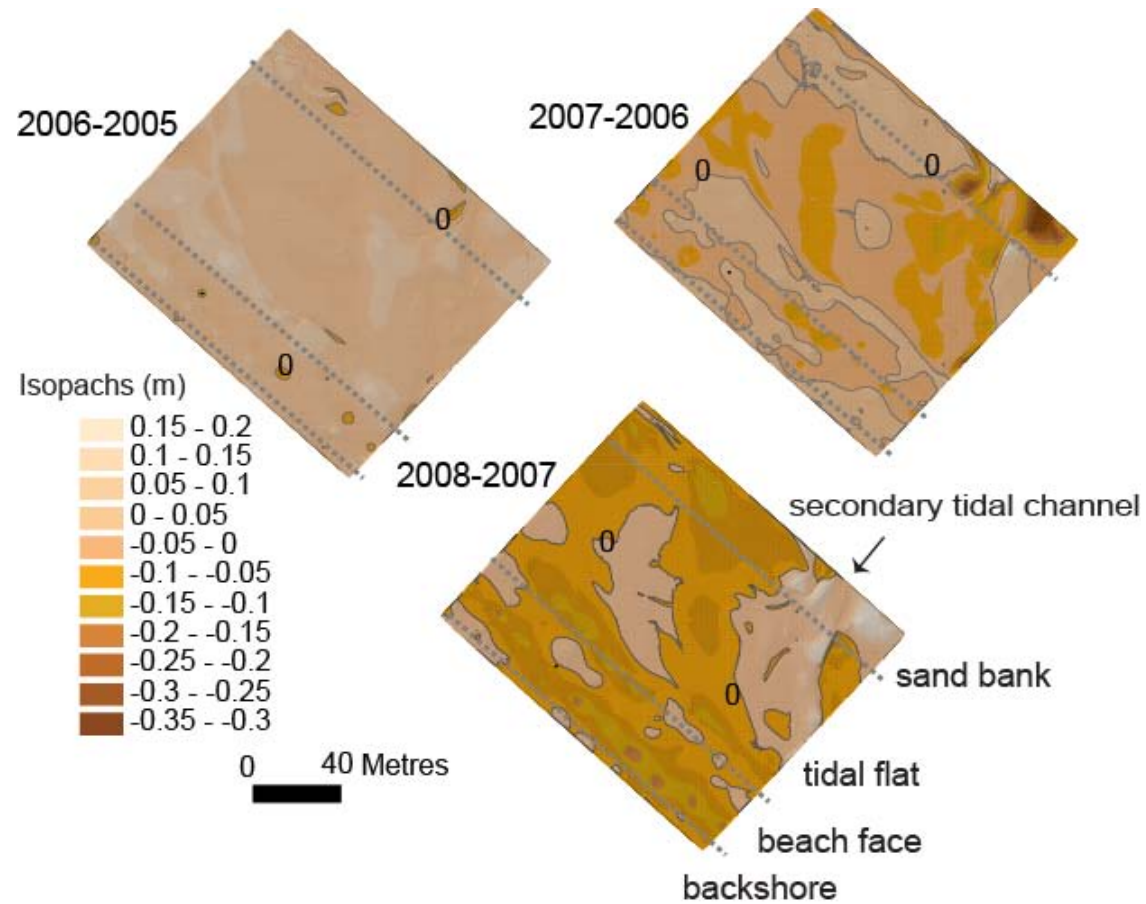


Figure 6.9. Inter-annual elevation changes between 2005 and 2008. Positive elevation changes are expressed with brighter color tones; DEMs were reconstructed as triangular irregular networks in ArcGis 9.3.

Table 6.4. Correlation coefficients between morphology volumes and wind conditions ($p < 0.05$ when $r > 0.39$).

Morphology volume	Correlation with maximum wind intensity	Correlation with mean wind direction
backshore	0.37	0.21
beach face	0.05	0.29
tidal flat	0.37	0.07
sand bank	0.03	0.05

Plan-view advance/retreat of both the beach-face and the nearshore (sand bank crest) was inferred based on reference limit displacements (section 6.3.1). With a few exceptions, the two morphologies presented a displacement tendency towards the Ancão channel (Figure 6.10). Most of the time, the foreshore and nearshore exhibited parallel variations. Displacements were of higher magnitude between 2005 and 2006 (e.g., maximum displacement of +1.40 m of the beach-face during 2005, Figure 6.10).

6. Discussion

6.1. Linking timescales

The studied backbarrier beach is itself a channel margin, and consequently vulnerable to changes performed in the respective tidal channel and surrounding areas (section 6.2.1). Two timescales were articulated to provide a broad overview of changes over the past 60 years. Each timescale denounced a different rate of evolution, the first (large-scale) reporting a modified beach response-type, and the second (small-scale) reporting a natural beach response-type. Besides operating at different time stamps, the timescales are complementary since information can be transferred from one to the other.

At the large-scale beach recorded significant seaward advance, partly from natural beach accretion, but was mostly human imposed (section 6.4.1). Two major periods of

change overcome: between 1947 and 1996 (before human interventions, with minor changes over the beach profile; and after 1996 (prior to human interventions) with deep

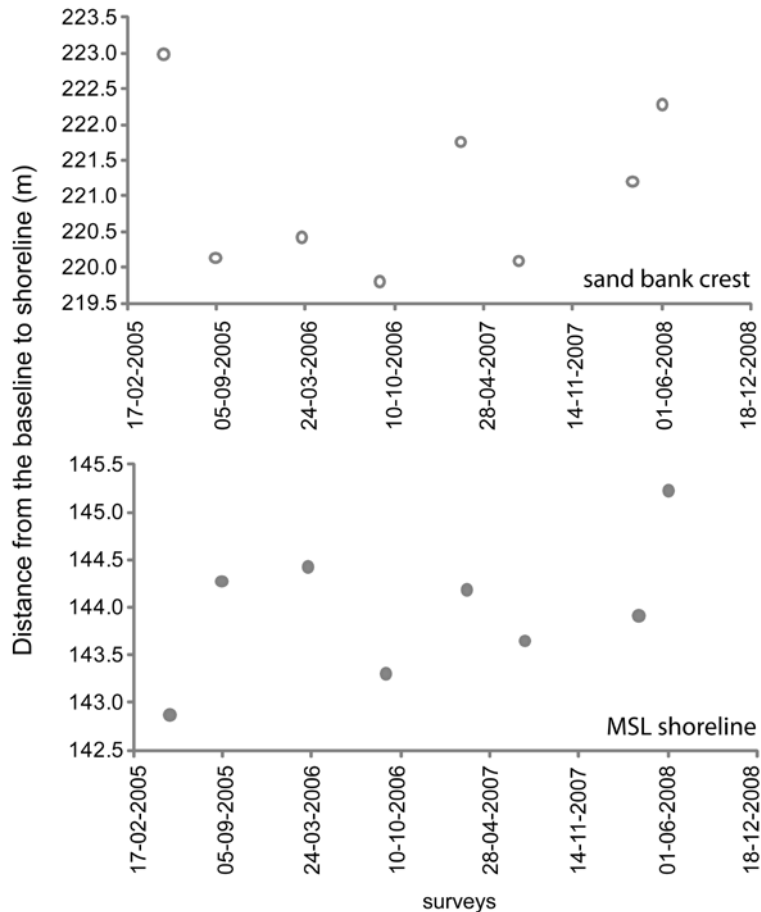


Figure 6.10. Beach and nearshore displacements towards Ancão channel between 2005 and 2008.

changes over beach profile (nearshore development) and surrounding tidal channel.

Human activities leading to change comprised dredging and inlet relocation. Before human interventions the natural backbarrier beach was originally composed of backshore, beach face, and various sand spits forming the tidal flat (between 1947 and 1996, Figure 6.5). The backbarrier, as a channel margin, was relatively stable, but Ancão tidal channel was suffering an intense infilling, like in other parts of the lagoon

(Carrasco et al., 2008). The area was affected by few sand spits and small tidal channels (photo 1989, Figure 6.5), probably relics of a former position of the Ancão Inlet flood delta. Old flood-tidal deltas following inlet/closure is one of the main sources of sediment to backbarriers contributing to lagoon infilling (Godfrey and Godfrey, 1974; Kraft et al., 1979).

Ancão tidal channel infilling motivated dredging operations to facilitate the passage of boats towards the inlet (see dredged volumes in section 6.2.2 and dredged channel at Figure 6.5). Dredging took place far from the backbarrier shoreline, and the Ancão channel axis was transposed seaward (i.e., towards the mainland). As deduced from aerial photograph interpretation, topographic datasets also showed a profound profile change between ~1944-1945 and 2005 (Figure 6.5); the large amount of dredged sand (section 6.2.2) illustrates the magnitude of changes in the tidal channel. Channel axis transposition promoted morphological changes in the landward margin, namely sand bank development. A new backbarrier state was then created integrating different morphologies (backshore, beach face, tidal flat and elongated sand bank; photo 2007, Figure 6.5). After 1996, both beach face and nearshore evolved at different rates. The newly detached sand bank operated as a natural protection to the beach, resulting in nearshore seaward displacement (between 2001 and 2005, Table 6.3; Figure 6.4). The backbarrier shore remained distant from Ancão channel, and became subject to a new hydrodynamic regime. Sheltered conditions were accentuated, with a decrease in currents near the shoreface. Since its artificial construction between 1996 and 2001, the sand bank has evolved by adjusting its shape to the time-varying forcing mechanisms (Figure 6.5). The induced morphological protection by the sand bank allowed the tidal flat to develop, with an increase in fine sediments in the protected area between the new elongated sand bank and the beach face.

Besides dredging, Ancão Inlet was relocated closer to the field site in June 1997 (Vila-Concejo et al., 2004b). Current velocities experienced new changes, with expected stronger currents at the study area (see distance to inlet, Figure 6.4a). Following its eastwards migration (Vila-Concejo et al., 2003) a slow and progressive decrease in current velocities occurred, leading to a new morphological equilibrium.

The small-scale analysis is relevant to understand the period between 2005 and 2007, and illustrates a natural beach response-type, since no human interventions were performed at that period. Rates of evolution between 2005 and 2008 (section 6.4.2) should be in agreement with the morphological changes observed in aerial photographs between 2005 and 2007 (section 6.4.1). Over a monthly time scale beach evolution was small and continuous (Figures 6.8 and 6.9), similar to the very sheltered mesotidal beaches described in Short (2006; tide-dominated beach and tidal flat, section 6.4.2). Beach face and nearshore were independent sub-systems operating in different ways (Figure 6.8d). The only direct relationship between them is that the nearshore offers protection to wind-induced waves that impact on the beach, mainly during mean to low tide. There was no demarcation of seasonal beach behaviour (Figure 6.8e), in contrast to the behaviour described for other low-energy beaches (e.g., Nordstrom 1980, Travers, 2007), and the beach underwent less conspicuous changes in response to relatively energetic events than is the case for high-energy beaches. Contrary to most oceanic beaches (e.g., Wright and Short, 1984; Dubois, 1988), the studied backbarrier showed a reluctance for cyclic changes (Figure 6.8); the small monthly shift between erosion and accretion around the mean volume suggests a slow respond to forcing (rate of reaction; Figure 6.8e). Volumetric changes were small because of the low to moderate prevailing wind intensities (average velocity 4 m s^{-1} , Figure 6.6), and consequently because of the low breaking wave energy due to the limited fetch conditions (the narrow Ancão

channel) and the extension of the low tide terrace (energy dissipation, Carrasco et al., 2011a). In fact, there was a relative independence between forcing and response at the small-scale (Table 6.4). Besides wind and wind-induced waves, tidal currents probably played a greater role in local sediment transfers, as observed by Carrasco et al. (2011a) for shorter (daily) time-scales.

Sedimentary similarities exist between the backbarrier morphologies and the nearby oceanic beach compartments, suggesting that sediment transfers between them had occurred in the past. For instance, the backshore ($d_{50} \sim 1.0 \phi$, Figure 6.7) is an active portion of the beach, being also part of the main barrier structure, and is sediment-fed by aeolian transport (Figure 6.2e), revealing similarities with the nearby dunes ($d_{50} \sim 1.2 \phi$, Matias, 2006). The beach face ($d_{50} \sim 0.6 \phi$, Figure 6.7) presented greater variation in grain-size distribution, and its sediments are related to those of the oceanic beach ($d_{50} \sim 0.5-0.6 \phi$, Matias, 2006). The tidal flat was formed with sediments delivered from Ancão channel and associated sand spits (see Figure 6.5; years 1989, 1996). The tidal flat is presently in a less dynamic stage (photo 2007, Figure 6.5) and is protected by the sand bank and fed through the secondary tidal channel (channel location shown in Figures 6.3 and 6.9). The flat is composed of finer sediments ($d_{50} \sim 1.3 \phi$ and 9% mud content) reworked and deposited in relatively very low-energy hydrodynamic conditions (Carrasco et al., 2011a); episodically, the grain size may increase (Figure 6.7) mainly due to the deposition of shells (Figure 6.2c). The sand bank ($d_{50} \sim 1.2 \phi$; Figures 6.2f and 6.7) was formed by sediments from Ancão channel and from pre-existing sand spits probably associated with a former westward position of the Ancão flood delta ($d_{50} \sim 1 \phi$, Matias, 2006; years 1989 and 1996, Figure 6.5). Presently is a very stable morphology with very small volumetric changes (section 6.2.1 and Figure 6.2f; Carrasco et al., 2011b).

6.5.2. Beach inheritance and resource value

Human activities left a strong imprint and consequent inheritance in the system, instilling morphological changes that were neither erased nor counteracted by the cumulative backbarrier evolution trends (section 6.4.1; Table 6.3). The momentary beach state at the backbarrier beach is not a contemporary response to prevailing hydrodynamics, but reveals the system memory and evolution associated with continuously acting processes (section 6.4.2). Prior to human activities, the backbarrier adjusted slowly (almost nil), and had enough time to defeat the impacts of the channel dredging activity. Morphological changes were of low magnitude proceeding at different spatial and temporal scales from those on the oceanside (as suggested in Nordstrom and Jackson, 1992).

It was demonstrated that a backbarrier stretch can remain relatively unchanged for a long period, due to low-energy conditions, revealing a beach lagging behind prevailing conditions. In the absence of dredging and inlet relocation, the field site would experience much smaller shoreline advance rates than those observed after such activities (between 2001 and 2005, Table 6.3), and the natural beach profile would look very similar to the observed in ~1944 - 1945 (backshore, beach face and sand spits). The backbarrier would remain in a quasi-equilibrium, and shoreline changes would be in phase with the prevailing local hydrodynamic factors (e.g., Houser et al., 2008), with a natural propensity to channel infilling (as observed until 1996, Figure 6.5). Results revealed that backbarrier beaches might present a small chance to reach a full morphological response before the same conditions change and the outcome is that it appears to change little over time (e.g., Figure 6.8e).

Although backbarrier resources may not be immediately appealing, they have value because of their uniqueness, and because they are sometimes close to human populations as is the case of Ancão backbarrier. Ancão backbarrier belongs to the Ria Formosa Natural Park and, as with other backbarrier beaches along the system, is often used for recreational purposes, mainly during summer. Moreover, Ancão channel is one of the most important channels in the Ria Formosa system (Figure 6.1; Andrade, 1990, Salles, 2001), and it allows passage into the inlet by local fishing boats and pleasure craft. Besides recreational uses, the nearshore morphology (tidal flat and sand bank) supports a range of habitats for benthic fauna and substrate for seagrass beds (e.g., Figure 6.2d). The low perceived value of backbarrier beaches often results in loss of beach habitats as the shoreline is modified to accommodate human uses or shore protection methods (Nordstrom, 1992). The results of this study provide reasonable approximations for the beach changes involving both natural and human dynamics (e.g., volumetric variability or shoreline displacement rates) and indicate the slow adjustment magnitude of these very low-energy systems, demonstrated by the longer return time (or even no return) to the previous morphodynamic beach stage. Therefore, any human action (even “building with nature” approaches such as dredging, dune fencing or nourishment) should be regarded as having a “permanent” (decades) imprint, disruptive of the past conditions and generating new conditions.

6.6. Conclusions

There is a paucity of morphological and hydrodynamic datasets collected in fetch-limited environments, and only a handful of studies have reported the morphological dynamics of backbarrier shores. The present study has helped to fill this gap by

analysing both the large- and small scale evolution for Ancão backbarrier beach, Ria Formosa barrier system (southern Portugal). The magnitude of variations within each timescales was evaluated, as was the crossover between the scales involved. The combined analysis revealed the importance of shorter term events caused by human activities in the overall evolution of very low-energy beaches. Results illustrate that regional and large-scale processes, which likely control system response, become overwhelmed by smaller-scale processes related to human activities. It was found that the momentary beach state at Ancão backbarrier beach is a response to prevailing hydrodynamics, but at very slow rates. The capacity of beach to exhibit major morphological changes is small and/or the response time of beach is not necessarily immediate. A backbarrier system does not easily return to previous conditions after human activities. Thus, any intervention will leave a long-term imprint, obliging such a system to adapt and evolve into a new morphodynamic state.

Predicting morphological changes in fetch-limited environments has been shown to be a non-trivial task due to the complexity of processes and the sensitivity of the system behaviour to both natural and human-induced variability. As in other backbarriers, the beach evolution at Ancão is extremely dependent on human modifications made to the dynamics of the surrounding tidal channels. The findings of the study lead to the improvement of management practices in these ecosystems by showing that human actions (even “building with nature” approaches) cause a large-scale environmental footprint.

CHAPTER 7

**FLOOD HAZARD ASSESSMENT AND
MANAGEMENT OF FETCH-LIMITED
COASTAL ENVIRONMENTS**

Abstract

Flooding is a significant environmental threat that can cause loss of human life, damage to infrastructure, disruption to economic activity, and decline in ecological resources in coastal areas. This paper presents a framework for assessing the potential implications of floods in fetch-limited coastal environments (with no significant wave setup), focused on hazard mapping and risk analysis. Hazard maps are based on defined return periods and risk estimates are determined by computing the extent of affected occupied and ecological areas lying below water levels associated with the return periods. For management purposes, this study chooses the adaptive management approach as the most feasible to improve local economies and to mitigate the loss of natural areas, and identifies/recommends specific types of occupation and activity for each flood hazard zone.

The proposed framework was applied to a low-energy fetch-limited beach, Ancão Peninsula backbarrier, located in the Ria Formosa barrier system (southern Portugal). Inundation levels predicted for 1, 10 and 100 year-return periods were 2.08 m, 2.45 m and 3.17 m above MSL (mean sea level), respectively. On this basis, flood impacts were found to be important in occupied areas, generating physical damage to residences and infrastructure. Ecological impacts of floods affected sub-aerial species inhabiting dunes. Several management options deriving from the framework's application were recommended for the Ancão Peninsula.

Key-words: *flooding, fetch-limited coastal environments, risk, adaptation.*

7.1. Introduction

Floods cause great damage in many parts of the world; in the last decade of the 20th century, floods killed about 100,000 people and affected over 1.4 billion in various ways. Six types of floods can be distinguished: coastal floods, flash floods, river floods, drainage problems, tsunamis, and tidal waves (Jonkman, 2005). Coastal flooding constitutes a significant hydrological and geomorphological threat. Besides the economic impacts resulting from damage to infrastructure and to property, hundreds (sometimes thousands) of human lives have been lost in association with coastal flooding (Stanchev et al., 2009). For example, the windstorm Xynthia resulted in the deaths of 47 people including 41 related to coastal flooding, while Hurricane Katrina with a death toll of 1,464 deaths from combined coastal and river flooding showed that deadly disasters do not exclusively affect poor countries (Vinet et al., in press).

Coastal floods (also known as storm surges) occur along the coasts of seas and large lakes, and also in estuaries and backbarrier environments. A storm surge is an abnormal rise of water generated by a storm associated with a particular weather system and with wind forcing water towards the shore (e.g., Komar, 1998; Masselink and Hughes, 2003). When this situation coincides with astronomical high tide at the coast, it can lead to high or extreme water levels and flooding of the coastal area (Jonkman, 2005). Along an open shore, the wave runup elevated by a combination of storm surge, wave setup, and astronomical tide is likely to overtop the elevation of the dunes, and as a result sand is transported across the shore (Sallenger 2000). In fetch-limited areas, wind, wave setup, and wave runup are often much less important compared to the other forcing agents (such as storm surge).

Human activities in the coastal zone increase susceptibility to flooding problems, and increases in both population and building density close to the shoreline contribute to magnify the risk of inundation (Stanchev et al., 2009). Effects of coastal flooding with global warming are also expected to be amplified, as the coastal areas themselves are vulnerable to degradation from sea level rise (SLR; e.g., Wolanski and Chappell, 1996; Morris et al., 2002; FitzGerald et al., 2008; Kirwan et al.; 2010). Although a fairly large number of studies have been dedicated to the examination of coastal flooding along open shores, only a few have been devoted to fetch-limited coastal environments (e.g., Fagherazzi and Priestas, 2011). Fetch-limited areas can experience a combination of two types of flood, coastal and river flooding. Coastal flooding results from the natural susceptibility to changes in water level as a result of fluctuations in tide, surge, and wave setup (e.g., lagoon sites). River flooding is generated by excesses in river discharge, often due to intense rainfall or to manipulation of river flow control structures. The two types of flooding can occur simultaneously (e.g., in estuarine shorelines), enhancing the effects on fetch-limited coastal flooding. The impacts of the combined flood events are strongly influenced by the characteristics of the flood itself and by the characteristics of the flooded area (Jonkman, 2005). Because fetch-limited environments are generally low-lying shores with very slow recovery rates (e.g., Nordstrom and Jackson, 1992; Carrasco et al., 2011a), flooding effects are often recognisable for a long time afterwards. Therefore, efforts to predict extreme hazard impacts and to calculate the expected damage for a given flood event requires an integrative approach that considers both types of flood.

Here we present a framework for assessing potential implications of floods in fetch-limited coastal environments. The main objectives of the research are: (1) to define a

methodology to assess the susceptibility of fetch-limited coastal environments to flooding (hazard mapping); and (2) to identify the most reasonable options available to prevent and mitigate the associated social, economic, and environmental damage. The main advantage of the proposed framework stems from the approach taken, which combines coastal and river flooding and includes hazard source identification and flood hazard mapping. A case study of the Ria Formosa, southern Portugal, is presented as an example of application in backbarrier coasts.

7.2. Methodology

7.2.1. Flood assessment terminology

The body of literature on risk and adaptation contains an array of terms, including vulnerability, sensitivity, resilience, adaptation, adaptive capacity, risk, hazard, coping range, and adaptation baseline, amongst others (IPCC, 2001; Burton et al., 2002; Adger et al., 2003). The relationships between these terms are often unclear, and the same term may have different meanings when used in different contexts and by different authors. Researchers from the natural hazards field tend to focus on the concept of risk, while those from the social sciences and climate change fields often prefer to talk in terms of vulnerability (Downing and Patwardhan, 2003). In order to calculate the damage expected for a given flood event, the most common approach involves combining data on the characteristics of the event (hazard) with information on the assets that would be affected by it (exposure) and with information about the susceptibility of those exposed assets to the particular hazard (e.g., de Moel and Aerts, 2010; Merz et al., 2010). In such studies, hazard is represented in the form of hazard maps, showing flood characteristics

such as inundation depth, flow velocity, inundation duration, and sediment or contamination load (Ward et al., 2011). Exposure is often represented by land use maps, whereby each land use class is assigned an economic value per hectare. Susceptibility is most commonly represented by the amount of damage that would occur per hectare for each land use class and for different values of the flood hazard (Merz et al., 2010).

The framework presented herein deals only with two main concepts: hazard and risk. Hazard is expressed as the characteristics of a particular flood (the flood level attained for a given return period); and risk is expressed as the damage expected from the flood, assessed by calculating the area (m^2) lying under the inundation level for a given return period (the probability of such event; as suggested by Ward et al., 2011). Risk qualitatively evaluates the flooding impacts at a given area in order to improve decisions and actions in the flood management process. Hereinafter, people and goods are referred to as ‘occupancy’, which includes population density, physical infrastructure (such as roads, phone lines, and power lines), residential houses, and commercial and industrial buildings and their contents.

In this study, risk analysis conceives inundation levels for three return periods: two shorter return periods of 1 year and 10 years, and a longer return period of 100 years. Shorter return period floods, i.e., more frequent floods, impact areas of low elevation, while the longer return period floods (i.e., lower probability floods) reach higher water levels. Three zones of inundation risk are distinguished according to flooding probability: the high-risk zone lies below the 1 year return period flood level, the moderate-risk zone lies between the 1 and 10 year return period flood levels, and the low-risk zone lies between the 10 and 100 year return period flood levels. Areas lying above the 100 year return period flood level have a very low risk of flooding under the

temporal frameworks used by most management plans. The 10 and 100 year return period flood levels have previously been used for coastal inundation mapping (e.g., Snoussi et al., 2008; Ward et al., 2011), as well as for river inundation mapping (Federal Emergency Management Agency, 2011). The 1 year return period is additionally herein introduced to provide an approximation of the minimum flood level, and consequently minimum flood impacts, from a baseline year.

7.2.2. Framework variables

Two types of variable are considered in the proposed framework: (a) variables affecting water levels; and (b) variables affecting flood impacts. The first type of variable considers any contributor that changes the water level at a fetch-limited site, and includes astronomical tide, storm surge, SLR, and river discharge. The second type of variable considers the main physical constraints able to interfere with (i.e., amplify or minimize) flood impacts, and includes geomorphology, ecology, and occupancy. Local geomorphology affects the delimitation of inundation levels, and consequently the impacts of a given flood. For instance, gentle, low-lying backbarriers are more easily inundated than are higher and steeper ones. A higher percentage of occupied area increases local susceptibility because, in comparison with pristine areas, higher flood impacts are expected. Ecological impacts need to be evaluated considering the amount of stress brought to bear by the flood, which may vary from small impacts (e.g., for sand bank benthic species) to total disruption (e.g., for sub-aerial dune species).

Astronomical tides, storm surge, and river discharge all combine to produce a local water level. Local tide gauges are the best instruments to obtain a time-series of such water levels. In the absence of local tide gauges, the three forcing agents need to be

evaluated separately. In such an evaluation, astronomical tides can be modelled. Storm surges can be obtained from tide gauges in the vicinity of the water body. River discharges can be obtained from river gauges or from dam control charts. SLR estimates can be obtained based on IPCC (2007) projections for future global warming scenarios involving different greenhouse gas emissions (e.g., B1, A1B, and A1FI).

7.2.3. Development of the framework

The development of the framework embraces three main steps (Figure 7.1):

(1) *Hazard sources*, involving the characterisation of variables affecting water levels, and the probability of occurrence of different water levels. Hazard source identification follows closely the traditional techniques used for coastal flooding hazard determination for open shores, yielding flood levels for 1, 10, and 100 year return period events;

(2) *Flood hazard mapping*, which is analogous to the flood hazard mapping defined in studies of river flooding. The respective flood extents for 1, 10, and 100 year return periods are determined by overlapping the obtained flood levels onto a digital elevation model (DEM). The result is a tri-zonal flood hazard map; and

(3) *Risk analysis and management*, which includes the identification and quantification of both ecological and occupancy risk by overlapping the flood hazard maps with variables affecting and affected by flood impacts (e.g., ecology, and occupation). The outcomes are risk evaluation and a local management strategy.

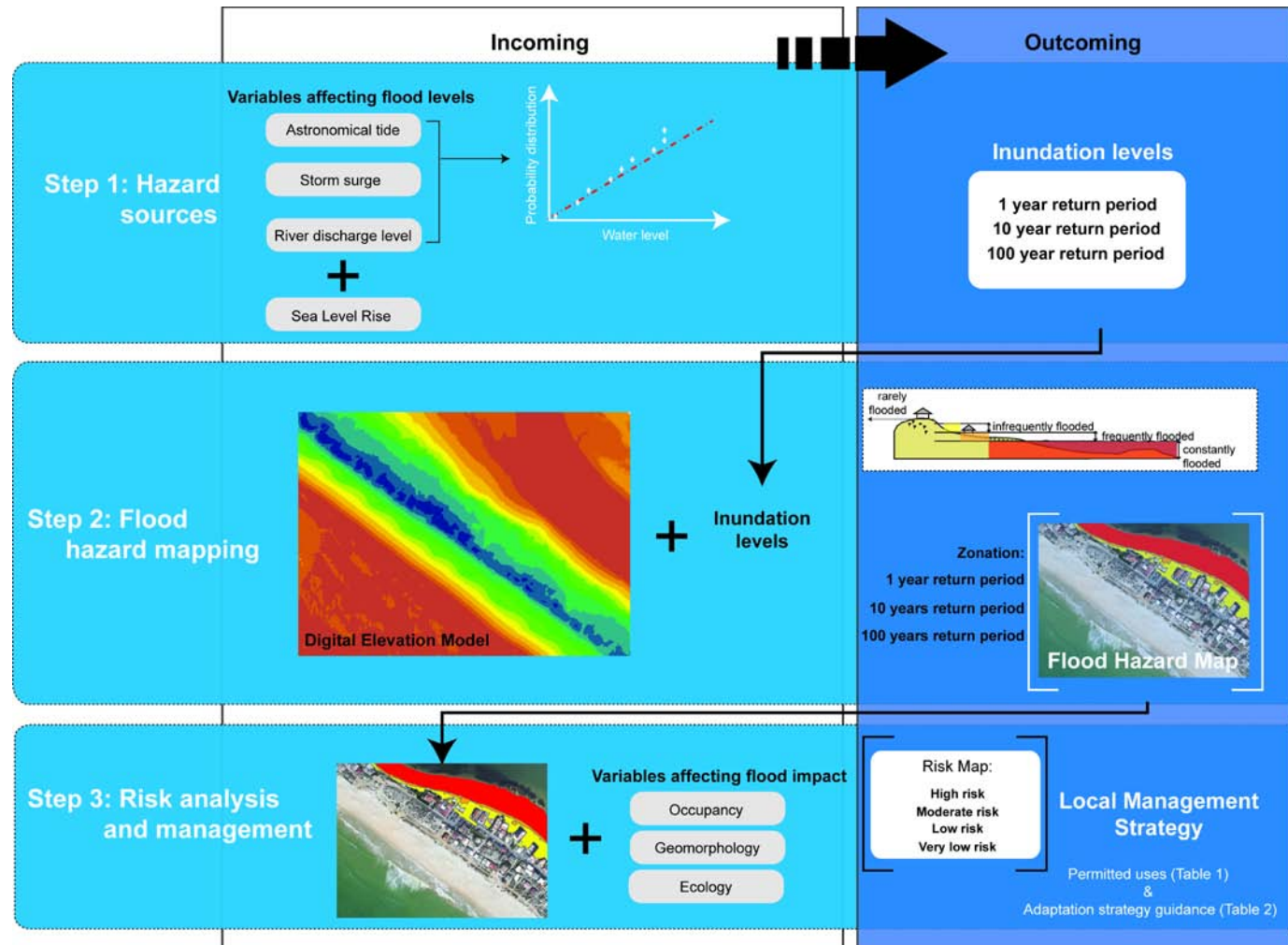


Figure 7.1. Schematic methodology for the flood hazard assessment and management of fetch-limited coastal environments.

Management options incorporate adequate usage/abandonment of flooded areas, and are discussed on the basis of the obtained maps.

7.2.3.1. Hazard sources

Flood levels for the chosen return periods are provided by the combination of variables affecting the water levels: astronomical tide, storm surge, SLR, and river discharge level (step 1 in Figure 7.1). Maximum annual astronomical tide, storm surge, and river discharge levels are determined along representative time series (based on tide level gauges). A probabilistic distribution (e.g., lognormal, normal, Gumbel, Weibull, amongst others) is chosen according to best-fit criteria to model the annual maxima probability distribution for each variable. From the distribution model, three water levels (each of which includes astronomical tide + storm surge + river discharge level) are calculated for the 1, 10, and 100 year return periods, respectively. SLR is also estimated for each of the 1 (actual level), 10, and 100 year return periods. Unlike the IPCC third assessment report (2001), the fourth assessment report by IPCC (AR4, 2007) does not provide time-series for SLR projections through the 21st century. However, SLR projections are provided by Hunter (2010), who scales the maximum and minimum values of IPCC AR4 projections between 1990 and 2100 and presents the projected sea-level values for the 5th and 95th percentiles. From Hunter's (2010) projections, and from a baseline year, SLR for the next 10 and 100 years can be determined.

7.2.3.2. Flood hazard mapping

The respective spatial limits of the three flooded zones depend on local morphology (for which a topographic map or DEM is needed; see step 2 in Figure 7.1). Flood hazard maps for fetch-limited beaches are built based on the flood hazard area definition for rivers by the Federal Emergency Management Agency (2011) in the Flood Insurance Programme. The floodway area (in the rivers approach) is hereinafter referred to as the ‘constantly flooded zone’, and represents the topographic area where the principal floodwater flow occurs (e.g., intertidal zones; step 2 in Figure 7.1). The lower limit of the constantly flooded zone is the principal floodwater flow (tidal channel), and the upper limit is the 1 year return period flood level. It can be alternatively defined as the area below the maximum spring high tide level for meso- and macro-tidal areas with low surge or river influence. The ‘frequently flooded zone’ lies above the constantly flooded zone and does not experience such strong currents as the constantly flooded zone; the upper limit of the frequently flooded zone is provided by the intersection of the topographic map with the defined 10 year return period level. The upper limit of the ‘infrequently flooded zone’ is defined by the 100 year return period flood (generally consisting of dunes and occupied areas), and represents the area that is occasionally flooded. Areas lying above the 100 year-return period coastal areas are classified as ‘rarely flooded zone’ (step 2 in Figure 7.1). If appropriate, other return periods might be considered, in accordance implying different spatial delineations to the hazard mapping. For example, shorter return periods (e.g., 5 or 25 year return period) might be helpful to bound small hazard areas of particular interest and to define readjustments to temporal changes in flood exposure.

7.2.3.3. Risk analysis and management

The flood damage assessment is obtained by overlapping the flood hazard areas (section 7.2.3.2) with geomorphology, ecology, and occupancy (step 3 in Figure 7.1). Risk is categorized by the estimate of the affected areas for each given return period (risk estimates), or can be perceived and qualitatively identified by direct map analysis. Risk analysis is conducted for both ecological and occupancy areas: ecological risk represents, for example, the potentially flooded dune areas, protected landscapes, and habitats; while occupancy risk represents the potential flooded occupied areas or the overall affected population. A given economic value can be attributed to the occupancy area (per m², for instance), thereby allowing an economic estimate of the risk. Ecological and occupancy areas contained in the constantly flooded zone exhibit high risk; whilst areas contained in the rarely flooded zone exhibit very low risk (consistent with the definitions provided in section 7.2.1).

Management is accomplished after reviewing past threats and effects, and must be in agreement with local uses and legislation, including coastal management policies. It requires site-planning and identifying priority management interventions to sustain the provision of ecological, economic, and cultural values (Gilman, 2002). After risk analysis, preventive and mitigation measures are proposed according to the frequency of flooding (step 3, Figure 7.1). The main objective is to solve flood damage problems (both ecological and occupancy) identified in the hazard maps. Management strategy depends on the prescribed policy. Klein et al. (1999), proposed three major responses in coastal management (in their case applied to sea level rise): the first was “classical” total protection (hold the line), trying to retain the current uses at all costs; the second was ecological and occupancy adaptation to hazard; and the third, “do nothing”,

corresponds to no action (assuming that there are economic and ecological values which are jeopardised). The present framework envisages just one response strategy to minimize flood risk, adaptation. The adaptation option is more suitable from an economic point of view since capital expenditure, which is diminished in such an option, could otherwise be a hindrance for the implementation of a given measure (Carter, 1988). In contrast, classical protection measures are often costly and require continuous maintenance, and do not discourage unwise development. The “do nothing” strategy allows risks to occur with important social and economic consequences that often oblige authorities and society at large to take *ad hoc* short-term economic measures such as emergency assistance, refunding, rebuilding, and financial compensation. The adaptation strategy engenders gradual costs, spread over time, but also allows both maintenance and modification of land uses and activities in flood hazard zones.

Table 7.1 summarizes potential uses and ‘added value’ uses contemplated for flood hazard zones. Foreseen uses (Table 7.1) are part of the proposed framework (step 3 in Figure 7.1), and were identified in accordance with the following management guidelines: natural processes should be subjected to minimal interference; the uses need to be in agreement with previous coastal and marine management planning, as well as with the relevant social and economic context; the plan foresees non-permanent uses (adaptable or transferable); management options assume that human residences in flood hazard areas represent higher risk than do non-residential facilities (e.g., sports facilities), and therefore require greater adaptation efforts; and each adaptation measure must be evaluated with respect to its economic, social, and environmental benefits.

Table 7.1. Permitted uses in flooded areas, developed within the proposed framework.

Zonation	Foreseen uses	Occupancy regime
<p>High risk (constantly flooded)</p>	<p>The user cannot erect any structure or obstruction, or open any excavation or deposit any material or substance. All construction/re-adaptation projects should be subject to a review process and to environmental assessment. Permitted uses include:</p> <ul style="list-style-type: none"> • aquaculture, shellfish and oyster exploitation, salt exploitation, and other economic exploitation related to marine resources; • recreational/sports use (jet skiing, canoeing, sailing, etc); • beach leisure features (umbrellas, tents and beach chairs); • facilities or structures for boat anchoring; • structures for improving navigation; • piers and pilings; • elevated footpaths; • facilities for educational purposes and ecotourism; and • maintenance of natural vegetation, and nature preservation areas. 	<p>Withdrawal of permanent structures</p> <p>Seasonal occupancy</p>
<p>Moderate risk (frequently flooded)</p>	<p>All construction/re-adaptation projects should be subject to a review process. Permitted uses include:</p> <ul style="list-style-type: none"> • manufactured homes, such as fishermen’s houses; if the flood damage is initially minimized, the elevation of the lowest floor should be located at a position higher than the projected level of inundation; • beach leisure; • parks and recreational uses; • facilities and structures supporting seasonal holiday houses, restaurants, and commercial stalls, if the flood damage is initially minimized. The structures should be elevated and anchored to a foundation system designed to resist flotation, collapse, and lateral movement; • elevated footpaths and boardwalks; 	<p>Seasonal and permanent occupancy (from years to decades)</p>

	<ul style="list-style-type: none"> • non-permanent facilities for sports practice (e.g., football and basketball fields, sports areas); • picnic areas and public garden facilities; • wildlife and nature preservation areas; and • environmental protection measures (e.g., sand fencing). 	
<p>Low risk (infrequently flooded)</p>	<p>All construction/re-adaptation projects should be subject to a review process. Permitted uses include:</p> <ul style="list-style-type: none"> • residential houses (elevated); • facilities and structures supporting commercial uses (elevated); • walkways and accesses to residences (non-vehicular); • permeable parking areas; • shallow water catchments and drainage systems; and • sand fencing. 	<p>Permanent occupancy (from years to decades)</p>

For continuum management purposes, besides the durability and effectiveness of any intervention proposed in Table 7.1, maintenance costs in the future must be resilience, such as the protection and regeneration/stabilization of dune plants, the maintenance of sediment supply, and the provision of buffer zones, amongst others (Defeo et al., 2009). Uses with ‘added value’ (Table 7.1) should therefore contribute to the sustainable use of coastal areas, including the enhancement of ecological value and the strengthening of economic activities simultaneously with the minimisation of potential risks. The proposed uses and strategy require the development of an Adaptation Strategy Guidance before the process of intervention (see Table 7.2 for an example). This is a generic guidance agreement detailing the milestones for adaptation, and the actors involved in each milestone. It helps to accelerate the adaptation process and to prioritize uses reported in Table 7.1 for a given location, according to local economic, social, and environmental constraints.

Table 7.2. Example of an Adaptation Strategy Guidance.

Milestones	Actors involved
(A) Hazard Maps: determination of inundation scenarios and generation of vulnerability maps	Field/cartography technicians and scientific community
(B) Social and economic survey: identification of all socio-economic partners	Socio-economic skilled technicians and scientific community
(C) Public participation: incorporation of community-based principles in planning and in collaborative activities	Decision-makers and community
(D) List of non-prohibited and prohibited interventions within the legal framework	Urban planning and legal skilled technicians
(E) Estimated expenses and contingency analysis report: identify possible uses and associated costs	Urban planning and economy skilled technicians
(F) Costs vs. benefits report: recognise other uses with ‘added value’	Decision-makers
(G) Prioritize goals and construct intervention plan	Decision-makers and community

7.2.4. Sites for application of the framework

The framework is specific to fetch-limited coastal areas with risk of inundation provided by changes in astronomical tide, storm surge, and river flow. The proposed framework cannot be applied to locations with greater fetch conditions or sheltered locations with relevant wave energy. Apposite coastal environments for the framework's application include the unvegetated or partially vegetated sand, gravel, or shell intertidal beaches in estuaries, enclosed bays, lagoons, and fjords connected to oceans or seas where the fetch distances for local wave generation are in the order of a few kilometres or less. They should be exposed only to very small local waves (significant wave heights $H_s < 0.2$ - 0.4 m; peak period, $T_{\text{mean}} < 2 - 3$ s), where wave setup and runup are negligible. In addition, adequate water level records and topographic data (step 2 in Figure 7.1) must be available.

The developed framework should be able to be applied to a wide geographic dispersion of sites, including: the tide-dominated and irregularly flooded south-east Australian estuaries, such as Port Stevens (e.g., Roy et al., 2001; Vila-Concejo et al., 2010); the estuarine beaches found at Duck, North Carolina (Nordstrom, 1992); the rias-type beaches, like those found along the Galician coast (e.g., Costas et al., 2005); bays such as the Delaware bay and Chesapeake bay, both large drowned river estuaries, (e.g., Jackson, 1999; Lewis et al., 2005) and San Francisco bay (Nordstrom, 1992); lagoons such as Patos Lagoon located in Rio Grande do Sul (e.g., Calliari and Silva, 1998); some coastal deltas, for example the very sheltered areas of Ebro Delta (e.g., Alvarado-Agillar and Jiménez, 2009); and the very low-energy environments at Florida Keys (e.g., Ragan and Smosna, 1987) or the very sheltered sandy beaches of Southwestern Australia (e.g., Hegge et al., 1996), if they do not present a significant wave setup

contribution. The specific requirements for management of these coastal areas (step 3 in Figure 7.1) will vary between the various fetch-limited environments as a function of type, oceanographic and climatic setting, level of development, institutional framework, and cultural norms, amongst other factors. Only small amounts of effort should be required in order to adjust the proposed methodology to each field site.

7.3. Test case: Ancão backbarrier

7.3.1. General characteristics

The framework as described was applied to a very fetch-limited backbarrier, Ancão Peninsula backbarrier, located in the westernmost part of Ria Formosa (Figure 7.2). Ria Formosa is a multi-inlet barrier island system located on the southern Portuguese coast, with a configuration that consists of one peninsula and six islands extending over a total distance of around 56 km. The entire Ria Formosa backbarrier covers an area of $8.4 \times 10^7 \text{ m}^2$ (Andrade, 1990), being characterised by: i) large salt marsh areas with a dense distribution of shallow secondary tidal channels and creeks, with sediment composed of silt and fine sand (Bettencourt, 1994); ii) large sand flats partially flooded and reworked during spring tides (Pilkey et al., 1989); and iii) a complex network of natural and partially-dredged channels, which narrow and shoal in the upper regions of the system (Salles, 2001). The inner coastline, along the backbarrier islands and peninsulas, is characterised by low, narrow sandy beaches with areas of salt marsh, and washover plains (Andrade et al., 1998).

Like many other lagoon systems, the Ria Formosa system is an ecologically rich environment, with areas of high-interest habitats. At the same time it is actively used for

aquaculture and shellfish exploitation. The lagoon is a very low-lying area with depths generally lower than 2 m below MSL, and supports marked sedimentary and morphological variability (Andrade, 1990). The Ria Formosa system was classified as a Natural Reserve in 1978, a Natural Park in 1987, and is now part of the Natura 2000 network. The system is characterized by high faunistic diversity, has national importance as a nest-building zone, and assumes international relevance for bird migration. Moreover, it is considered to be one of the world's noteworthy wetland areas, and is protected by the RAMSAR and BERNA conventions. The overall backbarrier has, therefore, an intrinsic natural/ecological susceptibility to natural hazard events, including flooding.

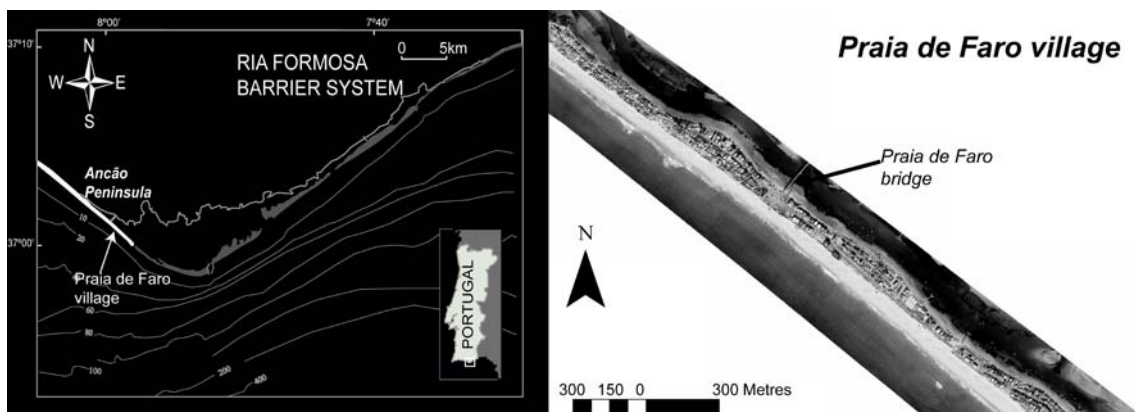


Figure 7.2. Map of Ria Formosa barrier system showing the locations of the Ancão Peninsula and Praia de Faro village (left), and aerial photograph of Praia de Faro village (right).

Tides in the area are semi-diurnal, with average ranges of 2.8 m and 1.3 m for spring and neap, respectively. However, maximum ranges of 3.5 m can be reached during spring tides. Offshore waves have mean annual H_s of 0.92 m (Costa et al., 2001);

however the field site is sheltered from ocean waves. Due to extremely small fetch conditions, wind-generated waves are in general small ($H_s < 0.1$ m; $T_{\text{mean}} < 1$ s, Carrasco et al., 2011a). Wind speed is on average 3 m s^{-1} (Andrade, 1990), with prevailing directions from W (~20 %) which do not causes wind setup at the backbarrier since they are generally directed offshore (from the barrier to the lagoon). There is no river draining into the water body, and the fluvial contribution from small streams is negligible.

The Ancão Peninsula backbarrier is dominated by sandy beaches backed by dunes, and has a high density of occupation, particularly in the central part of the peninsula (Table 7.3, Figures 7.2 and 7.3). The peninsula is a thin barrier, with several strips of infrastructural development running parallel to the shoreline, denoting problems of urban planning (Figure 7.3 and Table 7.3). The peninsula is connected to the mainland via a small bridge (built in the 1950s, Figure 7.2), and presents a high percentage of impermeable surfaces (mainly roads, small parking lots, and accesses to residences; Figure 7.3). Until the mid-1950s, Praia de Faro was occupied mainly by fishermen, since when recreational and touristic uses have increased significantly. Therefore, there is high potential occupancy damage by extreme events; multiple events over the past few decades have been reported by residents (recent examples are displayed in Figure 7.4).

Table 7.3. Morphological characterization of Ancão Peninsula backbarrier, and social context.

Features	Characteristics
Morphology	Uniform shoreline, dominated by sandy beaches, contacting the tidal channel through an extensive low tide terrace (finer sediment content, with silt and mud); sometimes intercepted by low lying vegetated areas (dune and salt marsh). Salt marsh portions occur at the westernmost parts of the backbarrier; and Important from the natural conservation perspective (birds, seagrass, sea horses).
Occupancy	Faro bridge connects the peninsula to mainland; Residences arranged continuously in alongshore line; densely occupied (mainly houses and other human facilities) in the central part of the peninsula; High percentage of impermeable substrata covered by small roads and piers for boat anchoring; Elevated footpath and dune fencing in the eastern half of the peninsula; Intense boat traffic (e.g., fishing boats and recreational) through the tidal channel (Ancão tidal channel); Major economic activities comprise shellfish gathering; and Commonly used for nautical sports (e.g., surfing, kite surfing, canoeing).
Coastal protection	Past sand renourishment, sand fencing, and elevated pathways.
<p><u>Community and stakeholders:</u> local habitants and end-users (including tourists), fishermen and other community members living off marine resources, Faro city council, and Natural Park of Ria Formosa.</p> <p><u>Decision-makers:</u> regional authorities, port authorities, Faro city council, and Natural Park of Ria Formosa.</p> <p><u>Main Legislation:</u> regulation of Natural Park of Ria Formosa, regulation of city council (POOC, Regional Coastal Management Plan), and legal rights conditioned by sectorized coastal plans.</p>	

7.3.2. Framework application

7.3.2.1. Step 1: hazard sources

Backbarrier flooding was estimated from the baseline year of 2010. Due to the very limited-fetch conditions, wave setup is minimal, which suits the application of the developed framework. Fluvial discharge is almost non-existent, therefore it does not

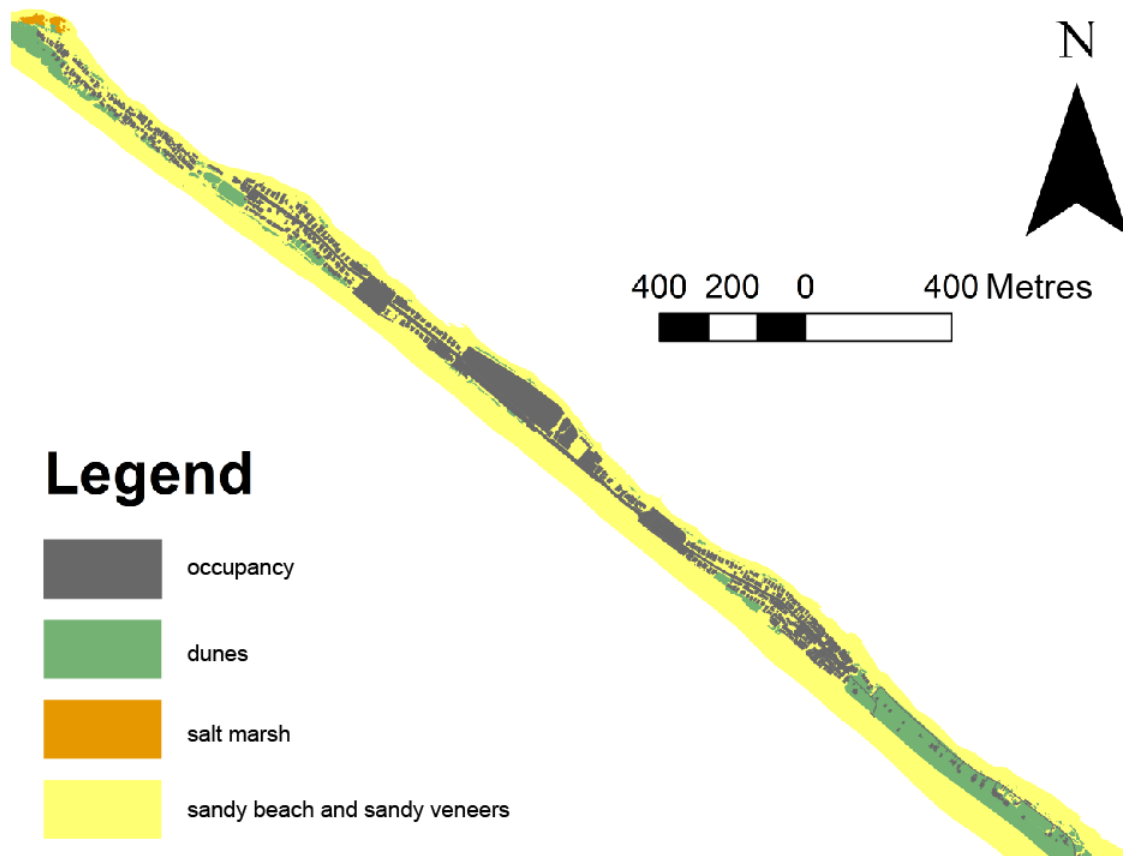


Figure 7.3. Land uses of Ancão Peninsula.

interfere with flood water level. Regional water sea levels (astronomical tide + storm surge) were obtained from Puertos del Estado (2011) datasets for Huelva tide gauge (around 60 km from the study area) for the period December 1996 to July 2011. The mean sea level (MSL), maximum annual astronomical tide, and storm surge levels were extracted. A probability distribution model was fitted to the water levels (Figure 7.5a), and the water levels associated with the 1, 10 and 100 year return periods were determined. Extreme value or reliability-type distributions (lognormal, normal, Rayleigh, Weibull, Gumbel) were tested, and the best fit was obtained using a lognormal distribution. SLR was further incorporated by using the moderate scenario, A1B, from IPCC (2007), which assumes a moderate rate of greenhouse gas emissions

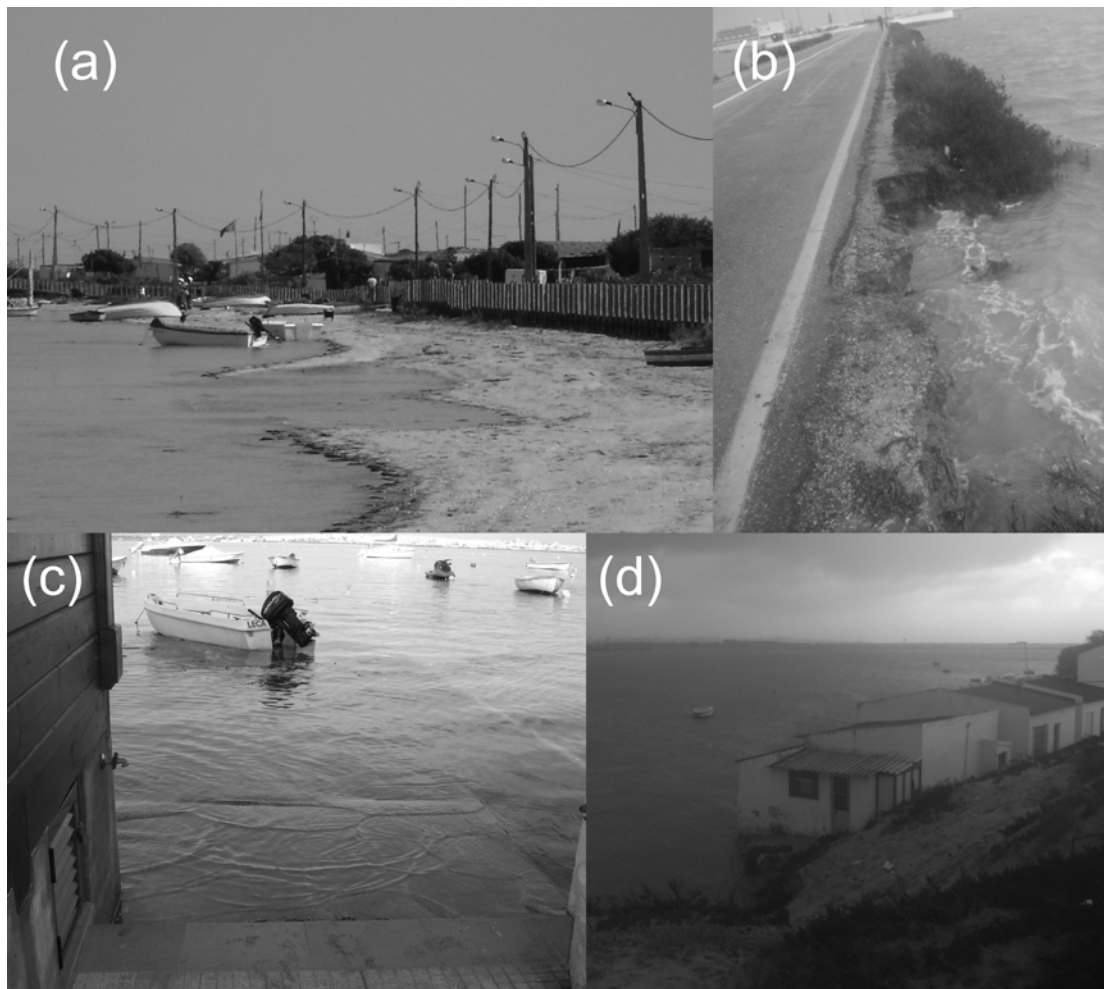


Figure 7.4. Examples of inundation attained at: (a) Ancão backbarrier during the equinoctial tide of October 2006 (with a maximum storm surge of 14 cm); (b) Praia de Faro bridge during the equinoctial tide of March 2010 (with a maximum storm surge of 58 cm; photograph courtesy of Elsa Caetano); (c) the eastern part of Ancão backbarrier during the equinoctial tide of September 2011 (with a maximum storm surge of 10 cm); and (d) the western part of Ancão backbarrier during the equinoctial tide of March 2010 (photograph courtesy of Elsa Caetano).

(related to the 95th percentile range projections; see Hunter, 2010). SLR projections for the 1, 10, and 100 year return periods, from the baseline year of 2010, under the A1B scenario are 0.059 m, 0.096 m, and 0.697 m, respectively. The final projected long-term

inundation levels predicted for the 1, 10, and 100 year return periods were, respectively, 2.08 m, 2.45 m, and 3.17 m above MSL (outcoming step 1 in Figure 7.1). Sources of uncertainty in the method's application are related to water level measurement uncertainty (tide gauge maximum error = 0.5×10^{-3} m) and lognormal distribution fitting (standard error of 0.01 m).

7.3.2.2. Step 2: flood hazard mapping

Local topography was derived from DEMs based on Airborne LIDAR data collected in November 2009. For analysis purposes, the irregularly spaced (around 10 points per m^2) LIDAR data were interpolated to DEMs with a 0.5 m grid resolution. The vertical and horizontal accuracies of the LIDAR measurements are estimated to be in the range 5-10 cm. Vertical and horizontal differences between LIDAR data and concurrent surveys at Ancão Peninsula are in the order of 7-10 cm, as reported in the LIDAR dataset. Flooded zones were delimited over the DEMs (Figure 7.6), following the methodology described in section 7.2.3.3 (step 2 in Figure 7.1).

7.3.2.3. Step 3: risk analysis and management

Different inundation scenarios are revealed with the delimitation of the 1, 10, and 100 year return periods (step 3 in Figure 7.1). The risk map (Figure 7.7) was obtained from the overlapping of the land-use map (Figure 7.4) with the hazard map (Figure 7.6). Risk estimates are presented in Table 7.4 as inundation areas (m^2). For Ancão backbarrier, the high-risk zone includes more than 148,000 m^2 of backbarrier sandy beaches and sandy veneers, and 2,500 m^2 of dunes.

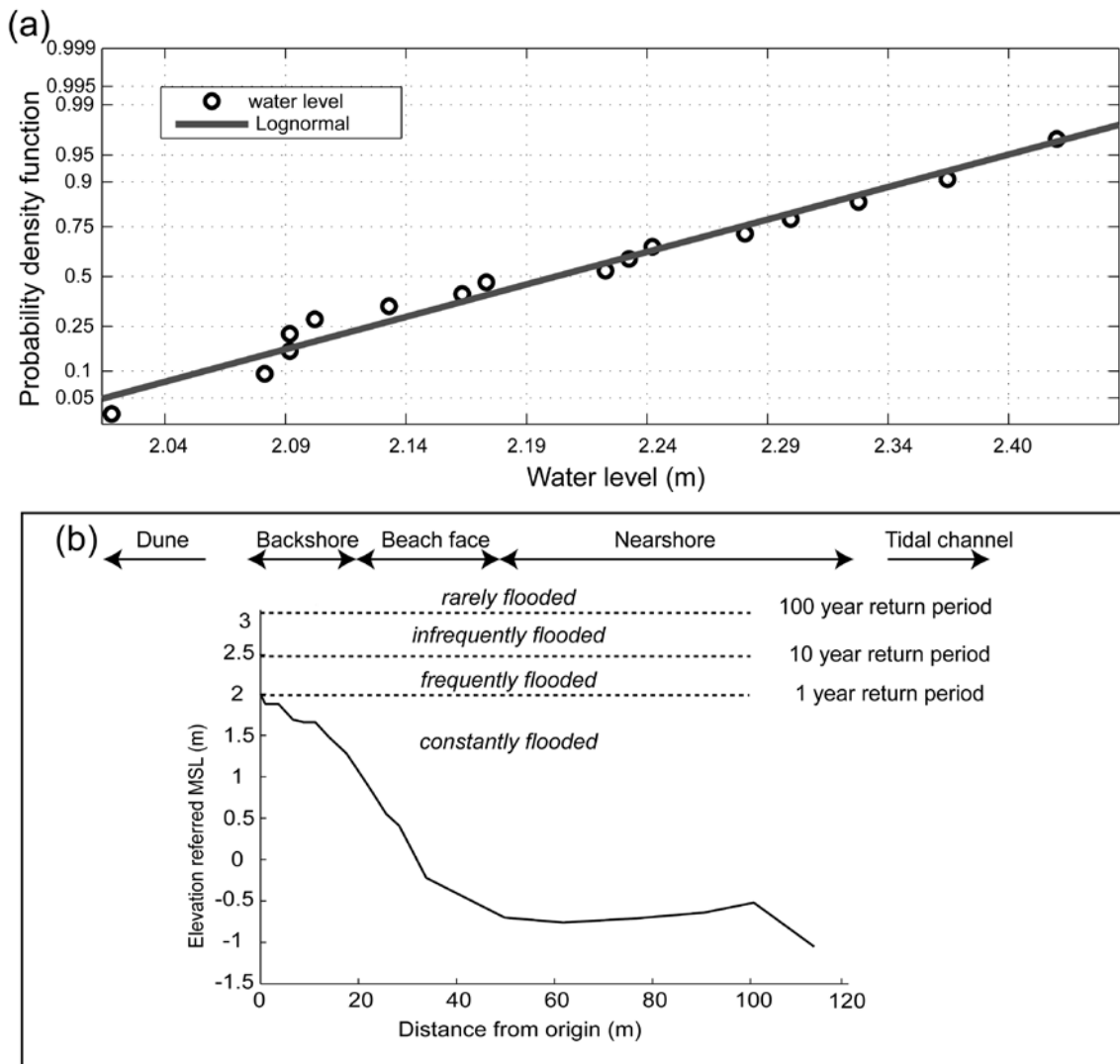


Figure 7.5. (a) Lognormal distribution fitting to annual maximum tide levels; and (b) representative topographic profile at Ancão backbarrier showing the main morphological segments (backshore, beach face, and nearshore) and inundation levels.

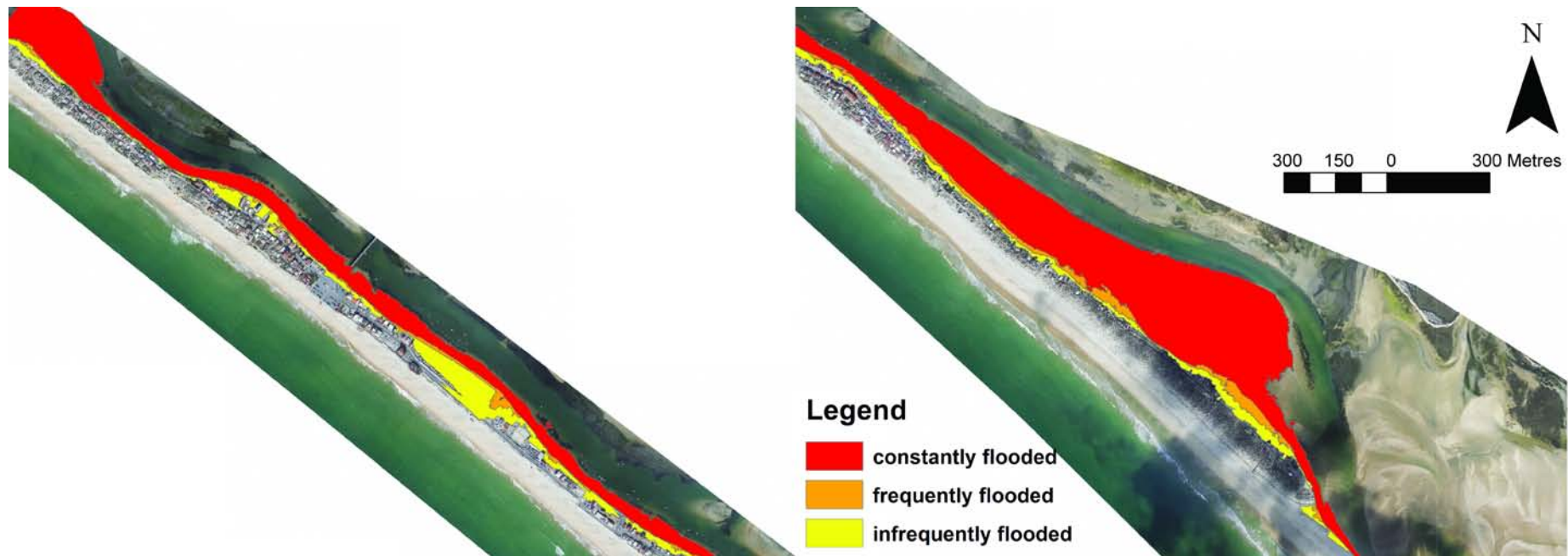


Figure 7.6. Hazard map for Ancão Peninsula for flood zones <1 yr return period (constant flooded), 1-10 yr (frequently flooded), and 10-100 (infrequently flooded) (lain over a 2009 orthophoto).

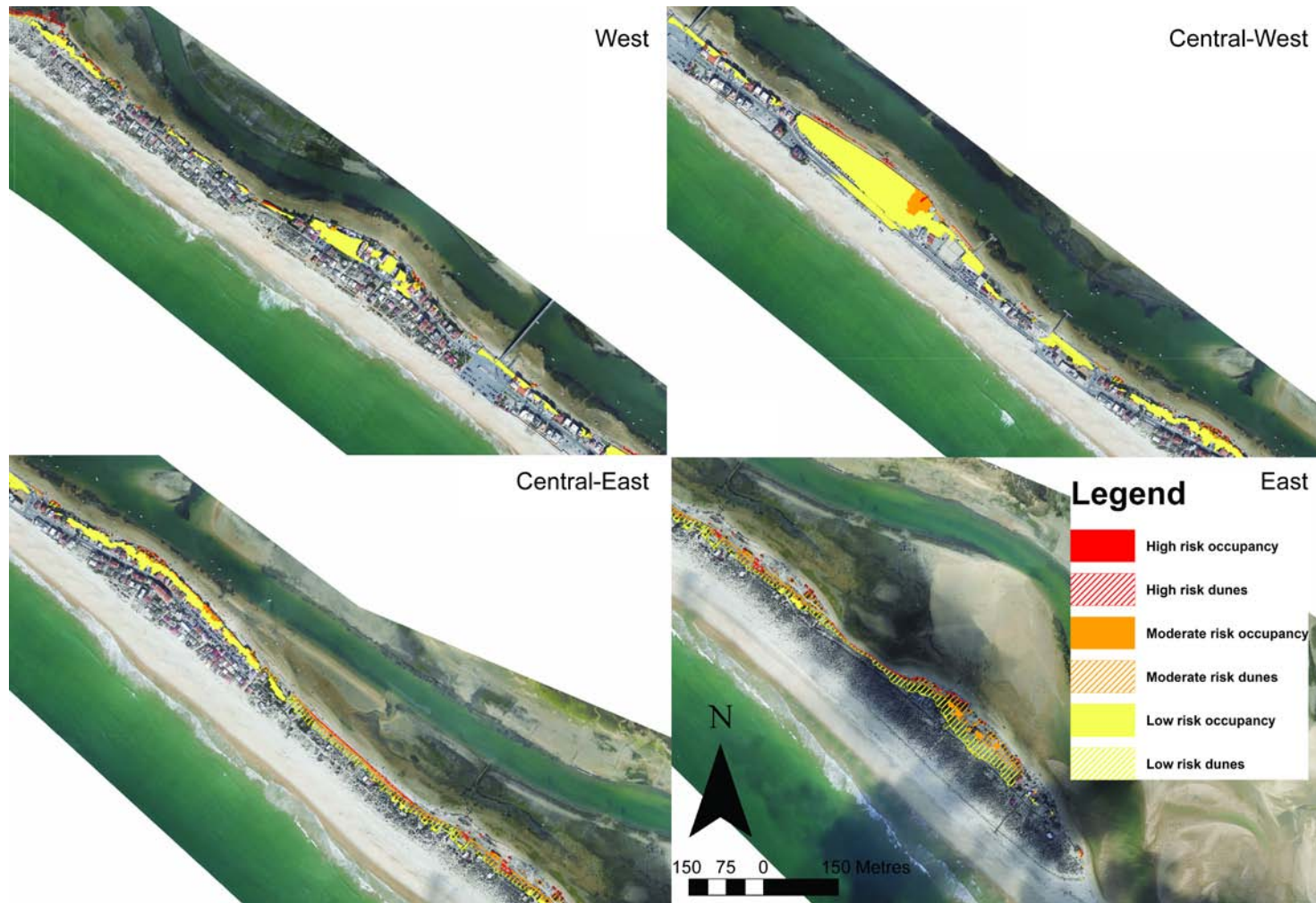


Figure 7.7. Risk map for occupancy and ecology at Ancão Peninsula.

The moderate-risk zone includes mostly backbarrier sandy beaches (20,400 m²) and dunes (12,000 m²), but also occupancy (3,500 m²). The low-risk zone includes mostly areas of occupancy and backbarrier sandy beaches (Table 7.4; Figure 7.7).

Table 7.4. Delimitation of flood hazard zones at Ancão Peninsula and risk estimates for each zone.

		Hazard zones		
		Low risk (100 year return period)	Moderate risk (10 year return period)	High risk (1 year return period)
Flood levels (m, MSL)		[3.17 ; 2.45]	[2.45 ; 2.08]	[2.08; -1.0]
Flooded areas (m ²)	occupancy	40,381	3,470	138
	backbarrier sandy beaches and sandy veneers	26,674	20,348	148,240
	dune	15,852	11,838	2,540
	salt marsh	-	-	2,509

The central part of the Ancão Peninsula (central-west and central-east, Figure 7.7) is the most susceptible, with a greater area of occupancy and ecological areas presenting moderate or low risk to flood. Occupancy with high risk is scattered alongshore through the backbarrier shorefront, but limited to a narrow fringe, which implies that a 100 year return period flood does not propagate into inner areas (with the exception of the central part, Figure 7.7). Impacts of flood on the ecology (mostly dunes) are greater in the eastern part of the peninsula (with less occupancy; Figure 7.7).

Impacts of floods on occupancy include damage to human residences (see Figure 7.3c and 3d), walkways, and accesses to residences (Figure 7.7). Artificial margins (e.g., central-west part) should have a different response to flood than should non-artificial margins (e.g., eastern part, Figure 7.7). For low-risk areas, management actions (in

agreement with Table 7.1) include: the elevation of facilities and structures supporting commercial uses (e.g., camping and restaurants located in central-west part of the peninsula, Figure 7.7); the rehabilitation of impermeable parking areas into permeable parking areas; and sand fencing (e.g., in the eastern part of the peninsula, Figure 7.7). For the moderate-risk area, elements include: the recovery of some concrete residences to wooden homes (e.g., in the central-east and eastern part of the peninsula, Figure 7.7); the adaptation of the flooded zone to recreational uses such as picnic areas and kidding garden facilities; and the creation of beach leisure facilities. For the high-risk area, elements include recreational/sports use (jet skiing, canoeing, sailing, etc) and the creation of beach leisure facilities (in agreement with Table 7.1). Economic exploitation of marine resources, elevated footpaths, facilities and structures for boat anchoring, and piers and piles are already in use in the high-risk zone. Residences and other permanent facilities not related to marine resource exploitation in this zone should be removed or relocated to the low-risk area (e.g., a few constructions on the shorefront of the central-west part of the peninsula, Figure 7.7).

Locally, the main benefit of the adoption of uses described in Table 7.1 is the reuse of abandoned non-occupied backbarrier stretches for recreational purposes and to avoid gradual physical damage to occupied areas. In contrast to the ocean shore, the backbarrier shore uses devoted to recreation (permanent facilities and structures supporting seasonal beach leisure and restaurants) have always been neglected. The adaptation to other uses with 'added value' and the correct management of the existing uses is both economically and socially profitable, as it minimizes the impacts of long-term floods (100 year return period) and contributes to the sustainable reclamation of the entire barrier. For instance, beach recreation along backbarrier beaches is an appraisal option for beach users that requires mild wave energy conditions (e.g.,

families with children, disabled people). This is an ‘added value’ of backbarrier areas under high risk of flood. To prevent further deterioration of houses in the high- and moderate-risk zones, the lowest floor level should be at an elevation higher than the projected flood level (Table 7.1).

The most significant impacts of flood on the ecology of Ancão backbarrier are associated with the local and temporary disruption of dune sub-aerial species (mostly in the eastern part of the peninsula, Figure 7.7). Mitigation measures are recommended only if the flood is extensive and/or considered to be an endangering factor to the medium-term evolution of dune species. To improve the natural coastal resilience of the dunes on Ancão backbarrier, the installation of sand fencing and planting dune grasses inside the fences is the best option.

Based on the geomorphological settings and socio-economic constraints, an adaptation strategy guidance plan was developed for Ancão backbarrier (Table 7.5). The plan identifies the procedures and milestones of the adaptation strategy and the actors involved in each milestone. The adaptation strategy guidance is suitable for application in a natural park context in which there is a recurrent conflict of uses and funding problems.

7.4. Applicability of the method

In this paper, a methodological framework has been developed for flood hazard assessment and management of fetch-limited coastal environments, with a test application to Ancão Peninsula. The framework has provided an overall picture of flood risk in the backbarrier (Figure 7.7) and has allowed the formulation of response strategies on the basis of the environmental, economic, and social context. Hazard

sources have been determined and qualitatively validated in the test case. The cross-referencing between the hazard maps generated (Figure 7.6) and information gathered during local flood events (e.g., photographs and field visits) enabled the flood zones to be validated.

Table 7.5. Adaptation Strategy Guidance for Ancão Peninsula.

Milestones	Actors involved
(A) Hazard and risk maps (Figures 7.6 and 7.7)	Faro city council and scientific community (e.g., University of Algarve)
(B) Social and economic survey	Decision-makers (Faro city council, Natural Park of Ria Formosa, regional authorities for coastal management); Economics skilled technicians (e.g., Universidade do Algarve, other universities or private economic consultants)
(C) Public participation	Community (Praia Faro fisherman's and community living from marine resources), Natural Park of Ria Formosa, ONGs and local associations, recreational users
(D) List of non-prohibited and prohibited interventions	Legal rights (Natural Park of Ria Formosa) POOC, Regional Coastal Management Authorities
(E) Contingency analysis report	Decision-makers (Faro city council, Natural Park of Ria Formosa, regional authorities for coastal management); Economy skilled technicians (e.g., Universidade do Algarve, other universities or private economics consultants)
(F) Costs vs. benefits report	Decision-makers (Faro city council, Natural Park of Ria Formosa, regional authorities for coastal management)
(G) Intervention plan	Decision-makers (Faro city council, Natural Park of Ria Formosa, regional authorities for coastal management)

The primary advantage of the proposed Adaptation Strategy Guidance (Table 7.2) and foreseen uses (Table 7.1) is that these represent an articulation of best-practice adaptation strategies, and therefore are likely to be implemented in other fetch-limited

coastal systems. Results obtained using the framework can be significantly improved with the involvement of observers or eyewitnesses, generally coastal residents (Bernatchez et al., 2011). It should be noted that the instigation of adaptive measures will not only require a rethinking of society's view of coastal resources but will also require management founded upon an understanding of how coastal landforms are likely to change in the future (Crooks, 2004).

The estimated inundation levels reveal some uncertainty related to errors resulting from extreme probabilistic distributions and from projected levels for SRL (section 7.3.2.1). Water-surface levels for different return periods may change over time and require regular reassessment. The framework was applied to Ancão Peninsula using a 15-year-long period of water level data; with a longer time-series of data (e.g., 30 years), the accuracies of the projected flood levels (and therefore of the demarcated flood and risk zones) should be able to be improved. Future research and planning when considering the potential implications of floods in fetch-limited environments should also consider human demographic trends, as well as additional physical damage induced by inland precipitation (Irish et al., 2010). For instance, in some lagoons, rainfall can also be responsible for water level rise, producing high frequency, small amplitude oscillations of water elevation in the bay (Fagherazzi and Priestas, 2011), and consequent flood washout (Figueiredo and Calliari, 2004). Such rainfall might, therefore, add to changes in water level, and consequently represents a variable that could be included in the framework in cases/sites where rainfall is deemed to be, or measured as, a significant contributor.

When undertaking risk analysis it is important to consider that the level of risk is unlikely remain constant through time, and it is often necessary to predict changes in risk estimates in the future in order to make better decisions. The main causes of

changes in exposure parameters are: (i) those factors that increase susceptibility, such as development, changing value of assets at risk, changing land use, behaviour of people during a flood, and capacity for recovery; and (ii) those that decrease susceptibility, including the delocalisation/movement of assets, improvement of flood warnings, changing land use, behaviour of people during a flood, and capacity for recovery.

7.5. Conclusions: benefits of the proposed framework

The main innovative element in this study is the development of a widely applicable methodological framework for analysing flood hazard and risk in fetch-limited coastal regions, which should have benefits for managing such regions. The framework involves the three steps of hazard source identification, flood hazard mapping, and risk analysis and management. The proposed framework was applied to a very low-energy system (Ancão backbarrier, south Portugal), but still requires further validation in other fetch-limited conditions. Proposed guidelines from the framework should assist coastal managers to: (a) identify high- and moderate-risk zones; (b) implement a flexible process-oriented adaptation approach to backbarrier uses; (c) organize a complex planning and management process with conflicting uses and multiple stakeholder groups with diverging interests; and (d) consider the appropriateness of management interventions, not only to address the priority given to conserving threatened areas but also to increase the economic potential of such areas.

The evolution of public policies is not a linear process and public decision makers may reject environmentally favourable management measures as a result of social and economic pressures. Recognition of the economic benefits resulting from coastal

conservation proposed in the adaptive framework presented denotes a positive step towards developing a sustainable management policy.

CHAPTER 8

FINAL CONSIDERATIONS

This chapter highlights the main thesis outcomes, presents the main innovative aspects and shortcomings, and includes some suggestions for future research.

8.1. General conclusions

The main conclusions of this thesis have been presented separately in the foregoing chapters. This final chapter brings those conclusions together into a unified whole.

The morphodynamic evolution of a fetch-limited beach was comprehensively analysed, producing definitions of the different types and rates of evolution for the dominant causative forcings. Factors governing sediment transport on a backbarrier beach were determined for a short-term scale (daily variability). Two different experiments with tracer techniques were undertaken during fair-weather conditions: (a) the first during a single tidal cycle (spring-tide conditions), and (b) the second during a full spring- to neap-tide cycle. Given the scarce information about tracer techniques under low energy conditions, both experiments afford new insights into such environments. They quantified vertical changes in the beach profile (on average $0.03 \text{ m}^3 \text{ m}^{-2}$ over one tidal cycle), grain-size (medium and coarse sands), and sediment transport (maximum $0.03 \text{ m}^3 \text{ d}^{-1}$), as well as the typical tidal currents, wind regime and wind-induced wave conditions underpinning local fair-weather conditions. Both experiments recorded low rates of sediment transport by advection, although tracer dispersion patterns revealed differences in the magnitude of the controlling forcing factors. In the first experiment (Chapter 3) tracer transport by advection was small (a few cubic centimetres per tidal cycle), in agreement with the observed tracer dispersion. In the second experiment tracer transport by advection was also small, but dispersion was in the order of metres per day, due to relatively higher wind intensities and consequently

higher wind-induced waves. The single tidal cycle experiment covered a very small time span that was probably not sufficient to fully characterise sediment transport under very low energy conditions. This highlights the need for a broad timescale of sediment transport data collection (i.e., more than a week) in order to better understand the influence of causative forcing mechanisms.

Comparison between published data and the measurements taken during the fieldwork campaigns demonstrated that the study area is not only a low-energy beach when compared with oceanic beaches, but is also within the lower-energy spectrum of fetch-limited coastal environments. The second experiment demonstrated that sediment transport along backbarrier beaches under very low wave-energy conditions (maximum fetch < 2 km) occurs mostly during spring tide, tending towards very small or zero values during neap tides (Chapter 4). In both experiments, tidal currents were the main factor governing net sediment transport (by advection and mostly alongshore), with relatively higher rates of tracer displacement taking place on the sand bank as a consequence of higher current velocities and smaller grain size. Discrimination of time-average shear velocity vs. critical shear velocity indicated a higher potential for sediment transport at the sandbank relative to the beach face, due to smaller grain size and higher velocities: maximum: \bar{u}^* velocities (time-average shear velocities) are close to 0.07 m s^{-1} on the sand bank, whereas on the beach face 0.03 m s^{-1} may be reached.

Analysis of sediment transport over several tidal cycles (from spring to neap tide) gave new insights into the application of tracers, highlighting the distinction between tracer advection and tracer dispersion in tidally controlled environments. Given the absolute speeds recorded during the second experiment (maximum current velocities of 0.5 m s^{-1}) and current asymmetry, it was expected that substantially greater net longshore transport would occur. Unexpectedly, tracer advection did not prevail over

diffusion and dispersion, bringing some methodological drawbacks associated with the application of tracers to attention. Tracer techniques revealed the need for improvements in very fetch-limited environments that are largely dependent on ebb and flood sediment reworking. Careful application of fluorescent tracer techniques is recommended in very low-energy environments, alongside a careful analysis of tracer results. The findings are innovative but require further research.

Analysis of beach variability on a daily scale was extended to a scale of analysis ranging from months to years (medium-term, Chapters 5 and 6). The results illustrate the limited capacity of very fetch-limited beaches to exhibit major morphological changes, revealing a response time which does not necessarily follow prevailing forcing conditions immediately. Chapter 5 was the first chapter devoted to medium-term analysis, reporting beach volumetric tendencies with respect to wind (wave driver) conditions over two years of monitoring. Chapter 6 also reported beach volumetric tendencies with respect to wind, but over a longer monitoring period (three years). Outcomes from the medium-term analysis corroborate the major trends identified in short-term experiments (Chapters 3 and 4), i.e., monthly variability in beach volume was low (maximum monthly variation of 47 m^3 for the entire analysed area, Chapter 6), in agreement with the very low daily sediment transport rates obtained in tracer experiments (cm^3 per day, Chapters 3 and 4). Maximum volumetric variation at the backshore and beach-face during the monitoring period was $+0.18 \text{ m}^3 \text{ m}^{-1}$ and $+4.88 \text{ m}^3 \text{ m}^{-1}$, respectively, whereas maximum volumetric variation on the tidal flat and sand bank between 2005 and 2008 was $+4.50 \text{ m}^3 \text{ m}^{-1}$ and $-3.45 \text{ m}^3 \text{ m}^{-1}$, respectively. Clearly, two response patterns were observed for the foreshore and nearshore, where site-specific controls revealed different local domains (Chapter 5). The nearshore evolved as an independent sub-system, with analogous volumetric variations, indicating the

absence of cross-shore transport between the tidal flat and the sand bank. No similar trend existed between the backshore and the beach face.

On the broad scale of an entire beach, fetch-limited beaches may present very low rates of change, with spatially limited sediment displacement (Chapters 3 and 4), and pronounced volumetric homogeneity (Chapter 5). However, on a smaller, morphological scale, volumetric changes and volumetric heterogeneity are indeed observed (Chapter 6). The Ancão backbarrier presented no significant seasonality in beach evolution, nor any significant correlation between volume and prevailing wind conditions. The dominant wind blowing was not coincident with the larger fetch length; some wind-induced beach changes were detected in grain-size variations, although they were not significant (Chapter 5).

Long-term analysis (from years to decades, Chapter 6) was relevant to understanding the (human-) modified beach response-type. From 1944 to 2007, key-changes were observed in the overall backbarrier and the neighbouring Ancão tidal channel, with a maximum rate of backbarrier shoreline change of 4.4 m yr^{-1} during the 1990s. Rates of change from this period were very different from rates of change determined for short- (Chapters 3 and 4) and medium-term analyses (Chapter 5), although the three timescales are complementary. The crossover between short- to long-term data it proved that backbarrier stretches might remain relatively unchanged for a long period, lagging considerably behind prevailing conditions. Because this type of environment is slow to adjust to causative forcing mechanisms (Chapters 4 and 5), disruptive/constructive changes, such as those produced by human interventions, oblige the system to adapt and evolve to a new morphodynamic state (Chapter 6). Human activities left a strong imprint on and consequent inheritance in the system, instilling morphological changes that were neither erased nor counteracted by cumulative

backbarrier evolution trends (as rates of change in the medium-term analysis testified). The analysis undertaken at the different timescales is an important contribution for the fully comprehension of beach responsiveness in very low-energy conditions (without wave energy contribution).

Besides human interventions, potential threats to fetch-limited coastal environments include natural hazards such as coastal flooding and sea-level rise. This thesis presents a framework for assessing the potential implications of flooding in fetch-limited coastal environments (with no significant wave setup; Chapter 7), with a focus on hazard mapping and risk analysis. The framework prioritizes site-based local management, so that appropriate interventions can be designed to minimize risks, and identifies alternative tools for sustainable coastal resources. It identifies tides, storm surges, sea-level-rise projections and river discharge as the main sources of flooding hazards, and was validated in a very low-energy system (Ancão backbarrier, southern Portugal). The main advantage of the proposed framework lies in its approach, which combines coastal and river flooding in fetch-limited coastal environments. Aside from the technical aspects, the presented framework proposes Adaptation Strategy Guidance for coastal management, which envisages uses with ‘added value’ in flooded zones. The proposed framework was easily applied to the test case, and likely to be implemented in other fetch-limited coastal systems (e.g., estuarine beaches, deltas, lagoons, coastal lakes).

8.2. Critical assessment

There is a paucity of morphological and hydrodynamic datasets collected in fetch-limited environments, and only a few studies have reported the morphological dynamics of backbarrier shores. It is worth pointing out that this thesis overcomes important

scientific problems in relation to the short- and longer-term morphodynamic behaviour of fetch-limited coastal beaches. In the absence of extensive published literature about fetch-limited beach evolution, most of the terminology, concepts, methods, and experimental designs presented were developed and modified during the course of this thesis. Some nomenclature adopted in Chapter 5 was further modified in Chapter 6 and subsequent chapters as understanding of the barrier system increased, namely ‘sand spit’ was replaced by ‘sand bank’, a more geomorphologically appropriate term. Other examples include the technical and scientific contributions of the first tracer experiment described in Chapter 3, compared to the second tracer experiment described in Chapter 4. Results from the first tracer experiment led into a better understanding of the system and were very important to the experimental design (e.g., amount of tracer to release) and dataset analysis undertaken in the second tracer experiment (Chapter 4). The short-term experiments described in Chapters 3 and 4 were motivated by the increasing need to produce accurate estimates of sediment transport on beaches facing very low-energy hydrodynamic conditions. Methods presented can be applied generally to other backbarrier beaches around the world; however, they might require some improvement or further validation in other coastal systems. Obtained results proved that most of the scientific methodologies (or expected behaviours) adopt in fetch-limited environments cannot be settle in methodologies developed for oceanic beaches. Results from Chapter 4 are conclusive in terms of applied methodology, but less definitive in regard to overall transport patterns over a spring-to-neap tidal cycle. As tracer techniques were not very enlightening about principal transport tendencies on a weekly time-scale, other sediment transport techniques (e.g., sediment traps) could have been employed to confirm bedload transport tendencies. Sediment transport analysis would also benefit from sediment transport experiments under stormy conditions (potentially increased wind

speed and wave height) and the influence of boat wakes could be considered. Notwithstanding, the results herein reported are thorough measurements of sediment transport rates in environments that have been hitherto neglected in the literature.

Chapter 6 and 7 are crucial from a management point of view. Chapter 6 provided an accurate picture of human impacts under very low-energy conditions. The adaptation strategies presented in Chapter 7 are an asset to management of flood hazard zones in any fetch-limited coastal environment. Besides being non-prohibitive management strategies, and therefore easily implemented in economic and social terms, these adaptation strategies also recommend a set of optional uses to better take advantage of beaches. Nevertheless, the framework proposed in Chapter 7 is mostly devoted to very fetch-limited environments, requiring adjustments for higher energy conditions (larger fetch with higher wave climate).

Application of the scientific findings for ecological purposes was not an objective of this thesis. However, the results are extremely important for integrated coastal studies and management strategies concerning biodiversity and conservation, given the recognised importance of biotic interactions on beach foreshores (see Nordstrom 2000; Jackson et al., 2002b).

8.3. Future Work

This thesis clearly demonstrates that work on fetch-limited beaches is far from being complete. Many questions are still to be answered, in respect to both the oceanographic and morphodynamic tendencies acting on these types of environments. Further research should be focussed on the definition of thresholds for hydrodynamic conditions driving medium-term evolution, including wind direction, wind intensity and tidal currents, and

to the role of cumulative beach inheritance on beach mobility (e.g., definition of equilibrium beach profile). Other sediment transport studies should discriminate the suspended load contribution from the overall sediment transport budget (e.g., short-term experiments).

After characterising the lower spectrum of fetch-limited backbarrier beaches, research should now move towards higher energy conditions (i.e., larger fetch). The role of wind-induced waves (and refracted ocean waves) should be progressively integrated, including swash excursion, determination of runup limits and testing the adequacy of existing formulae in this type of environment. This work would entail the establishment of the three scales of variability for larger fetch-limited conditions, similar to the studies developed within this thesis. Efforts should be concentrated in developing a new morphodynamic classification (morphology *vs.* wave energy), considering different types of fetch-limited conditions. For that reason, it is very important to ensure that future works contemplates the same type of data acquisition. Other research directions include:

- a determination of backbarrier morphological variability during infrequent high-energy events, which would require adequate methods and equipment, and improvement of accuracy levels;
- an investigation of coastal dunes and foreshores, evaluating the aeolian transport contribution to beach robustness in backbarrier beaches;
- an analysis of the contribution of boat wakes to small-scale beach variability;
- and
- an analysis of ecological factors, and the dependence of species on backbarrier morphology (e.g., role of natural vegetation on the upper foreshore); the

interactions between organisms, waves, currents and sediment movement should be investigated.

Literature on low energy beaches is scarce. Any new information on these environments should be welcomed as a significant contribution to knowledge.

REFERENCES

- Adger, W.N., Huq, S., Brown, K., Conway, D. and Hulme, H., 2003. Adaptation to climate change in the developing world. *Progress in Development Studies*, 3(3), 179-195.
- Almeida, L.P., Ferreira, Ó. and Pacheco, A., 2010. Thresholds for morphological changes on an exposed sandy beach as a function of wave height. *Earth Surface and Landforms*, 36, 523-532.
- Alvarado-Agillar, D. and Jiménez, J.A., 2009. Flood hazard mapping for coastal storms in the Delta Ebro. In: Samuels et al. (eds.), *Flood Risk Management: Research and Practice*, Taylor & Francis Group, London, pp. 375-384.
- Andrade, C., 1990. *O ambiente barreira da Ria Formosa, Algarve-Portugal*. PhD thesis, Universidade de Lisboa, Portugal, 626 p. (in Portuguese).
- Andrade, C., Cunha, J. and Paulino, J., 1998. Geochemical signature of extreme marine flooding in the Boca do Rio lowland (Algarve, Portugal). *Proceeding of Congresso Nacional de Geologia*. IGN, SGP, Lisboa, C-51/C-54.
- Andrade, C., Freitas, M., Moreno, J. and Craveiro, S., 2004. Stratigraphical evidence of Late Holocene barrier breaching and extreme storms in lagoonal sediments of Ria Formosa, Algarve, Portugal. *Marine Geology*, 210, 339-362.
- Anthony, E., Vanhee, S. and Ruz, M., 2006. Short-term beach-dune sand budgets on the north sea coast of France: sand supply from shoreface to dunes, and the role of wind and fetch. *Geomorphology*, 81, 316-329.

-
- Ashton, A.D., Murray, A.B., Littlewood, R., Lewis, D.A. and Hong, P., 2009. Fetch-limited self-organization of elongate water bodies. *Geology*, 37, 187-190.
- Balouin, Y., Howa, H., Pedreros, R. and Michel, D., 2005. Longshore sediment movements from tracers and models, Praia de Faro, South Portugal. *Journal of Coastal Research*, 21(1), 146-156.
- Battjes, J.A., 1974. Surf similarity. *Proceedings of the 16th Conference on Coastal Engineering*, ASCE, 466-480.
- Bernatchez, P., Fraser, C., Lefaivre, D. and Dugas, S., 2011. Integrating anthropogenic factors, geomorphological indicators and local knowledge in the analysis of coastal flooding and erosion hazards. *Ocean & Coastal Management*, 54, 621-632.
- Bertin, X., Castelle, B., Anfuso, G. and Ferreira, Ó., 2007. Improvement of sand activation depth prediction under conditions of oblique wave breaking. *Geo-Marine Letters*, 28, 65-75.
- Bertin X., Fortunato A.B. and Oliveira A., 2009a. Simulating morphodynamics with unstructured grids: description and validation of an operational model for coastal applications. *Ocean Modelling Online*, 28, 75-873.
- Bertin X., Fortunato A.B. and Oliveira A., 2009b. Morphodynamic modeling of the Ancão Inlet, South Portugal. *Journal of Coastal Research*, SI56, 10-14.
- Bettencourt, P., 1994. *Les Environnements Sédimentaires de la Côte Sotavento (Algarve, Sud Portugal) et leur Évolution Holocène et Actuelle*. PhD thesis, University Bordeaux, France, 92 p. (in French).

- Blott, S.J. and Pye, K., 2001. GRADISTAT: A grain size distribution and statistics package for the analysis of unconsolidated sediments. *Earth Surface Processes and Landforms*, 26, 1237-1248.
- Botton, M.L. and Lovelan, R.L., 2003. Abundance and dispersal potential of horseshoe crab (*Limulus polyphemus*) larvae in the Delaware Estuary. *Estuaries*, 26(6), 1472-1479.
- Brown, J.M. and Davies, A.G., 2009. Methods for medium-term prediction of the net sediment transport by waves and currents in complex coastal regions. *Continental Shelf Research*, 29, 1502-1514.
- Burton, I., Huq, S., Lim, B., Pilifosova, O. and Schipper, E.L., 2002. From impacts assessment to adaptation priorities: the shaping of adaptation policy. *Climate Policy*, 2, 145-159.
- Calliari, L.J. and Silva, R.P., 1998. Erosion processes associated to storm surge and washout along Brazilian coastline. *Journal of Coastal Research*, SI26, 1-7.
- Carrasco, A.R., Ferreira, Ó., Davidson, M.A., Matias, A. and Dias, J.A., 2008. An evolutionary categorisation model for backbarrier environments. *Marine Geology*, 251, 156-166.
- Carrasco, A.R., Ferreira, Ó., Freire, P. and Dias, J.A., 2009. Morphological changes in a low-energy backbarrier. *Journal of Coastal Research*, SI56, 173-177.

-
- Carrasco, A.R., Ferreira, Ó., Matias, A., Pacheco, A. and Freire, P., 2011a. Short-term sediment transport at a backbarrier beach. *Journal of Coastal Research*, 27(6), 1076-1084.
- Carrasco, A.R., Ferreira, Ó., Matias, A., Freire, P. and Dias, J.A., 2011b. Backbarrier evolution at medium-term scale. *Journal of Coastal Research*, SI64, 175-179.
- Carter, R.W.G., 1988. *Coastal environments - an introduction to the physical, ecological and cultural systems of coastlines*. Academic Press, London, 617 p.
- Ciavola, P., Taborda, R., Ferreira, Ó. and Dias, J.A., 1997a. Field measurements of longshore sand transport and control processes on a steep meso-tidal beach in Portugal. *Journal of Coastal Research*, 13(4), 1119-1129.
- Ciavola, P., Taborda, R., Ferreira, Ó. and Dias, J.A., 1997b. Field observations of sand-mixing depths on steep beaches. *Marine Geology*, 141(1-4), 147-156.
- Ciavola, P., Dias, N., Ferreira, Ó., Taborda, R. and Dias, J.A., 1998. Fluorescent sands for measurements of longshore transport rates: a case study from Praia de Faro in southern Portugal. *Geo-Marine Letters*, 18, 49-57.
- Cooper, J.A.G., Pilkey, O.H. and Lewis, D.A., 2007. Islands behind islands: an unappreciated coastal landform category. *Journal of Coastal Research*, SI50, 907-911.
- Costa, M., Silva, R., Vitorino, J., 2001. Contribuição para o estudo do clima de agitação marítima na costa portuguesa. *Proceedings of 2as Jornadas Portuguesas de*

Engenharia Costeira e Portuária, International Navigation Association PIANC, Sines, Portugal (in Portuguese).

Costas, S., Alejo, I., Vila-Concejo, A. and Nombela, M., 2005. Persistence of storm-induced morphology on a modal low-energy beach: a case study from NW Iberian peninsula. *Marine Geology*, 224, 43-56.

Cowart, L., Walsh, J.P. and Corbett, D.R., 2010. Analyzing estuarine shoreline change: a case study of Cedar Island, North Carolina. *Journal of Coastal Research*, 26(5), 817-830.

Cowell, P.J. and Thom, B.G., 1994. Morphodynamics of coastal evolution. In: R.W.G. Carter and C.D. Woodroffe (eds.), *Coastal Evolution*, University Press, Cambridge, pp. 39-71.

Crooks, S., 2004. The effect of sea-level rise on coastal geomorphology. *IBIS*, 146, 18-20.

Crowell, M., Leatherman, S.P. and Buckley, M.K., 1991. Historical shoreline change: error analysis and mapping accuracy. *Journal of Coastal Research*, 7(3), 839-852.

Curtiss, G.M., Osborne, P.D. and Horner-Devine, A.R., 2009. Seasonal patterns of coarse sediment transport on a mixed sand and gravel beach due to vessel wakes, wind waves, and tidal currents. *Marine Geology*, 259, 73-85.

Dail, H.J., Merrifield, M.A. and Bevis, M., 2000. Steep beach morphology changes due to energetic wave forcing. *Marine Geology*, 162(2-4), 443-458.

-
- de Moel, H. and Aerts, J.C.J.H., 2010. Effect of uncertainty in land use, damage models and inundation depth on flood damage estimates. *Natural Hazards*, 58, 407-425.
- Dean, R. G. and Darlymple, R.A., 2002. *Coastal Processes with Engineering Applications*. United Kingdom: Cambridge University Press, 475 p.
- Defeo, O., McLachlan, A., Schoeman, D.S., Schlacher, T.A., Dugan, J., Jones, A., Lastra, M. and Scapini, F., 2009. Threats to sandy beach ecosystems: a review. *Estuarine Coastal and Shelf Science*, 81, 1-12.
- Dias, J., 1988. Aspectos geológicos do litoral Algarvio. *Geonovas*, 10, 113-128.
- Dias, J. and Neal, W., 1992. Sea cliff retreat in Southern Portugal: profiles, processes and problems. *Journal of Coastal Research*, 7(3), 839-852.
- Dias, J.A., Ferreira, Ó., Matias, A., Vila-Concejo, A. and Sá-Pires, C., 2003. Evaluation of soft protection techniques in barrier islands by monitoring programs: case studies from Ria Formosa (Algarve-Portugal). *Journal of Coastal Research*, SI35, 117-131.
- Dias, J.M., Sousa, M.C., Bertin, X., Fortunato, A.B. and Oliveira, A., 2009. Numerical modeling of the impact of the Ancão Inlet relocation (Ria Formosa, Portugal). *Environmental Modelling & Software*, 24(6), 711-725.
- Dodet G, Bertin X, Taborda R. 2010. Wave climate variability in the North-East Atlantic Ocean over the last six decades. *Ocean Modelling Online*, 31, 120-131.
- Dolan, R., Fenster, M.S. and Holme, S.J., 1991. Temporal analysis of shoreline recession and accretion. *Journal of Coastal Research*, 7(3), 723-744.

- Dolphin, T.J. and Green, M.O., 2009. Patter of wave-orbital and skin friction under estuarine (fetch-limited waves). *Journal of Coastal Research*, SI56, 178-182.
- Downing, T. E. and Patwardhan, A., 2003. *Vulnerability assessment for climate adaptation, adaptation policy framework: a guide for policies to facilitate adaptation to climate change*, UNDP. Available via <http://www.undp.org/cc/apf-outline.htm>
- Dubois, R., 1988. Seasonal changes in beach topography and beach volume in Delaware. *Marine Geology*, 81, 79-96.
- Eliot, M.J., Travers, A. and Eliot, I.G., 2006. Morphology of a low-energy beach, Como Beach Western Australia. *Journal of Coastal Research*, 22(1), 63-77.
- Fagherazzi, S. and Priestas, A.M., 2011. Back-barrier flooding by storm surges and overland flow. *Earth Surface Processes and Landforms*. doi: 10.1002/esp.2247
- Federal Emergency Management Agency. Regulatory Floodway. Available via <http://www.fema.gov/plan/prevent/floodplain/nfipkeywords/floodway.shtm>; accessed November 2011.
- Ferreira Ó., 2011. Morphodynamic impact of inlet relocation to the updrift coast: Ancão Peninsula (Ria Formosa, Portugal). *Proceedings of Coastal Sediments 2011*, ASCE, 1, 497-504.
- Figueiredo, S.A. and Calliari, L.J., 2004. Washouts in the central and northern littoral of Rio Grande do Sul state, Brazil: distribution and implications. *Journal of Coastal Research*, SI39, 366-370.

-
- FitzGerald, D.M., Fenster, M.S., Argow, B.A. and Buynevich, I.V., 2008. Coastal impacts due to sea-level rise. *Annual Review of Earth and Planetary Sciences*, 36, 602-647.
- Folk, R. and Ward, W., 1957. Brazos River Bar: a study in the significance of grain size parameters. *Journal of Sedimentary Petrology*, 27, 3-26.
- Fortunato A.B., Pinto L, Oliveira A. and Ferreira J.S., 2002. Tidally generated shelf waves off the Western Iberian Coast. *Continental Shelf Research*, 22, 1935-1950.
- Fortunato A.B. and Oliveira A., 2004. A modelling system for tidally driven long-term morphodynamics. *Journal of Hydraulic Research*, 42, 426-434.
- Freire, P. and Andrade, C., 1999. Wind-induced sand transport in Tagus estuarine beaches. First Results. *Aquatic Ecology*, 33, 225-233.
- Freire, P., Ferreira, Ó., Taborda, R., Oliveira, F.S.B.F., Carrasco, A.R., Silva, A., Vargas, C., Capitão, R., Fortes, C.J., Coli, A.B. and Santos, J.A., 2009. Morphodynamics of fetch-limited beaches in contrasting environments. *Journal of Coastal Research*, SI56, 183-187.
- Friedrichs, C. and Aubrey, D.G., 1988. Non-linear tidal distortion in a shallow well-mixed estuaries: a synthesis. *Estuarine Coastal and Shelf Science*, 57, 521-545.
- Garcia, T., Ferreira, Ó., Matias, A. and Dias, J.A., 2010. Overwash vulnerability assessment based on long-term washover evolution. *Natural Hazards*, 54, 225-244.

- Gilman, E., 2002. Guidelines for coastal and marine site-planning and examples of planning and management intervention tools. *Ocean & Coastal Management*, 45(6-7), 377-404.
- Godfrey, P.J. and Godfrey, M.M., 1974. The role of overwash and inlet dynamics in the formation of salt marshes on North Carolina Barrier Islands. In: R.A. Reinold (ed.), *Ecology of Halophytes*, Academic Press, New York, pp. 407-427.
- Gómez-Pujol, L., Orfila, A., Cañelas, B., Alvarez-Allacuria, A., Méndez, F.J., Medina, R. and Tintoré, J., 2007. Morphodynamic classification of sandy beaches in low energetic marine environments. *Marine Geology*, 242, 235-246.
- Goodfellow, B.W. and Stephenson, W.J., 2005. Beach morphodynamics in a strong-wind bay: a low-energy environment? *Marine Geology*, 214, 101-116.
- Hayes, M.O., 1979. Barrier island morphology as a function of tidal and wave regime. In: S.P. Leatherman (ed.), *Barrier Islands from the Gulf of St. Lawrence to the Gulf of Mexico*. Academic Press, New York, pp. 211-236.
- Hegge, B., Eliot, I.G. and Hsu, J., 1996. Sheltered Sandy beaches of Southwestern Australia. *Journal of Coastal Research*, 12(3), 748-760.
- Houser, C., Hapke, C. and Hamilton, S., 2008. Controls on coastal dune morphology, shoreline erosion and barrier island response to extreme storms. *Geomorphology*, 100, 223-240.
- Hunter, J., 2010. Estimating sea-level extremes under conditions of uncertain sea-level rise. *Climate Change*, 99, 331-350.

- Inman, D., Zampol, J.A., Thomas, E.W., Hanes, D.M., Waldorf, B.W. and Kastens, K.A., 1980. Field measurements of sand motion in the surf zone. *Proceedings of the 17th Conference on Coastal Engineering*, ASCE, 1215-1235.
- Intergovernmental Panel on Climate Change (IPCC), 2001. *Climate Change 2001: Impacts, adaptation, and vulnerability. Contribution of working Group II to the Third Assessment Report of the Intergovernmental Panel on Climate Change*. Available via http://www.grida.no/publications/other/ipcc_tar/; accessed October 2011.
- Intergovernmental Panel on Climate Change (IPCC), 2007. *Intergovernmental panel on climate change fourth assessment report working group 1 report: the physical science basis*. Available via <http://www.ipcc.ch/ipccreports/ar4-wg1.htm>; accessed October 2011.
- Irish, J.L., Frey, A.E., D. Rosati, J.D., Olivera, F., Dunkin, L.M., Kaihatu, J. M. Ferreira, C.M. and Edge, B.L., 2010. Potential implications of global warming and barrier island degradation on future hurricane inundation, property damages, and population impacted. *Ocean & Coastal Management*, 53, 645-657.
- Jackson, N.L., 1995. Wind and waves: influence of local and non-local waves on mesoscale beach behavior in estuarine environments. *Annals of the Association of American Geographers*, 85(1), 21-37.
- Jackson, N.L., 1999. Evaluation of criteria for predicting erosion and accretion on an estuarine sand beach, Delaware, New Jersey. *Estuaries*, 22(2A), 215-223.

- Jackson, N.L. and Nordstrom, K.F., 1992. Site specific controls on a wind and wave processes and beach mobility on estuarine beaches in New Jersey, U.S.A. *Journal of Coastal Research*, 8(1), 88-98.
- Jackson, N.L., Horn, D.P., Spalding, V. and Nordstrom, K.F., 1999. Changes in beach water table elevation during neap and spring tides on a sandy estuarine beach, Delaware Bay, New Jersey. *Estuaries*, 22(3B), 753-762.
- Jackson, N., Nordstrom, K., Eliot, I. and Masselink, G., 2002a. "Low energy" sandy beaches in marine and estuarine environments: a review. *Geomorphology*, 48, 147-162.
- Jackson, N.L., Nordstrom, K.F., Eliot, I.G. and Masselink, G., 2002b. Geomorphic – biotic interactions on beach foreshores in estuaries. *Journal of Coastal Research*, SI36, 414-424
- Jackson, N.L., Nordstrom, K.F., Sainia, S. and Smith, D.R., 2010. Effects of nourishment on the form and function of an estuarine beach. *Ecological Engineering*, 36, 1709-1718.
- Jonkman, S.N., 2005. Global perspectives on loss of human life caused by floods. *Natural Hazards*, 34, 151–175.
- Karunaratna, H., Reeve, D.E. and Spivack, M., 2009. Beach profile evolution as an inverse problem. *Continental Shelf Research*, 29, 2234–2239.

-
- Kirwan, M.L., Guntenspergen, G.R., D'Alpaos, A., Morris, J.T., Mudd, S. M., Temmerman, S., 2010. Limits on the adaptability of coastal marshes to rising sea level. *Geophysical Research Letters*, 37, L23401.
- Klein, R.J.T., Nicholls, R.J. and Mimura, N., 1999. Coastal adaptation to climate change: can the IPCC technical guidelines be applied? *Mitigation and Adaptation Strategies for Global Change*, 4, 239-252.
- Komar, P.D., 1998. *Beach processes and sedimentation*. Prentice-Hall, New Jersey, 544p.
- Kraeuter, J.N. and Fegley, S.R., 1994. Vertical disturbance of sediments by horseshoe crabs (*Limulus polyphemus*) during their spawning season. *Estuaries*, 17(B), 288-294.
- Kraft, J.C., Allen, E.A. and Belknap, D.F., 1979. Processes and morphologic evolution of an estuarine and coastal barrier system. In: S.P. Leatherman (ed.), *Barrier Islands from the Gulf of St. Lawrence to the Gulf of Mexico*. Academic Press, New York, pp. 149-184.
- Kraus, N.C., Isobe, M., Igarashi, H., Sasaki, T.O. and Horikawa, K., 1982. Field experiments on longshore sand transport in the surf zone. *Proceedings 18th International Conference on Coastal Engineering*, ASCE, 969-988.
- Larson, M. and Kraus, N.C., 1995. Prediction of cross-shore sediment transport at different spatial and temporal scales. *Marine Geology*, 126, 111-127.

- Larson, M., Rosati, J.D. and Kraus, N.C., 2002. *Overview of regional coastal sediment processes and controls*. Vicksburg, MS, ERDC/CHL CHETN-XIV-4.
- Lewis, D.A., Cooper, J.A.G. and Pilkey, O.H., 2005. Fetch limited barrier islands of Chesapeake Bay and Delaware Bay. *Southeastern Geology*, 44(1), 1-17.
- Lewis, D.A., Cooper, J.A.G., Pilkey, O.H. and Short, A.D., 2007. Fetch-limited barrier islands of Spencer Gulf, South Australia. *Journal of Coastal Research*, SI50, 912-916.
- Lippman, T.C. and Holman, R.A., 1990. The spatial and temporal variability of sand bar morphology. *Journal of Geophysical Research*, 95(C7), 11575-11590.
- Madsen O.S., 1987. Use of tracers in sediment transport studies. *Proceedings of Coastal Sediments'87*, ASCE, 424-435.
- Makaske, B. and Augustinus, P., 1998. Morphologic changes of a micro-tidal, low wave energy beach face during spring-neap tide cycle, Rhône-Delta, France. *Journal of Coastal Research*, 14(2), 632-645.
- Masselink, G. and Hughes, M.G., 2003. *Introduction to coastal processes and geomorphology*. Holder Arnold, U.K., 354 p.
- Masselink, G. and Pattiartchi, C.B., 2001. Seasonal changes in beach morphology along the sheltered coastline of Perth, Western Australia. *Marine Geology*, 172(3-4), 243-263.

- Matias, A., 2006. *Overwash sediment dynamics in the Ria Formosa Barrier Islands*. PhD thesis, Universidade Algarve, Portugal, 253 p. (in Portuguese).
- Matias, A., Ferreira, Ó., Dias, J. and Vila-Concejo, A., 2004. Development of indices for the evaluation of dune recovery techniques. *Coastal Engineering*, 51, 261-276.
- Matias, A., Ferreira, Ó., Vila-Concejo, A., Garcia, T. and Dias, J.A., 2008. Classification of washover dynamics in barrier islands. *Geomorphology*, 97, 655-674.
- Merz, B., Kreibich, H., Schwarze, R. and Thieken, A., 2010. Assessment of economic flood damage. *Natural Hazards Earth System Science*, 10, 1679-1724.
- Moore, R.D., Wolf, J., Souza, A.J. and Flint, S.S., 2009. Morphological evolution of the Dee Estuary, Eastern Irish Sea, UK: a tidal asymmetry approach. *Geomorphology*, 103, 588–596.
- Morris, J.T., Sundareshwar, P.V., Nietch, C.T., Kjerfve, B. and Cahoon, D.R., 2002. Responses of coastal wetlands to rising sea level. *Ecology*, 83(10), 2869–2877.
- Nordstrom, K.F., 1977. Bayside beach dynamics: implications for simulation modeling on eroding sheltered tidal beaches. *Marine Geology*, 25, 333-342.
- Nordstrom, K.F., 1980. Cyclic and seasonal beach response: a comparison of oceanside and bayside beaches. *Physical Geography*, 1(2), 177-196.

- Nordstrom, K.F., 1992. *Estuarine beaches: an introduction to physical and human factors affecting use and management of beaches in estuaries, lagoons, bays and fjords*. Elsevier Applied Science, New York, 225 p.
- Nordstrom, K.F. and Jackson, N.L., 1992. Two-dimensional change on sandy beaches in meso-tidal estuaries. *Zeitschrift fur Geomorphologie*, 36(4), 465-478.
- Nordstrom, K.F. and Roman, C.T. 1996. Emerging research needs related to interactions on estuarine shores. In: K.F. Nordstrom and C. Roman (eds.), *Estuarine shores: evolution, environments and human alterations*. John Wiley & Sons, USA, pp. 469-480.
- Nordstrom, K.F., Jackson, N.L., Allen, J.R. and Sherman, D.J., 1996. Wave and current processes and beach changes on a microtidal lagoonal beach at Fire Island, New York, USA. In: K.F. Nordstrom and C. Roman (eds.), *Estuarine shores: evolution, environments and human alterations*. John Wiley & Sons, USA, pp. 213-231.
- Nordstrom, K.F., Jackson, N.L., Allen, J.R. and Sherman, D.J., 2003. Longshore sediment transport rates on a microtidal estuarine beach. *Journal of Waterway, Port, Coastal and Ocean Engineering*, 129, 1-4.
- Oertel, G.F., 1985. The barrier island system. *Marine Geology*, 63, 1-18.
- Oliveira, F.S.B.F., Vargas, C.I.C. and Coli, A.B., 2006. Longshore sediment transport of an estuarine beach: numerical investigation. *Proceedings of the 5th Symposium on the Iberian Atlantic Margin*, 1-2.

-
- Pacheco, A., Ferreira, Ó., Williams, J.J., Garel, E., Vila-Concejo, A., Dias, J.A., 2010. Hydrodynamics and equilibrium of a multiple-inlet system. *Marine Geology*, 274(1-4), 32-42.
- Pilkey, O., Neal, W., Monteiro, J. and Dias, J., 1989. Algarve barrier islands: a noncoastal-plain system in Portugal. *Journal of Coastal Research*, 5(2), 239-261.
- Pilkey, O., Cooper, J. and Lewis, D., 2009. Global distribution and geomorphology of fetch-limited barrier islands. *Journal of Coastal Research*, 25(4), 819–837.
- Pizzuto, J.E., 1986. Barrier island migration and onshore sediment transport, southwestern Delaware Bay, Delaware, U.S.A. *Marine Geology*, 71, 299-325.
- Ragan, J. and Smosna, R., 1987. Sedimentary characteristics of low-energy carbonate beaches, Florida Keys. *Journal of Coastal Research*, 3(1), 15-28.
- Ramos, L. and Dias, J.A., 2000. Overwash vulnerability attenuation in Ria Formosa system through soft interventions. *Proceedings of the 3rd Symposium on the Iberian Atlantic Margin*, 361-632.
- Roy, P.S. Williams, R.J., Jones, A.R., Yassin, I., Gibbs, P.J., Coaters, B., West, R.J., Scanes, P.R., Hudson, J.P. and Nichol, S., 2001. Structure and function of south-east Australian estuaries. *Estuarine Coastal and Shelf Science*, 53, 351-384.
- Sallenger, A.H., 2000. Storm impact scale for barrier islands. *Journal of Coastal Research*, 16(3), 890-895.

- Salles, P., 2001. *Hydrodynamic controls on multiple tidal inlet persistence*. PhD thesis, Massachusetts Institute of Technology and Woods Hole Oceanographic Institution, USA, 272 p.
- Salles, P., Voulgaris, G. and Aubrey, D.G., 2005. Contribution of nonlinear mechanisms in the persistence of multiple tidal inlet systems. *Estuarine, Coastal and Shelf Science*, 65, 475-491.
- Sherman, D.J., Nordstrom, K.F., Jackson, N.L. and Allen, J.R., 1994. Sediment mixing-depths on a low-energy reflective beach. *Journal of Coastal Research*, 10(2), 297-305.
- Short, A., 2006. Australian beach systems - nature and distribution. *Journal of Coastal Research*, 22(1), 11-27.
- Silva, A.M., Taborda, R., Rodrigues, A., Duarte, J. and Cascalho, J., 2007. Longshore drift estimation using fluorescent tracers: new insights from an experiment at Comporta Beach, Portugal. *Marine Geology*, 240, 137-150.
- Silveira, T.M. and Psuty, N.P., 2009. Morphological responses of adjacent shoreline segments on a fetch-restricted estuarine beach. *Journal of Coastal Research*, SI56, 208-212.
- Snoussi, M., Ouchani, T. and Niazi, S., 2008. Vulnerability assessment of the impact of sea-level rise and flooding on the Moroccan coast: The case of the Mediterranean eastern zone. *Estuarine Coastal and Shelf Science*, 77, 206-213.

- Soulsby, R.L. and Humphery, J.D., 1990. Field observations of wave-current interaction at the sea bed. In: A. Torum and O.T. Gudmestad (eds.), *Water Wave Kinematics*. Dordrecht, Kluwer Academic Publishers, pp. 413-428.
- Soulsby, R.L., 1997. *Dynamics of marine sands: a manual for practical applications*. Thomas Telford, 249 p.
- Stanchev, H., Palazov, A. and Stancheva, M., 2009. 3D GIS model for flood risk assesment of Varna Bay due to extreme sea level rise. *Journal of Coastal Research*, SI 56, 1597-1601.
- Stutz, M.L. and Pilkey, O.H., 2002. Global distribution and morphology of deltaic barrier island systems. *Journal of Coastal Research*, SI36, 694-707.
- Tanner, W.F. and Demirpolat, S., 1988. New beach ridge type: severely limited fetch, very shallow water. *Transactions Gulf Coast Association of Geological Societies*, 38, 367-373.
- Thieler, E.R. and Danforth, W.W., 1994. Historical shoreline mapping (II), Applications of the Digital Shoreline Mapping Analysis System (DSMS/DSAS) to shoreline change mapping in Puerto Rico. *Journal of Coastal Research*, 10, 600-620.
- Thieler, E.R., Himmelstoss, E.A., Zichichi, J.L., and Miller, T.L., 2005. *Digital Shoreline Analysis System (DSAS) version 3.0, an ArcGIS extension for calculating shoreline change*. U.S. Geological Survey Open-file Report 1304.

- Tonk, A. and Masselink, G., 2005. Evaluation of longshore transport equations with OBS sensors, streamer traps, and fluorescent tracer. *Journal of Coastal Research*, 21(5), 915-931.
- Travers, A., 2007. Low-energy beach morphology in respect to physical setting: a case study from Cockburn Sound, Southwestern Australia. *Journal of Coastal Research*, 23(2), 429-444.
- Vila, A., Dias, J.M.A., Ferreira, Ó. and Matias, A., 1999. Natural evolution of an artificial inlet. *Proceedings of the Coastal Sediments '99*, ASCE, 1478-1488.
- Vila-Concejo, A., Matias, A., Ferreira, Ó., Duarte, C. and Dias, J.M.A., 2002. Recent evolution of the natural Inlets of a barrier island system in southern Portugal. *Journal of Coastal Research*, SI 36, 741-752.
- Vila-Concejo, A., Ferreira, Ó., Matias, A. and Dias, J.M.A., 2003. The first two years of an inlet: sedimentary dynamics. *Continental Shelf Research*, 23, 1425-1445.
- Vila-Concejo, A., Ferreira, Ó., Ciavola, P., Matias, A. and Dias, J.M.A., 2004a. Tracer studies on the updrift margin of a complex inlet system. *Marine Geology*, 208, 43-72.
- Vila-Concejo, A., Ferreira, Ó., Morris, B., Matias, A. and Dias, J.M.A., 2004b. Lessons from inlet relocation: examples from Southern Portugal. *Coastal Engineering*, 51, 967-990.

- Vila-Concejo, A., Matias, A., Pacheco, A., Ferreira, Ó. and Dias, J.A., 2006. Quantification of inlet-hazards in barrier island systems: an example from the Ria Formosa (Portugal). *Continental Shelf Research*, 26, 1045-1060.
- Vila-Concejo, A., Hughes, M.G., Short, A.D. and Ranasinghe, R., 2010. Estuarine shoreline processes in a dynamic low-energy system. *Ocean Dynamics*, 60, 285-298.
- Vinet, F., Lumbroso, D., Defosse, S. and Boissier, L., in press. A comparative analysis of the loss of life during two recent floods in France: the sea surge caused by the storm Xynthia and the flash flood in Var. *Natural Hazards*.
- Voulgaris, G. and Collins, M.B., 2000. Sediment resuspension on beaches: response to breaking waves. *Marine Geology*, 167, 167-187.
- Wang, P., Davis Jr, R.A. and Kraus, N.C., 1998. Cross-shore distribution of sediment exchange texture under breaking waves along low-wave-energy coasts. *Journal of Coastal Research*, 14(1), 269-282.
- Ward, P.J., de Moel, H. and Aerts, J.C.J.H., 2011. How are flood risk estimates affected by the choice of return-periods? *Natural Hazards and Earth System Sciences*, 11, 3181-3195.
- Weather underground. History: Weather Underground, Faro, Portugal. Available via <http://www.wunderground.com/history/station/08554/>; accessed January 2006; March 2008; and December 2008.

White, T.E., 1998. Status of measurement techniques for coastal sediment transport.

Coastal Engineering, 35, 17–45.

Wolanski, E. and Chappell, J., 1996. The response of tropical Australian estuaries to a

sea level rise. *Journal of Marine Systems*, 7(2-4), 267-279.

Wright, L. and Short, A., 1984. Morphodynamic variability of surf zones and beaches: a

synthesis. *Marine Geology*, 56, 93-118.

